Synthesis of [3:1] Site-Differentiated [4Fe-4S] Clusters Having Tridentate Thiolate and Carboxylate/Imidazole Ligands: Models of Unusual [4Fe-4S] Clusters in Metalloproteins

三座チオラート配位子とカルボキシラート／イミダゾールを有する
四鉄四硫黄クラスターの合成：
生体内に存在する特異な四鉄四硫黄クラスターのモデル

Tamaki TERADA

寺田　玲季

Table of Contents

Chapter 1

General Introduction

1.1 [4Fe-4S] Clusters in Proteins

1.1.1 General information of [4Fe-4S] clusters in proteins

[4Fe-4S] Cluster is one of the common clusters in iron-sulfur proteins. Most of [4Fe-4S] clusters in proteins are involved in electron transfer processes such as electron uptake, storage, donation, and exchange between intramolecular/intermolecular. Usual [4Fe-4S] clusters exhibit reversible oxidation and reduction between $[4Fe\text{-}4S]^{2+}$ and $[4Fe\text{-}4S]^{+}$ state.[1] On the other hand, some clusters exhibit $[4Fe\text{-}4S]^{3+/2+}$ redox couplings, such as cluster in high potential iron-sulfur proteins (HiPIP).[2] The other roles of [4Fe-4S] clusters are catalysis in enzyme,[3] stabilization of protein structure, substrate recognition,[4] and so on.[5] [4Fe-4S] Cluster has the distorted cube structure called "cubane", which is constituted by four iron and four sulfur atoms alternating at the vertices of cube. In many cases, each of four irons is coordinated by thiolate ligand from the cysteine residue of protein (Figure 1-1), but one cysteine thiolate of some [4Fe-4S] clusters is replaced by other ligand such as hydrosulfide, carboxylate from aspartic acid residue, or imidazole from histidine. They are termed [3:1] site-differentiated [4Fe-4S] clusters.

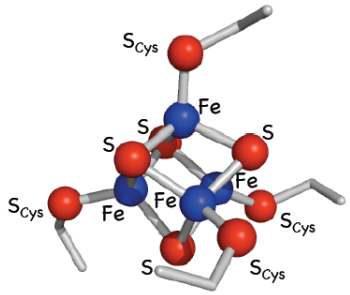

Figure 1-1. The structure of [4Fe-4S] cluster in the ferredoxin I from *Desulfovibrio africanus* (PDB: 1fxr).[1a]

1.1.2 [3:1] Site-differentiated [4Fe-4S] clusters in proteins

Recently, various site-differentiated [4Fe-4S] clusters have been discovered in various organisms. Their properties would be different from usual [4Fe-4S] clusters. We describe some types of [3:1] site-diffrentiated [4Fe-4S] clusters; (i) coordinated by a hydrosulfido and a cysteine thiolate connecting with another bioinorganic component, (ii) coordinated by a carboxylate from aspartic acid and from glutamic acid, (iii) coordinated by a carboxylate and/or an alkoxydo from substrate of enzymatic reaction and by a hydroxydo, (iv) coordinated by an imidazole from histidine residue.

[4Fe-4S] Clusters coordinated by a hydrosulfido and a cysteine thiolate connecting with another bioinorganic component: Very recently, the structure of (*R*)-2-hydroxyisocaproyl-CoA dehydratase from *Clostridium difficile* has been elucidated (Figure 1-2),[6] which contains two [4Fe-4S] clusters coordinated by three cysteines and one terminal ligand. The terminal ligand of cluster in the α-subunit is a water/hydroxido ion. The catalytic reaction is occurred on this site after binding substrate, similar to aconitase and IspH protein, described later. The cluster in the β-subunit has a terminal hydrosulfido/sulfido ligand and could control the electron transfer system in this protein.

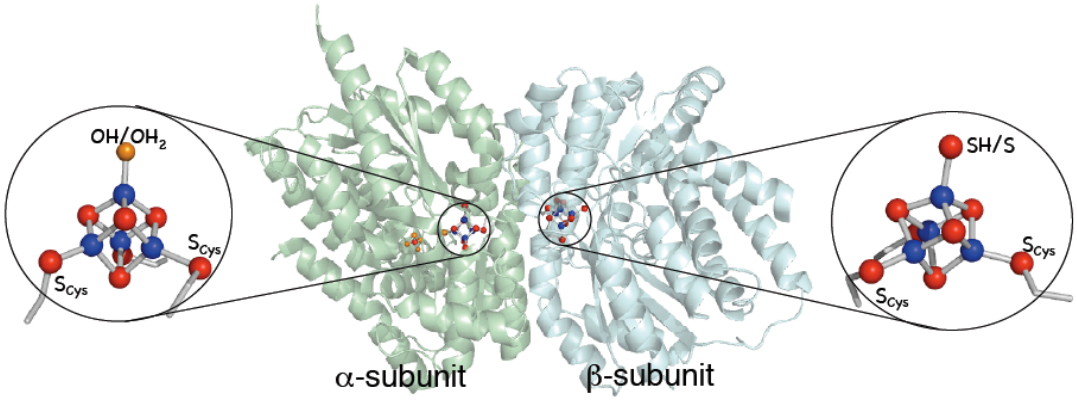

Figure 1-2. The structure of (*R*)-2-hydroxyisocaproyl-CoA dehydratase including two kind of [4Fe-4S] cluster (PDB: 3o3m).[6]

[4Fe-4S] Clusters in [FeFe] hydrogenase from *Clostridium pasteurianum* and *Desulfovibrio desulfuricans*,[7] sulfite reductase from *Escherichia coli*,[8] and acetyl CoA synthase from *Carboxydothermus hydrogenoformans*[9] are unique. Their [4Fe-4S] cores are bridged to another bioinorganic component of the active site of enzymes through each a common cysteine thiolate ligand, respectively. The active site of [FeFe] hydrogenase[7] has a dinuclear irons complex coordinated by some CO/CN ligand and cysteine thiolate connecting with [4Fe-4S] cluster (Figure 1-3),[7ab] and catalyzes the activation of hydrogen. Connecting [4Fe-4S] cluster to the active site could be relevant for the redox process of active site. The [4Fe-4S] clusters in sulfite reductase[8] and in acetyl CoA synthase[9] have one kind of iron-porphyrine complexes "siroheme"[8a] and dinuclear nickel complex connecting with two cysteines and one glycine residue,[9c] respectively (Figure 1-3). These clusters also help in transferring electrons to active sites.

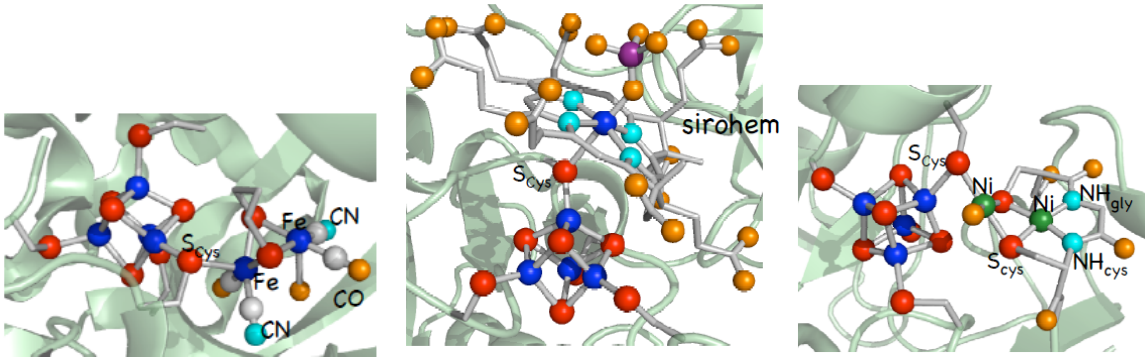

Figure 1-3. The structure of active site of *Dd* [FeFe] hydrogenase (left, PDB: 1hfe),[7ab] *Ec* sulfite reductase (center, PDB: 1aop),[8a] and *Ch* acetyl CoA synthase (right, PDB: 1ru3).[9c]

[4Fe-4S] Clusters coordinated by a carboxylate from aspartic acid and glutamic acid: The [4Fe-4S] clusters carrying one carboxylate ligand from amino acid residue on the unique iron site are found in three proteins at least. Dark-operative protochlorophilide oxidoreductase (DPOR) from *Rhodobacter capsulatus*[10] and ferredoxin from *Pyrococcus furiosus*[11] have an [4Fe-4S] cluster carrying one aspartate and three cysteine thiolates. They play an important role as electron transfer to/from active site of enzyme. The [4Fe-4S] cluster in IspG protein from *Aquifex aeolicus*[12] is coordinated by glutamate, and catalyzes the enzymatic reaction with reduction.

DPOR[10] is the photosynthetic enzymes and catalyzes the stereospecific reduction of protochlorophilide (Scheme 1-1). The NB-protein of the catalytic component of DPOR contains the [4Fe–4S] cluster at interface, which is coordinated by three cysteine residues and one aspartic acid residue.[10d] The location of the aspartate-ligated cluster is suitable to mediate the electron transfer from the [4Fe–4S] cluster having four cysteines of L-protein, which contact with NB-protein, to the substrate of protochlorophilide (Figure 1-4). In the study of mutants,[10d] this aspartic acid was replaced with cysteine, serine, and alanine. The replacement

by cysteine and by serine almost abolished the activity; nevertheless the cysteine substitution expressed all cysteine-coordinated [4Fe-4S] cluster. However the replacement by alanine exhibited low activity (13%) and its crystal structure contains an [4Fe–4S] cluster coordinated by three cysteines and non-protein ligand likely to be water/hydroxido. These results indicated that aspartate ligation is not essential for assembly of the cluster but is important for the enzymatic activity, such as electron transfer mediate.

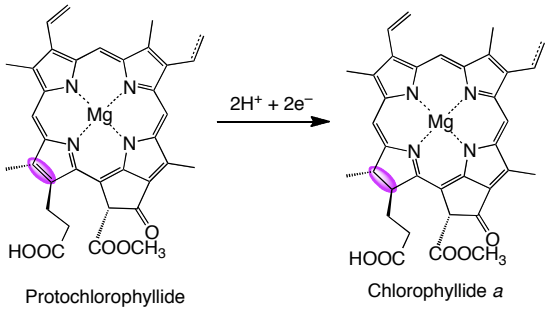

Scheme 1-1. The enzymatic reaction of DPOR.

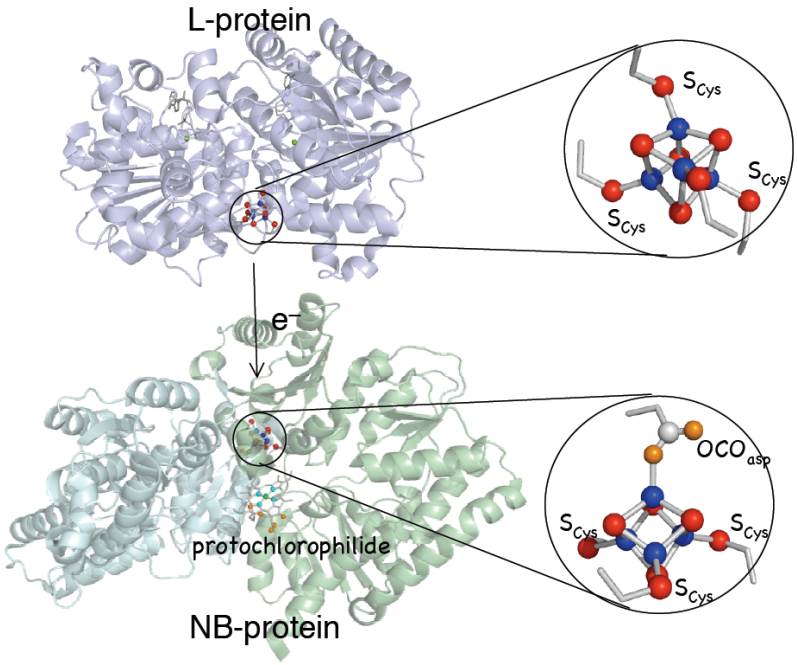

Figure 1-4. The structure of L-protein and NB protein in DPOR concluding two types [4Fe-4S] clusters (PDB: 3fwy, 3aek).[10cd]

Pf ferredoxin[11] also has an aspartate coordinated [4Fe-4S] cluster. One of *Pf* ferredoxin contacts with formaldehyde ferredoxin oxidoreductase (FOR), which is tungstopterin-containing protein.[11c] The electron transfer pathway of FOR is proposed that begins at the tungsten center, leads to the [4Fe-4S] cluster having an aspartate of *Pf* ferredoxin via [4Fe-4S] cluster having four cysteines of FOR, reversed DPOR electron transfer pathway. The mutation of aspartate to cysteine also expressed [4Fe-4S] clusters, which have the reduction potentials at E_m = –426, and –501 mV, respectively, while the reduction potential of WT *Pf* ferredoxin is E_m = –368 mV.[11b] It is conceivable that the coordination of aspartate give the different reduction potential.

IspG protein[12] serves as the penultimate enzyme of the non-mevalonate pathway for the biosynthesis of the universal isoprenoid precursors, isopentenyl diphosphate (IPP) and dimethylallyl diphosphate (DMAPP). IspG protein contains an [4Fe-4S] cluster which is coordinated by one glutamate and three cysteines (Figure 1-5),[12a] and catalyzes the reductive opening of the eight-membered ring of 2C-methyl-D-erythritol 2,4-cyclodiphosphate (MEcPP), which yields 1-hydroxy-2-methyl-2-(E)-butenyl 4-diphosphate (HMBPP) (Scheme 1-2). The study of replacement of this glutamic acid by aspartic acid resulted in loss of activity.[12a] In contrast, replacement by glutamine retained 28% relative activity. Thus, the mutation studies indicate that this glutamic acid residue does not directly participate in the activation of the substrate. Hence, the most likely functions are proposed; (i) the stabilization of the [4Fe–4S] cluster against loss of the unique iron ion, (ii) the acting as a site for coordination of the substrate to the iron of [4Fe-4S] which may involve weak binding, (iii) the tuning of the cluster's redox potential.

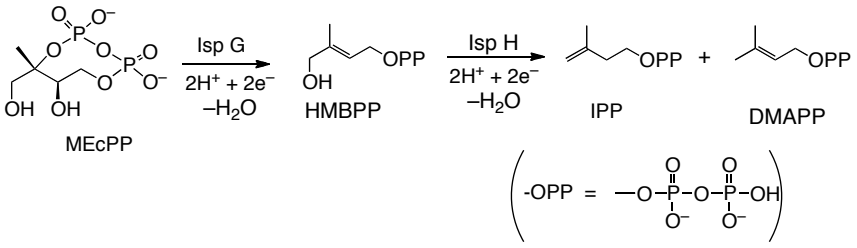

Scheme 1-2. The enzymatic reaction of IspG and IspH.

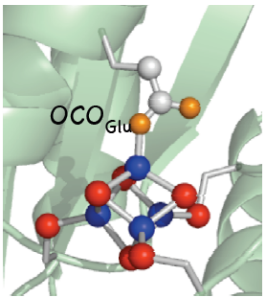

Figure 1-5. The structure of active site of IspG (PDB: 3noy).[12a]

[4Fe-4S] Clusters coordinated by an carboxylate and/or an alkoxydo from substrate of enzymatic reaction, and by a hydroxydo: The [4Fe-4S] clusters catalyzing enzymatic reactions were found in IspH proteins,[13] aconitase[14], and previous described (*R*)-2-hydroxyisocaproyl-CoA dehydratase.[6] These cluster have three cysteines and one terminal ligand as substrate of catalytic reaction or as hydroxido/water during substrate free state. On the other hand, the radical S-adenosylmethionine (SAM) super family enzymes[15] have [3:1] site-differentiated clusters carrying a SAM, which helps various radical reactions.

IspH protein[13] is the last enzyme of the non-mevalonate pathway for the biosynthesis, shown in Scheme 1-2. It synthesizes IPP and DMAPP from the dehydroxylation and reduction of HMBPP. IspH has one [4Fe-4S] cluster carrying three cysteines on three iron sites, of which forth iron is coordinated by the hydroxyl group of HMBPP and by the allyl of

intermediate (Figure 1-6).[13c] The mechanism of enzymatic reaction is unclear, but the crystal structures indicated that the catalytic reaction proceeds on the unique iron site.

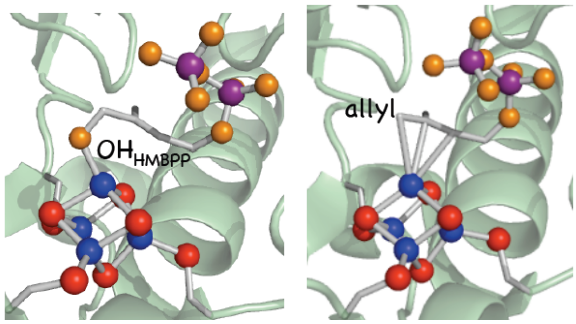

Figure 1-6. The structures of active site of IspH; alcohol/alkoxydo of HMBPP ligation (left, PDB: 3ke8), and allyl intermediate from HMBPP to IPP/DMAPP ligation (right, PDB: 3ke9).[13c]

Aconitase[14] is one [4Fe-4S] cluster containing enzyme of the tricarboxylic acid cycle. It catalyzes the stereospecific isomerization of citrate to isocitrate via *cis*-aconitate by a dehydration-hydration mechanism (Scheme 1-3). The each three iron of [4Fe-4S] cluster has one cysteine thiolate, while the unique iron has one terminal ligand relating to enzymatic reaction. So far, the X-ray structural analysis shows the existence of the clusters, which were coordinated by the carboxylate and the hydroxyl group of isocitrate and an oxygen atom of water molecular,[14b] by a hydroxido,[14d] and by the carboxylate and the hydroxyl group of citrate and an water molecular from the mutation experiment[14f] (Figure 1-7). The absence of direct protein ligand on the unique iron confers the flexibility of coordination, which is capable of binding to only a hydroxido, to a hydroxyl and a carboxylate of the substrate and water, and so on. Therefore, the [4Fe-4S] cluster having one ligand-free iron is essential to enzyme activity.

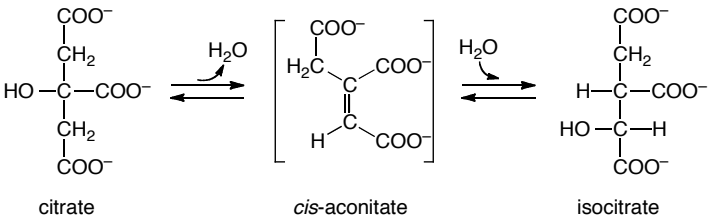

Scheme 1-3. The enzymatic reaction of aconitase.

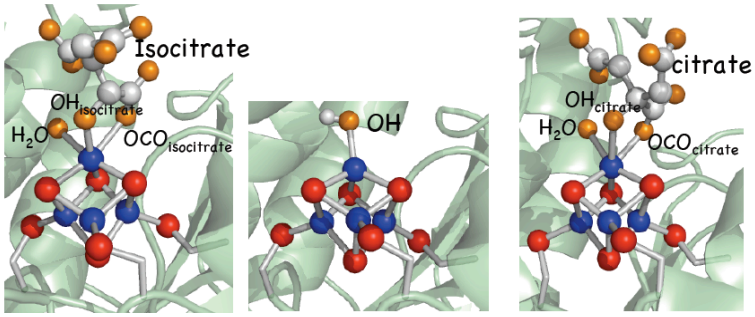

Figure 1-7. The structures of active site of aconitase; isocitrateand water ligation from wild type aconitase (left, PDB: 7acn),[14b] hydroxydo ligation from wild type (center, PDB: 1amj),[14d] and citrate and water ligation from S642A mutant (right, PDB: 1c96).[14f]

Radical SAM enzymes[15] include pyruvate formate-lyase activating enzyme (PFL-AE),[15ef] oxygen-independent coproporphyrinogen III oxidase (HemN),[15h] biotin synthase (BioB),[15b] molybdenum cofactor biosynthesis protein MoaA,[15c] and lysine aminomutase (LAM).[15d] These enzymes generate the radical by the reductive cleavage of a much simpler cofactor SAM. This radical acts the substrate, and then radical reaction proceeds. For example, PFL-AE[15ef] catalyzes the formation of glycyl radical from glycine using SAM, and LAM[15d] catalyzes the interconversion of L-lysine and L-β-lysine (Scheme 1-4). Several radical SAM enzymes catalyze sulfur insertion reactions with radicals, such as RimO[15g] and BioB[15b] (Scheme 1-4). The structures of PFL-AE,[15f] BioB,[15b] MoaA,[15c] and LAM[15d] were investigated by X-ray analysis. They have the [4Fe-4S] cluster carrying three cysteines and a SAM. SAM binds directly to the [4Fe-4S] cluster through its amino nitrogen and carboxylate oxygen.

Ligation to the cluster presumably helps to secure SAM in the binding site and to position SAM for radical generation, properly.

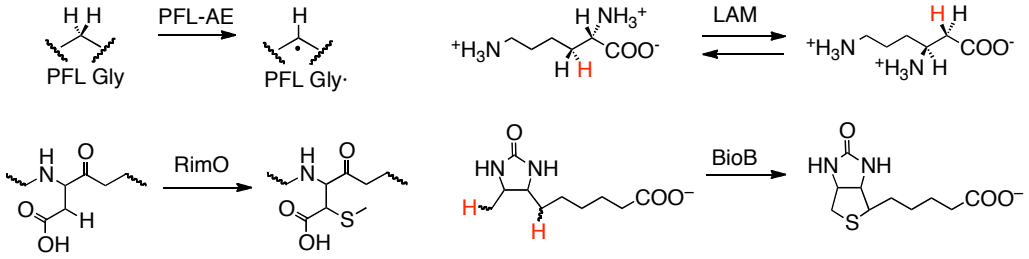

Scheme 1-4. The reactions catalyzed by radical SAM super family enzymes.

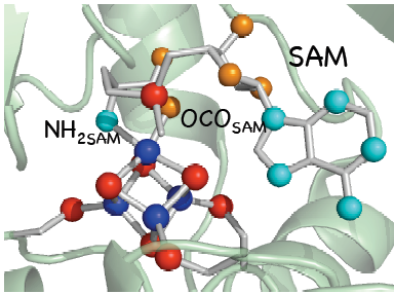

Figure 1-8. The structure of radical SAM coordinated [4Fe-4S] cluster in PFL-AE (PDB: 3cb8).[15f]

[4Fe-4S] Clusters coordinated by an imidazole from histidine residue: The [4Fe-4S] clusters carrying one histidine imidazole and three cysteine thiolates were found in [NiFe] hydrogenase from *Desulfovibrio gigas* and *Desulfovibrio fructosovorans*,[7de,16] [FeFe] hydrogenase from *Clostridium pasteurianum*,[7acde] Edihydronicotinamide adenine dinucleotide (NADH)–ubiquinone oxidoreductase (Complex I) from *Thermus thermophilus*,[17] membrane-bound quinol-nitrate oxidoreductase (nitrate reductase A; NarGHI) from *Escherichia coli*,[18] and 4-hydroxybutyryl-CoA dehydratase (4-BUDH) from *Clostridium aminobutyricum*.[19] The imidazole-ligation in 4-BUDH catalyzes enzymatic reaction with

radical activation, while the others play the important role as transferring electrons to/from active site of enzyme, other iron-sulfur cluster, and other protein. Two types of histidine coordination were observed (Figure 1-9). One is coordinated to the iron by N_δ atom of imidazole (e.g. in [NiFe] hydrogenase and nitrate reductase A), and the other is coordinated by N_ε atom (e.g. in [FeFe] hydrogenase, Complex I, and 4-BUDH). However, the properties of both clusters would not be different except for the distance between [4Fe-4S] core and protein chain.

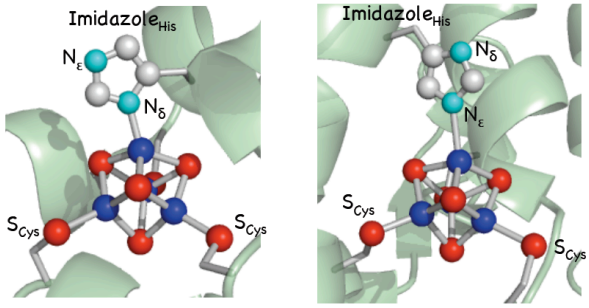

Figure 1-9. Two type hystidine ligation: coordination by N_δ atom of histidine imidazole in *Dg* [NiFe] hydrogenase (left, PDB: 2frv)[16c] and by N_ε atom in 4-BUDH (right, PDB: 1u8v).[19b]

In *Dg* and *Df* [NiFe] hydrogenases,[7de,16] the electrons are transferred from the active site nickel-iron complex to the redox partner of [NiFe] hydrogenase via four cysteines coordinated [4Fe-4S] cluster, [3Fe-4S] cluster, and the surface-exposed [4Fe-4S] cluster having one histidine and three cysteines (Figure 1-10). The mutation study of *Df* [NiFe] hydrogenase was reported,[16e] on which this histidine was changed into cysteine and glycine. The clusters in these mutants were assembled but the oxidative activity of the mutants was only 1.5 and 3% of that of the WT, respectively. It would result from the changing electron transfer ability in intra- or intermolecular.

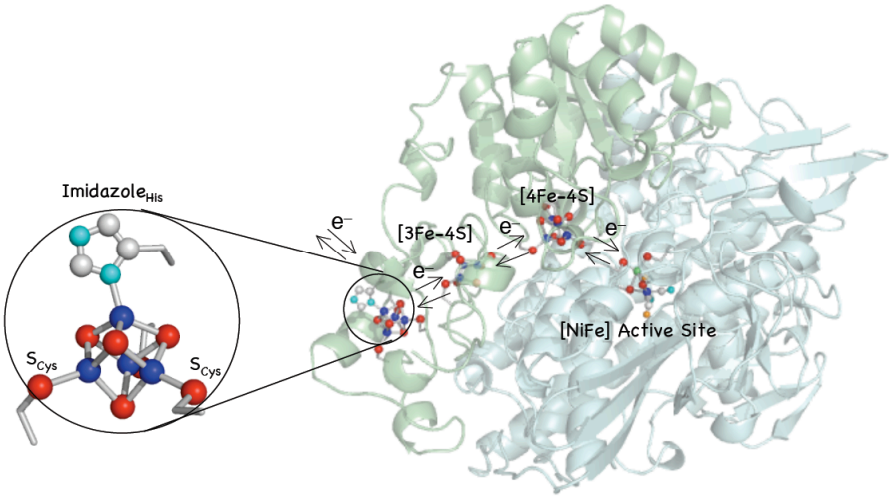

Figure 1-10. The structure of *Dg* [NiFe] hydrogenase concluding histidine imidazole coordinated [4Fe-4S] cluster on protein surface (PDB: 1frv).[16b]

The membrane-bound nitrate reductase A[18] is composed of a molybdenum cofactor-containing catalytic subunit, an iron-sulfur cluster-containing electron transfer subunit, and a heme-containing membrane anchor subunit. One of the iron-sulfur clusters is histidine-ligation, of which direct role is the electron transfer between the molybdenum-cofactor and other [4Fe-4S] cluster.[18b] The importance of histidine coordinated [4Fe-4S] cluster in electron transfer to the active site is supported by mutagenesis studies.[18ac] The midpoint potentials of the cluster lost histidine imidazole for H50C mutant enzyme shows a shift of 500 mV from the value of that of wild type.[18c]

The [4Fe-4S] cluster in 4-BUDH[19] has three cysteine thiolates and one histidine imidazole. The reversible dehydration of 4-hydroxybutyryl-CoA (Scheme 1-5) is catalyzed on the iron having histidine imidazole. Interestingly, the Fe-N (imidazole) bond length is 2.4 Å, although those in other metalloproteins such as [FeFe] hydrogenase are observed for 1.9-2.1 Å.[19bc] This long bond could contribute to the tuning of the electronic and bonding properties of iron,

which is ideally positioned for interaction with the hydroxyl group of the substrate. The occurrence of imidazole ligand could make this residue acted as a catalytic base.

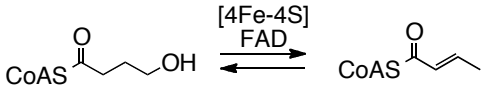

4-hydroxybutyryl CoA

Scheme 1-5. The catalytic reaction of 4-BUDH.

Conclusion: The properties of several [3:1] site-differentiated [4Fe-4S] clusters are clearly different from those of usual clusters; (i) having different redox potential tunes the electron transfer system in protein, (ii) having weak bond between the unique iron and the ligand is capable of proceeding catalytic reaction on the unique iron. However, these differences might be affected from amino acids around [4Fe-4S] clusters. Therefore it is necessary for revealing the properties of unusual cluster to synthesize their model clusters.

1.2 Synthetic [4Fe-4S] clusters

Synthetic [4Fe-4S] clusters were also investigated around the same time of revealing [4Fe-4S] clusters in metalloproteins. Herein, the clusters revealed X-ray crystal structures are described. In 1965, the first synthetic [4Fe-4S] cluster $[Fe_4S_4(\eta^5\text{-}C_5H_5)_4]$ was reported by Prewitt *et al* and Dahl *et al*.[20] However, it only has non-biological cyclopentadienyls and its oxidation state $[4Fe\text{-}4S]^{4+}$ is higher than the oxidation state in protein ($[4Fe\text{-}4S]^{3+}$, $[4Fe\text{-}4S]^{2+}$, and $[4Fe\text{-}4S]^{1+}$). Later, Holm *et al* reported the synthesis and the crystal structure of four benzylthiolates coordinated [4Fe-4S] cluster $[Fe_4S_4(SCH_2Ph)_4]^{2-}$ in 1972,[21] of which oxidation state is $[4Fe\text{-}4S]^{2+}$. Therefore, this cluster is termed for first model of [4Fe-4S] clusters in proteins. Until recent year, various aryl-, and alkyl-thiolates ligation $[Fe_4S_4(SR)_4]^{2-}$ (R = H, Me, ^{t}Bu, Ad, Ph, etc) were reported.[22] Moreover, thiolates-ligated $[4Fe\text{-}4S]^{3+}$ [23] or $[4Fe\text{-}4S]^{+}$ [24] cluster were also synthesized. Their properties were investigated by not only single crystal X-ray analysis but also by ^{1}H NMR, Mössbauer, UV-Vis, ESR spectroscopy, and so on.

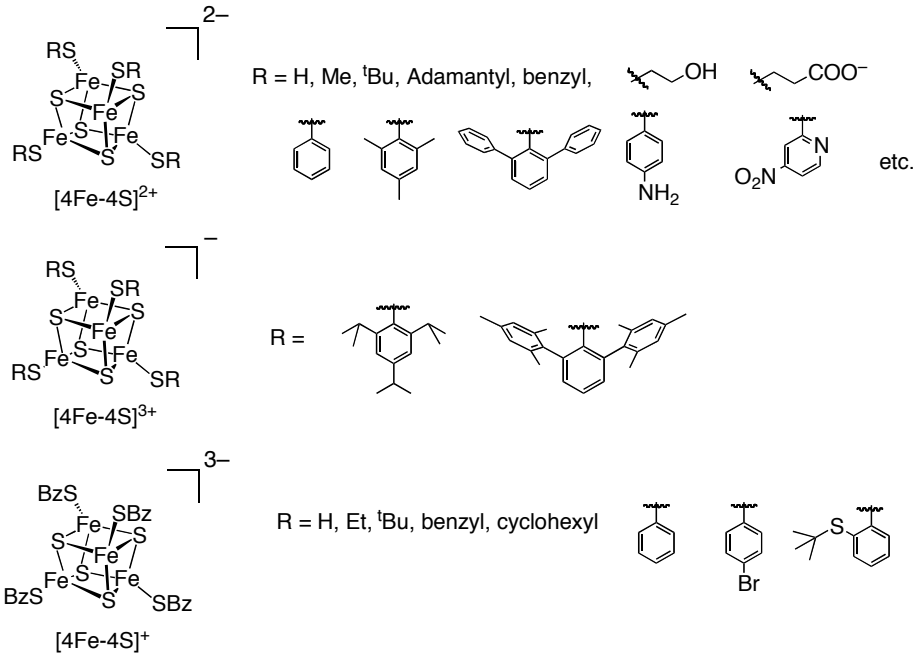

Chart 1-1. The four thiolate coordinated [4Fe-4S] clusters.

On the other hand, non-thiolate coordinated [4Fe-4S] clusters such as first synthetic [4Fe-4S] cluster were also reported.[20,23b,25] They have cyclopentadienyls,[20,25ab] trimethylsilylamides,[23b,25nt] phosphines,[25j] halides,[25ciq] phenolates,[25f] cyanides,[25np] N-heterocycliccarbenes,[25r] and so on. Their oxidation states of cubane cores are various. For example, cyclopentadienyl-ligation is capable of being the oxidation state of $[4Fe\text{-}4S]^{6+}$ [25b] and reduced cyanide-ligation has $[4Fe\text{-}4S]^{0}$ core.[25p]

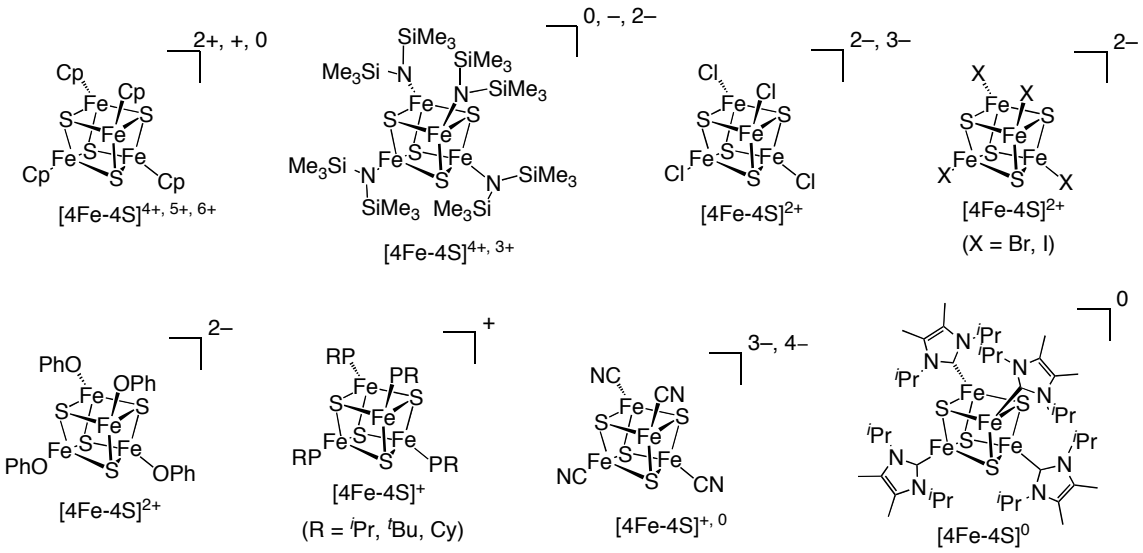

Chart 1-2. The four non-thiolate coordinated [4Fe-4S] clusters.

Additionally, synthetic site-differentiated [4Fe-4S] clusters were also synthesized for investigating whether or not they have different properties from usual types.[23b,26] They are coordinated by three halides and one thiourea/dithiocarboxylate,[26be] by three phosphines and one selenate/halide/siloxide,[26jqr] by two halides and two thioureas/phenolates/ dithiocarboxylates/diphosphines,[26abegp] and so on. The clusters having one or two thiolate ligands were also reported;[23b,26abfjkmnqr] such as cluster having one thiolate and three phosphines,[26qr] and having two thiolates and two chloride/phenolate/phosphines/

thioureas/dithiocarboxylates.[26abfk] The author's group reported three thiolates coordinated [3:1] site-differentiated clusters, which have very balky thiolates $DmpS^-$ (Dmp = 2,6-dimesitylphenyl) on each three irons and one tetramethylimidazole or three THF on the unique iron site.[23b] [4Fe-4S] Clusters having three $DmpS^-$ and one tetramethylimidazole are only one example of the model of [3:1] site-differentiated [4Fe-4S] cluster revealing its crystal structure. Unfortunately, the synthesis of site-differentiated [4Fe-4S] clusters could not be controlled well, and therefore it is needed for modeling [4Fe-4S] clusters in metalloproteins to use strategy.

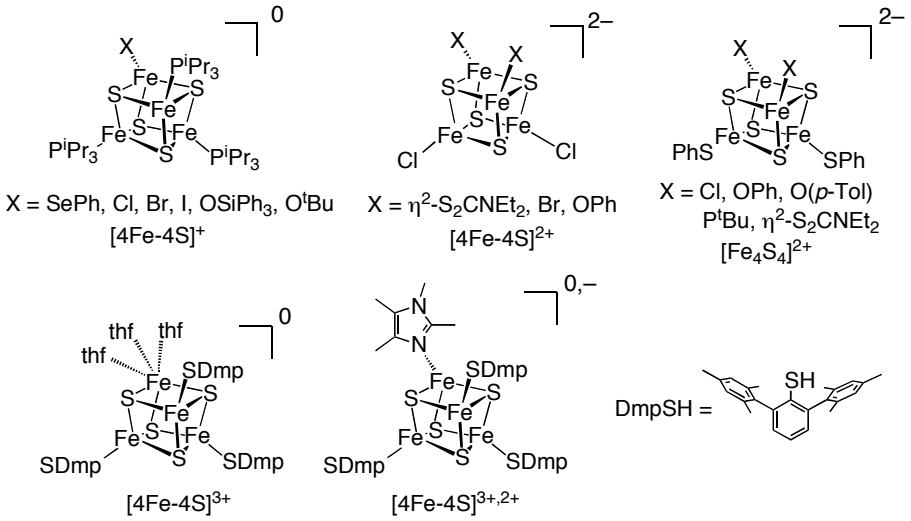

Chart 1-3. The synthetic [3:1] or [2:2] site-differentiated [4Fe-4S] clusters.

Strategic method for synthesis of models is to introduce a tridentate thiolate ligand.[27-29] Holm *et al* have developed a tridentate ligand LS_3^{3-} ($L(SH)_3$ = 1,3,5-tris(4,6-dimethyl-3-mercaptophenylthio)-2,4,6-tris(*p*-tolylthio)benzene) that tightly chelates three irons of the [4Fe-4S] core leaving one iron site for further functionalization, and they have reported the synthesis of various [3:1] site-differentiated [4Fe-4S] clusters $[Fe_4S_4(L')(LS_3)]^{2-}$ (L' = Cl, SR, etc).[28] Pohl *et al* have also reported one cluster coordinated by benzenethiolate and the

tridentate ligand $TriS^{3-}$ ($TriSH_3$ = 1,3,5-triethyl-2,4,6-tris(3-sulfanylindolyl[1]methyl)benzene).[29] However, the S-donor ligand or chlorido coordinated clusters were only investigated by X-ray structural analysis, and therefore the clusters having tridentate thiolate LS_3^{3-} and $TriS^{3-}$ are not good models of [3:1] site-differentiated [4Fe-4S] clusters in metalloproteins.

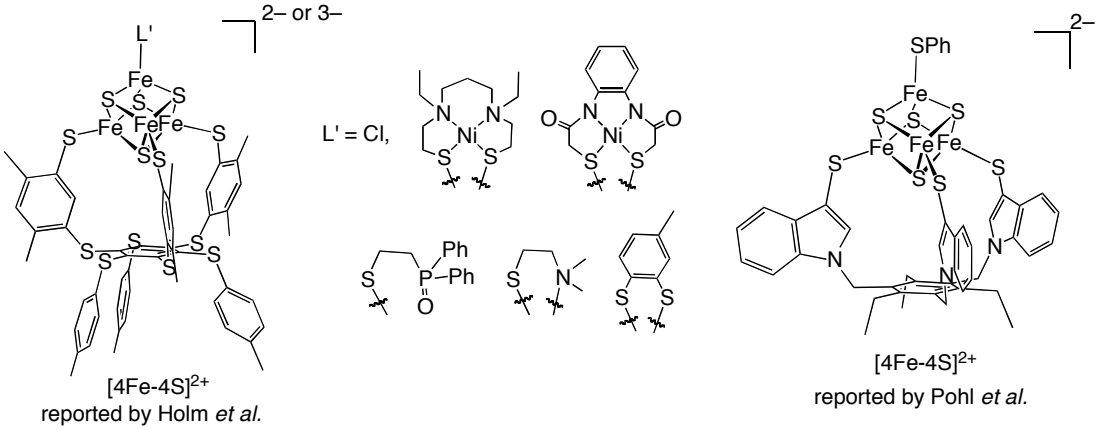

Chart 1-4. The [3:1] site-differentiated [4Fe-4S] clusters using tridentate thiolate ligand.

1.3 Overview of this thesis

For the purpose of elucidating the properties of [3:1] site-differentiated [4Fe-4S] clusters in the proteins using models, the author synthesized the [4Fe-4S] cluster having tridentate thiolate $TempS_3^{3-}$ and $TefpS_3^{3-}$ designed by the author's group. These clusters were investigated their X-ray structures and their redox properties, and were feedbacked to metalloprotein chemistry.

In chapter 2, design and preparation of the new tridentate thiolate ligands $TempS_3^{3-}$ and $TefpS_3^{3-}$ were described. These ligands were introduced to [4Fe-4S] cluster, which gave an ethanethiolate and tridentate thiolate coordinated clusters $[Fe_4S_4(SEt)(TempS_3)]^{2-}$ and $[Fe_4S_4(SEt)(TefpS_3)]^{2-}$. Their ethanethiolate ligands were selectively substituted by benzenethiolate and hydrosulfide. The hydrosulfide ligations convert to sulfide-bridged double cubane clusters with dissociation of H_2S. Finally, the hydrosulfide clusters were related to the cluster in (*R*)-2-hydroxyisocaproyl-CoA dehydratase. In chapter 3, the reaction of [4Fe-4S] cluster having a tridentate thiolate $TempS_3^{3-}$ and an ethanethiolate with carboxylic acids gave the carboxylate coordinated [4Fe-4S] clusters. Their carboxylate ligands coordinate to the each unique iron in η^1 manner, which is similar to the coordination mode of [4Fe-4S] clusters in proteins. The redox potentials of carboxylate-ligation are a little positive from ethanethiolate coordinated cluster, which would be relevant to [4Fe-4S] cluster in metalloproteins. In chapter 4, the [4Fe-4S] cluster having a tridentate thiolate $TempS_3^{3-}$ and an imidazole were synthesized, and were characterized by X-ray structural analysis. Their cyclic voltammograms indicated that the imidazole ligands would dissociate from the unique iron along reduction. The redox behavior is dependent on the concentration of imidazole in acetonitrile. The redox potentials of imidazole-ligation under the existence of imidazole are

more positive than that of ethanethiolate coordinated cluster. In chapter 5, the author investigated the synthesis, structure, and magnetic properties of $[4Fe\text{-}4S]^{+}$ cluster carrying a tridentate thiolate $TefpS_3^{3-}$. When the chloride coordinated cluster $[Fe_4S_4(Cl)(TefpS_3)]^{2-}$ was reacted with sodium tetrahydroborate, the edge-bridged double-cubane cluster $[\{Fe_4S_4(TefpS_3)\}_2]^{4-}$ was formed. Its oxidation state is reduced from starting material. Addition of benzenethiolate to the edge-bridged double-cubane cluster provided $[4Fe\text{-}4S]^{+}$ cluster having benzenethiolate and $TefpS_3^{3-}$, which was investigated by electron spin resonance spectroscopy and magnetic susceptibility.

References for Chapter 1

[1] a) A. Séry, D. Housset, L. Serre, J. Bonicel, C. Hatchikian, M. Frey, M. Roths, *Biochemistry* **1994**, *33*, 15408–15417; b) P. J. Stephens, D. R. Jollie, A. Warshel, *Chem. Rev.* **1996,** *96*, 2491–2513, Ferredoxin; c) I. Bertini, A. Sigel, H. Sigel, *Handbook on Metalloproteins*, Marcel Dekker, New York, **2001**, Chapter 10; d) A. Messerchmidt, R. Huber, T. Poulos, K. Wiehardt, *Handbook of Metalloproteins vol. 1,* John Wiley & Sons, Chichester, UK, **2001**, pp543–552, 560–592.

[2] a) C. W. Carter, Jr., J. Kraut, S. T. Freer, N.-H. Xuong, R. A. Alden, R. G. Bartsch, *J. Biol. Chem.* **1974**, *249*, 4212–4225; b) A. Messerchmidt, R. Huber, T. Poulos, K. Wiehardt, *Handbook of Metalloproteins vol. 1,* John Wiley & Sons, Chichester, UK, **2001**, pp602–609.

[3] a) S. Nasu, F. D. Wicks, R. K. Gholson, *J. Biol. Chem.* **1982**, *257*, 626–632; b) D. H. Flint, R. M. Allen, *Chem. Rev.* **1996**, *96*, 2315–2334; c) A. H. Saunders, A. E. Griffiths, K.-H. Lee, R. M. Cicchillo, L. Tu, J. A. Stromberg, C. Krebs, S. J. Booker, *Biochemistry* **2008**, *47,* 10999–11012

[4] a) M.-P. Golinelli, N. H. Chmiel, S. S. David, *Biochemistry* **1999**, *38*, 6997-7007; b) T. E. Messick, N. H. Chmiel, M.-P. Golinelli, M. R. Langer, L. Joshua-Tor, S. S. David, *Biochemistry* **2002,** *41,* 3931–3942.

[5] D. P. Bhave, J. A. Hong, R. L. Keller, C. Krebs, K. S. Carroll, *ACS Chem. Biol.* **2012**, *7*, 306−315.

[6] S. H. Knauer, W. Buckel, H. Dobbek, *J. Am. Chem. Soc.* **2011**, *133*, 4342–4347.

[7] a) J. W. Peters, W. N. Lanzilotta, B. J. Lemon, L. C. Seefeldt, *Science* **1998**, *282*, 1853–1858; b) Y. Nicolet, C. Piras, P. Legrand, C. E. Hatchikian, J. C. Fontecilla-Camps, *Structure* **1999**, *7*, 13–23; c) A. Messerchmidt, R. Huber, T. Poulos, K. Wiehardt, *Handbook of Metalloproteins vol. 2,* John Wiley & Sons, Chichester, UK, **2001**, pp738–751; d) J. C. Fontecilla-Camps, A. Volbeda, C. Cavazza, Y. Nicolet, *Chem. Rev.* **2007**, *107*, 4273–4303; e) C. Tard, C. J. Pickett, *Chem. Rev.* **2009**, *109,* 2245–2274.

[8] a) B. R. Crane, L. M. Siegel, E, D. Getzoff, *Science* **1995**, *270*, 59–67 b) A. Messerchmidt, R. Huber, T. Poulos, K. Wiehardt, *Handbook of Metalloproteins vol. 1,* John Wiley & Sons, Chichester, UK, **2001**, pp471–485. c) A. Messerchmidt, *Handbook of Metalloproteins vol. 4,* John Wiley & Sons, Chichester, UK, **2011**, pp103–110.

[9] a) T. I. Doukov, T. M. Iverson, J. Seravalli, S. W. Ragsdale, C. L. Drennan, *Science* **2002**, *298*, 567–572; b) C. Darnault, A. Volbeda, E. J. Kim, P. Legrand, X. Vernède, P. A. Lindahl, J. C. Fontecilla-Camps, *Nature Structural Biology*, **2003**, *10*, 271–279; c) V. Svetlitchnyi, H. Dobbek, W. Meyer-Klaucke, T. Meins, B. Thiele, P. Römer, R. Huber, O. Meyer, *Proc. Natl. Acad. Sci.* **2004**, *101*, 446-451; d) A. Messerchmidt, *Handbook of Metalloproteins vol. 4,* John Wiley & Sons, Chichester, UK, **2011**, pp397–412.

[10] a) Y. Fujita, C. E. Bauer, *J. Biol. Chem.* **2000**, *275*, 23583–23588; b) J. Nomata, T. Ogawa, M.

Kitashima, K. Inoue, Y. Fujita, *FEBS Lett*. **2008**, *582*, 1346–1350; c) R. Sarma, B. M. Barney, T. L. Hamilton, A. Jones, L. C. Seefeldt, J. W. Peters, *Biochemistry* **2008**, *47*, 13004–13015; d) N. Muraki, J. Nomata, K. Ebata, T. Mizoguchi, T. Shiba, H. Tamiaki, G. Kurisu, Y. Fujita, *Nature* **2010**, *465*, 110–115.

[11] a) Z. H. Zhou, M. W. W. Adams, *Biochemistry* **1997,** *36,* 10892-10900; b) P. S. Brereton, M. F. J. M. Verhagen, Z. H. Zhou, M. W. W. Adams, *Biochemistry* **1998,** *37,* 7351-7362; c) Y. Hu, S. Faham, R. Roy, M. W. W. Adams, D. C. Rees, *J. Mol. Biol*. **1999**, *286*, 899–914; d) A. Messerchmidt, R. Huber, T. Poulos, K. Wiehardt, *Handbook of Metalloproteins vol. 2,* John Wiley & Sons, Chichester, UK, **2001**, pp1086-1096.

[12] a) M. Lee, T. Gräwert, F. Quitterer, F. Rohdich, J. Eppinger, W. Eisenreich, A. Bacher, M. Groll, *J. Mol. Biol*. **2010**, *404*, 600–610; b) W. Wang, J. Li, K. Wang, C. Huang, Y. Zhang, E. Oldfield, *Proc. Natl. Acad. Sci*. **2010**, *107*, 11189–11193; c) Y. Xiao, R. L. Nyland II, C. L. F. Meyers, P. Liu, *Chem. Commun*. **2010**, *46*, 7220–7222; d) W. Xu, N. S. Lees, D. Adedeji, J. Wiesner, H. Jomaa, B. M. Hoffman, E. C. Duin, *J. Am. Chem. Soc*. **2010**, *132*, 14509–14520.

[13] a) I. Rekittke, J. Wiesner, R. Röhrich, U. Demmer, E. Warkentin, W. Xu, K. Troschke, M. Hintz, J. H. No, E. C. Duin, E. Oldfield, H. Jomaa, U. Ermler, *J. Am. Chem. Soc*. **2008**, *130*, 17206–17207; b) T. Gräwert, F. Rohdich, I. Span, A. Bacher, W. Eisenreich, J. Eppinger, M. Groll, *Angew. Chem. Int. Ed*. **2009**, *48*, 5756 –5759; c) T. Gräwert, I. Span, W. Eisenreich, F. Rohdich, J. Eppinger, A. Bacher, M. Groll, *Proc. Natl. Acad. Sci*. **2010**, *107*, 1077–1081; d) T. Gräwert, I. Span, A. Bacher, M. Groll, *Angew. Chem. Int. Ed*. **2010**, *49*, 8802 – 8809; e) I. Span, T. Gräwert, A. Bacher, W. Eisenreich, M. Groll, *J. Mol. Biol*. **2012**, *416*, 1–9.

[14] a) A. H. Robbins, C. D. Stout *Proc. Natl. Acad. Sci. USA* **1989**, *86*, 3639–3643; b) H. Lauble, M. C. Kerinedy, H. Beinert, C. D. Stout, *Biochemistry* **1992**, *31*, 2135–2748; c) H. Lauble, M. C. Kennedy, H. Beinert, C. D. Stout, *J. Mol. Biol*. **1994**, *237*, 437–451; d) H. Lauble, C. D. Stout, *Proteins: Structure, Function, and Genetics* **1995**, *22*, 1–11; e) H. Beinert, M. C. Kennedy, C. D. Stout, *Chem. Rev*. **1996,** *96*, 2335–2373; f) S. J. Lloyd, H. Lauble, G. S. Prasad, C. D. Stout, *Protein Sci*. **1999** *8*, 2655–2662; g) A. Messerchmidt, *Handbook of Metalloproteins vol. 4,* John Wiley & Sons, Chichester, UK, **2011**, pp147–159.

[15] a) H. J. Sofia, G. Chen, B. G. Hetzler, J. F. Reyes-Spindola, N. E. Miller, *Nucleic acids Research* **2001**, *29*, 1097–1106; b) F. Berkovitch, Y. Nicolet, J. T. Wan, J. T. Jarrett, C. L. Drennan, *Science* **2004***, 303*, 76–79; c) P. Hänzelmann, H. Schindelin, *Proc. Natl. Acad, Sci. USA* **2004**, *101*, 12870–12875; d) B. W. Lepore, F. J. Ruzicka, P. A. Frey, D. Ringe, *Proc. Natl. Acad, Sci. USA*, **2005**, *102*, 13819–13824; e) C. J. Walsby, D. Ortillo, J. Yang, M. R. Nnyepi, W. E. Broderick, B. M. Hoffman, J. B. Broderick, *Inorg. Chem*. **2005**, *44*, 727–741; f) J. L. Vey, J. Yang, M. Li, W. E. Broderick, J. B. Broderick, C. L. Drennan, *Proc. Natl. Acad, Sci. USA* **2008**,

105, 16137–16141; g) K.-H. Lee, L. Saleh, B. P. Anton, C. L. Madinger, J. S. Benner, D. F. Iwig, R. J. Roberts, C. Krebs, S. J. Booker, *Biochemistry* **2009**, *48*, 10162–10174; h) F. Yan, J. M. LaMarre, R. Röhrich, J. Wiesner, H. Jomaa, A. S. Mankin, D. G. Fujimori, *J. Am. Chem. Soc.* **2010**, *132*, 3953–3964; i) J. L. Vey, C. L. Drennan, *Chem. Rev.* **2011**, *111*, 2487–2506.

[16] a) M. Teixeira, I. Moura, A. V. Xavier, J. J. G. Moura, J. LeGall, D. V. DerVartanian, H. D. Peck, Jr., B.-H. Huynh, *J. Biol. Chem.* **1989**, *264*, 16435–16450; b) A. Volbeda. M.-H. Charon, C. Piras, E. C. Hatchikian, M. Frey, J. C. Fontecilla-Camps, *Nature* **1995**, *373*, 580–587; c) A. Volbeda, E. Garcin, C. Piras, A. L. de Lacey, V. M. Fernandez, E. C. Hatchikian, M. Frey, J. C. Fontecilla-Camps**,** *J. Am. Chem. Soc.* **1996**, *118,* 12989–12996; d) A. Messerchmidt, R. Huber, T. Poulos, K. Wiehardt, *Handbook of Metalloproteins vol. 2,* John Wiley & Sons, Chichester, UK, **2001**, pp880-896; e) S. Dementin, V. Belle, P. Bertrand, B. Guigliarelli, G. Adryanczyk-Perrier, A. L. De Lacey, V. M. Fernandez, M. Rousset, C. Léger, *J. Am. Chem. Soc.*, **2006**, 128, 5209–5218; f) S. Dementin, B. Burlat, V. Fourmond, F. Leroux, P.-P. Liebgott, A. A. Hamdan, C. Léger, M. Rousset, B. Guigliarelli, P. Bertrand, *J. Am. Chem. Soc.* **2011**, *133*, 10211–10221.

[17] a) L. A. Sazanov, P. Hinchliffe, *Science* **2006***, 311*, 1430–1436; b) A. Messerchmidt, *Handbook of Metalloproteins vol. 4,* John Wiley & Sons, Chichester, UK, **2011**, pp47–61; c) H. R. Bridges, E. Bill, J. Hirst, *Biochemistry* **2012**, *51*, 149−158.

[18] a) A. Magalon, M. Asso, B. Guigliarelli, R. A. Rothery, P. Bertrand, G. Giordano, F. Blasco, *Biochemistry* **1998**, *37*, 7363–7370; b) M. G Bertero, R. A Rothery, M. Palak, C. Hou, D. Lim, F. Blasco, J. H. Weiner, N. C. J. Strynadka, *Nature Structural Biology* **2003**, *10*, 681–687; c) R. A. Rothery, M. G. Bertero, T. Spreter, N. Bouromand, N. C. J. Strynadka, J. H. Weiner, *J. Biol. Chem.* **2010**, *285*, 8801–8807; d) A. Messerchmidt, *Handbook of Metalloproteins vol. 5,* John Wiley & Sons, Chichester, UK, **2011**, pp524–532.

[19] a) U. Müh, I. Çinkaya, S. P. J. Albracht, W. Buckel, *Biochemistry* **1996**, *35,* 11710–11718; b) B. M. Martins, H. Dobbek, I. Çinkaya, W. Buckel, A. Messerschmidt, *Proc. Natl. Acad. Sci. USA* **2004**, *101*, 15645–15649; c) A. Messerchmidt, *Handbook of Metalloproteins vol. 4,* John Wiley & Sons, Chichester, UK, **2011**, pp172–182.

[20] a) R. A. Schunn, C. J. Fritchie C. T. Prewitt, *Inorg. Chem.* **1966**, *5*, 892–899; b) C. H. Wei, G. R. Wilkes, P. M. Treichel, L. F. Dahl, *Inorg. Chem.* **1966**, *5*, 900–905.

[21] a) T. Herskovitz, B. A. Averill, R. H. Holm, J. A. Ibers, W. D. Phillips, J. F. Weiher, *Proc. Nat. Acad. Sci. USA* **1972***, 69*, 2437–2441; b) B. A. Averill, T. Herskovitz, R. H. Holm, J. A. Ibers, *J. Am. Chem. Soc.* **1973**, *95*, 3523–3534.

[22] a) L. Que Jr., M. A. Bobrik, J. A. Ibers, R. H. Holm, *J. Am. Chem. Soc.* **1974**, *96*, 4168–4178; b) H. L. Carrell, J. P. Glusker, R. Job, T. C. Bruice, *J. Am. Chem. Soc.* **1977**, *99*, 3683–3690; c) G. Christou, C. D. Garner, M. G. B. Drew, R. Cammack, *J. Chem. Soc., Dalton Trans.* **1981**,

1550–1555; d) P. K. Mascharak, K. S. Hagen, J. T. Spence, R. H. Holm, *Inorg. Chim. Acta* **1983**, *80*, 157–170; e) N. Euyama, T. Sugawara, M. Fuji, A. Nakamura, N. Yasuoka, *Chem. Lett.* **1985**, 175–178; f) T. J. Ollerenshaw, C. D. Garner, B. Odell, W. Clegg, *J. Chem. Soc., Dalton Trans.* **1985**, 2161–2165, g) A. Muller, N. H. Schladerbeck, H. Bogge, *J. Chem. Soc., Chem. Commun.* **1987**, 35–36; h) H. Kambayashi, H. Nagao, K. Tanaka, M. Nakamoto, S.-M. Peng, *Inorg. Chim. Acta* **1993**, *209*, 143–149; i) J. Silver, G. R. Fern, J. R. Miller, C. A. McCammon, D. J. Evans, G. J. Leigh, *Inorg. Chem.* **1999**, *38*, 4256–4261; j) C. Zhou, J. W. Raebiger, B. M. Segal, R. H. Holm, *Inorg. Chim. Acta* **2000**, *300*, 892–902; k) L. M. L. Daku, J. Pecaut, A. Lenormand-Foucaut, B. Vieux-Melchior, P. Iveson, J. Jordanov, *Inorg. Chem.* **2003**, *42*, 6824–6850; l) A. Kern, C. Nather, F. Studt, F. Tuczek, *Inorg. Chem.* **2004**, *43*, 5003–5010; m) Y. Kim, J. Han, *Bull. Korean Chem. Soc.* **2012**, *33*, 48–54; n) D. L. Gerlach, D. Coucouvanis, J. Kampf, N. Lehnert, *Eur. J. Inorg. Chem.* **2013**, 5253–5264.

[23] a) T. O'Sullivan, M. M. Millar, *J. Am. Chem. Soc.* **1985**, *107*, 4096–4097; b) Y. Ohki, K. Tanifuji, N. Yamada, M. Imada, T. Tajima, K. Tatsumi, *Proc. Nat. Acad. Sci. USA* **2011**, *108*, 12635–12640.

[24] a) E. J. Laskowski, R. B. Frankel, W. O. Gillum, G. C. Papaefthymiou, J. Renaud, J. A. Ibers, R. H. Holm, *J. Am. Chem. Soc.* **1978**, *100*, 5322–5337; b) J. M. Berg, K. O. Hodgson R. H. Holm, *J. Am. Chem. Soc.* **1979**, *101*, 4586–4593; c) D. W. Stephan, G. C. Papaefthymiou, R. B. Frankel, R. H. Holm, *Inorg. Chem.* **1983**, *22*, 1550–1557; d) K. S. Hagen. A. D. Watson, R. H. Holm, *Inorg. Chem.* **1984**, *23*, 2984–2990; e) M. J. Carney, G. C. Papafthymiou, K. Spartalian, R. B. Frankel, R. H. Holm, *J. Am. Chem. Soc.* **1988**, *110*, 6084–6095; f) M. J. Carney, G. C. Papaefthymiou, M. A. Whitener, K. Spartalian, R. B. Frankel, R. H. Holm, *Inorg. Chem.* **1988**, *27*, 346–352; g) M. J. Carney, G. C. Papaefthymiou, R. B. Frankel, R. H. Holm, *Inorg. Chem.* **1989**, *28*, 1497–1503; h) B. M. Segal, H. R. Hoveyda, R. H. Holm, *Inorg. Chem.* **1998**, *37*, 3440–3443.

[25] a) Trinh-Toan, W. P. Fehhammer, L. F. Dahl, *J. Am. Chem. Soc.* **1977**, *99*, 402–407; b) Trinh-Toan, B.-K. Teo, J. A. Ferguson, T. J. Meyer, L. F. Dahl, *J. Am. Chem. Soc.* **1977**, *99*, 408–416; c) M. A. Bobrik, K. O. Hodgson, R. H. Holm, *Inorg. Chem.* **1977**, *16*, 1851–1858; d) T. H. Lemmen, J. A. Kocal, F. Y.-K. Lo, M. W. Chen, L. F. Dahl, *J. Am. Chem. Soc.* **1981**, *103*, 1932–1941; e) C. T.-W. Chu, F. Y.-K. Lo, L. F. Dahl, *J. Am. Chem. Soc.* **1982**, *104*, 3409–3422; f) W. E. Cleland, D. A. Holtman, M. Sabat, J. A. Ibers, G. C. DeFoits, B. A. Averil, *J. Am. Chem. Soc.* **1983**, *105*, 6021–6031; g) R. E. Johnson, G. C. Papaefthymiou, R. B. Frankel, R. H. Holm, *J. Am. Chem. Soc.* **1983**, *105*, 7280–7287; h) W. Saak, S. Pohl, *Z. Naturforsch., B: Chem. Sci.* **1985**, *40*, 1105–1112; i) A. Muller, N. H. Schladerbeck, E. Krickemeyer, H. Bogge, K. Schmitz, E. Bill, A. X. Trautwein, *Z. Anorg. Allg. Chem.* **1989**, *570*, 7–36; j) C. Goh, B. M. Segal, J. Huang, J. R. Long, R. H. Holm, *J. Am. Chem. Soc.* **1996**, *118*, 11844–11853; k) N. Zhu, R. Appelt, H.

Vahrenkamp, *J. Organomet. Chem.* **1998**, *565*, 187–192; l) M. Ueda, T. Mochida, *Inorg. Chim. Acta* **2003**, *353*, 306–309, (m) A. Kern, C. Nather, F. Studt, F. Tuczek, *Inorg. Chem.* **2004**, *43*, 5003–5010; n) T .A. Scott, H.-C. Zhou, *Angew. Chem., Int. Ed.* **2004**, *43*, 5628–5631; o) Y. Ohki, Y. Sunada, K. Tatsumi, *Chem. Lett.* **2005**, *34*, 172–173; p) T. A. Scott, C. P. Berlinguette, R. H. Holm, H.-C. Zhou, *Proc. Nat. Acad. Sci. USA* **2005**, *102*, 9741–9744; q) K. S. Hagen, M. Uddin, *Inorg. Chem.* **2008**, *47*, 11807–11815; r) L. Deng, R. H. Holm, *J. Am. Chem. Soc.* **2008**, *130*, 9878–9886; s) C.-C. Tsou, Z.-S. Lin, T.-T. Lu, W.-F. Liaw, *J. Am. Chem. Soc.* **2008**, *130*, 17154–17160; t) C. R. Sharp, J. S. Duncan, S. C. Lee, *Inorg, Chem.* **2010**, *49*, 6697–6705; u) M. G. G. Fuchs, S. Dechert, S. Demeshko, F. Meyer, *Eur. J. Inorg. Chem.* **2010**, 3247–3251.

[26] a) M. G. Kanatzidis, N. C. Baenziger, D. Coucouvanis, A. Simopoulos, A. Kostikas, *J. Am. Chem. Soc.* **1984**, *106*, 4500–4511; b) M. G. Kanatzidis, D. Coucouvanis, A. Simopoulos, A. Kostikas, V. Papaefthymiou, *J. Am. Chem. Soc.* **1985**, *107*, 4925–4935; c) W. Saak, S. Pohl, *Z. Naturforsch., B: Chem. Sci.* **1988**, *43*, 813–817; d) J. A. Weigel, K. K. P. Srivastava, E. P. Day, E. Munck, R. H. Holm, *J. Am. Chem. Soc.* **1990**, *112*, 8015–8023; e) S. Pohl, U. Bierbach, *Z. Naturforsch., B: Chem. Sci.* **1991**, *46*, 68–74; f) U. Bierbach, W. Saak, D. Haase, S. Pohl, *Z. Naturforsch., B: Chem. Sci.* **1991**, *46*, 1629–1634; g) S. Pohl, U. Bierbach, *Z. Naturforsch., B: Chem. Sci.* **1992**, *47*, 1266–1270; h) S. Inomata, K. Hitomi, H. Tobita, H. Ogino, *Inorg. Chim. Acta* **1994**, *225*, 229–238; i) S. Inomata, K. Hiyama, H. Tobita, H. Ogino, *Inorg. Chem.* **1994**, *33*, 5337–5342; j) C. Goh, J. A. Weigel, R. H. Holm, *Inorg. Chem.* **1994**, *33*, 4861–4868; k) M. A. Tyson, K. D. Demadis, D. Coucouvanis, *Inorg. Chem.* **1995**, *34*, 4519–4520; l) F. Osterloh, W. Saak, D. Haase, S. Pohl, *Chem. Commun.* **1996**, 777–778; m) F. Osterloh, W. Saak, S. Pohl, *J. Am. Chem. Soc.* **1997**, *119*, 5648–5656; n) M. Harmjanz, W. Saak, D. Haase, S. Pohl, *Chem. Commun.* **1997**, 951–952; o) J. Han, D. Coucouvanis, *J. Am. Chem. Soc.* **2001**, *123*, 11304–11305; p) J. Han, D. Coucouvanis, *Inorg. Chem.* **2002**, *41*, 2738–2746; q) H.-C. Zhou, R. H. Holm, *Inorg. Chem.* **2003**, *42*, 11–21; r) L. Deng, A. Majumdar, W. Lo, R. H. Holm, *Inorg. Chem.* **2010**, *49*, 11118–11126.

[27] a) T. D. P. Stack, M. J. Carney, R. H. Holm, *J. Am. Chem. Soc.* **1989**, *111,* 1670–1676; b) S. Ciurli, M. Carrié, J. A. Weigel, M. J. Carney, T. D. P. Stack, G. C. Papaefthymiou, R. H. Holm, *J. Am. Chem. Soc.* **1990**, *112,* 2654–2664; c) J. A. Weigel, R. H. Holm, *J. Am. Chem. Soc.* **1991**, *113,* 4184–4191; d) H. Y. Liu, B. Scharbert, R. H. Holm, *J. Am. Chem. Soc.* **1991**, *113,* 9529–9539; e) M. A. Whitener, G. Peng, R. H. Holm, *Inorg. Chem.* **1991**, *30*, 2411–2417; f) D. J. Evans, G. Garcia, G. J. Leigh, M. S. Newton, M. D. Santana, *J. Chem. Soc., Dalton Trans.* **1992**, 3229–3234; g) L. Cai, R. H. Holm, *J. Am. Chem. Soc.* **1994**, *116*, 7177–7188; h) G. P. F. van Strijdonck, J. A. E. H. van Haare, J. G. M. van der Linden, J. J. Steggerda, R. J. M. Nolte, *Inorg. Chem.* **1994**, *33*, 999–1000; i) C. Zhou, L. Cai, R. H. Holm, *Inorg. Chem.* **1996**, *35,* 2767–2772;

j) G. P. F. van Strijdonck, J. A. E. H. van Haare, P. J. M. Hönen, R. C. G. M. van den Schoor, M. C. Feiters, J. G. M. van der Linden, J. J. Steggerda, R. J. M. Nolte, *J. Chem. Soc., Dalton Trans.* **1997**, 449–461; k) J. E. Barclay, M. I. Diaz, D. J. Evans, G. Garcia, M. D. Santana, M. C. Torralba, *Inorg. Chim. Acta* **1997**, *258*, 211–219; l) G. P. F. van Strijdonck, P. T. J. H. ten Have, M. C. Feiters, J. G. M. van der Linden, J. J. Steggerda, R. J. M. Nolte, *Chem. Ber./Recueil* **1997**, *130,* 1151–1157; m) P. V. Rao, R. H. Holm, *Chem. Rev.* **2004**, *104*, 527–559; n) C. Tard, X. Liu, S. K. Ibrahim, M. Bruschi, L. D. Gioia, S. C. Davies, X. Yang, L.-S. Wang, G. Sawers, C. J. Pickett, *Nature* **2005**, *433*, 610–613; o) E. P. L. van der Geer, G. van Koten, R. J. M. K. Gebbink, B. Hessen, *Inorg. Chem.* **2008**, *47*, 2849–2857, p) D. L. Gerlach, D. Coucouvanis, N. Lehnert, *Eur. J. Inorg. Chem.* **2013**, 3883–3890.

[28] a) T. D. P. Stack, R. H. Holm, *J. Am. Chem. Soc.* **1987**, *109,* 2546–2547; b) T. D. P. Stack, R. H. Holm, *J. Am. Chem. Soc.* **1988**, *110*, 2484–2494; c) C. Zhou, R. H. Holm, *Inorg. Chem.* **1997**, *36,* 4066–4077; d) P. V. Rao, S. Bhaduri, J. Jiang, D. Hong, R. H. Holm, *J. Am. Chem. Soc.* **2005**, *127*, 1933–1945; e) R. Panda, C. P. Berlinguette, Y. Zhang, R. H. Holm, *J. Am. Chem. Soc.* **2005**, *127*, 11092–11101; f) J. Sun, C. Tessier, R. H. Holm, *Inorg. Chem.* **2007**, *46*, 2691–2699.

[29] C. Walsdorff, W. Saak, S. Pohl, *J. Chem. Soc., Dalton Trans.* **1997**, 1857–1861.

Chapter 2

Preparation of Tridentate Thiolate Ligands $TempS_3^{3-}$ and $TefpS_3^{3-}$ and Synthesis of [4Fe-4S] Cluster Having a Tridentate Thiolate and a Ethanethiolate/Benzenethiolate/ Hydrosulfide Ligands

2.1 Introduction

[3:1] Site-differentiated [4Fe-4S] clusters carrying one non-cysteine ligand attract much attention due to their biological significance, described as chapter 1.[1] However, details of their chemistry have not been established, and studies of synthetic analogues are needed. A common method to synthesize site-differentiated clusters is to introduce a tridentate thiolate ligand. Along with previous approach,[2-5] we extended the scope of the synthesis of site-differentiated [4Fe-4S] clusters by designing the new tripodal trithiols $Temp(SH)_3$ (**1a**) and $Tefp(SH)_3$ (**1b**) shown in Figure 2-1. Although the use of tripodal trithiol is the same as previous strategy,[2,3] the new ligands have advantage in that they can be prepared easily in short steps, and in that they tend to give crystalline [4Fe-4S] clusters suitable for X-ray structural analysis. This property is notable because detailed structural knowledge of biologically significant molecules aids in understanding their enzymatic roles. In this chapter, the author reports the synthesis and structures of the $[4Fe\text{-}4S]^{2+}$ clusters with EtS^-, PhS^-, HS^- as unique ligands, and double cubane clusters bridged by S^{2-} at the unique iron sites. Their redox properties have also been investigated.

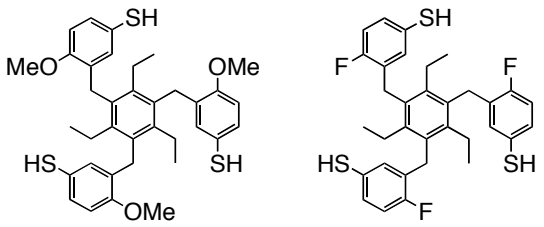

$Temp(SH)_3$ (**1a**) $Tefp(SH)_3$ (**1b**)

Figure 2-1. The tripodal trithiols.

2.2 Results

2.2.1 Preparation of the trithiols Temp(SH)$_3$ (1a) and Tefp(SH)$_3$ (1b)

The tripodal trithiols were designed according to the following requirements: (i) three thiol units are arranged to hold a [4Fe-4S] cubane core naturally, (ii) the arrangement of the three thiols are pre-organized so as to avoid the formation of polymeric products during the encapsulation of the [4Fe-4S] cluster, (iii) the ligand is semi-flexible and facilely affording the products as crystals suitable for X-ray analysis, and (iv) the synthetic route to the ligands is convenient. To achieve semi-flexibility, the trithiols Temp(SH)$_3$ (**1a**) and Tefp(SH)$_3$ (**1b**) are composed of arene units. Each basal arene is bonded to three mercaptobenzyl units at the 1,3,5-positions and to three ethyl groups at 2,4,6. This alternating substitution encourages the six substituents to adopt an *ababab* arrangement to avoid steric crowding. The methoxy groups and the fluorides on the mercaptobenzyl units hinder rotation of the mercaptoarenes and favor the orientation with the methoxy groups and the fluorines pointing outward.[6] Accordingly, the three thiols are lined up so as to capture an [4Fe-4S] core as was the case for the tridentate ligands reported by Holm and Pohl.[2,4]

The synthetic routes to the ligands **1a**,**b** are shown in Scheme 2-1. The basal arene component 1,3,5-triethyl-2,4,6-triformylbenzene[7] was reacted with 3 equiv of 4-bromo-2-lithioanisole prepared by treatment of 2,4-dibromoanisole with butyllithium, which gave the benzyl alcohol compound **2a** as a diastereomeric mixture.[8] Compound **2b** was also obtained similarly using 4-bromo-2-lithiofluorobenzene prepared from 4-bromofluorobenzene and lithium diisopropylamide.[9] After removal of all of the OH groups of **2a**,**b** by treatment with triethylsilane and borontrifluoride etherate,[10] the bromides of **3a**,**b** were lithiated by butyllithium, followed by treatment with elemental sulfur. After addition of $LiAlH_4$, the reaction was quenched by aqueous HCl, which afforded the trithiol **1a**,**b**.[11] X-ray analysis of **1b** confirms the substituents are arranged as expected (Figure 2-2).

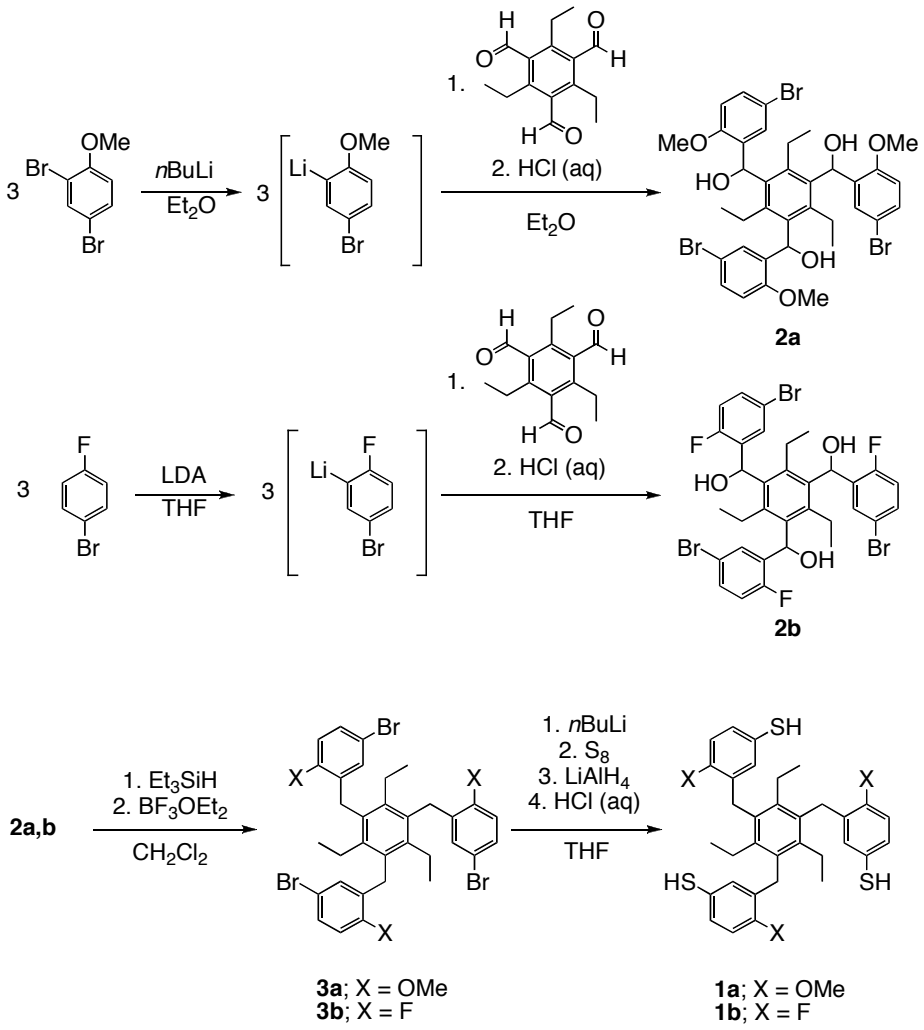

Scheme 2-1. Synthesis of Temp(SH)$_3$ (**1a**) and Tefp(SH)$_3$ (**1b**).

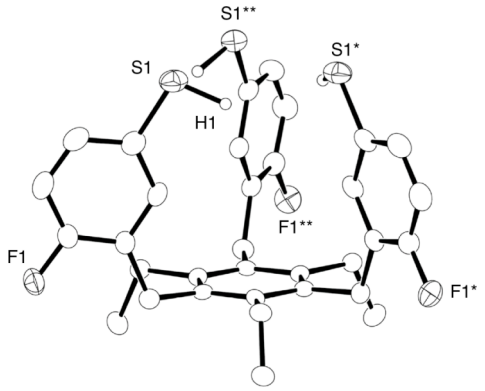

Figure 2-2. Molecular structure of Tefp(SH)$_3$ (**1b**) with 40% thermal ellipsoids. Hydrogen atoms except for H1 are omitted for clarity.

2.2.2 Synthesis and structures of $(PPh_4)_2[Fe_4S_4(SEt)(TempS_3)]$ (4a) and $(PPh_4)_2[Fe_4S_4(SEt)(TefpS_3)]$ (4b)

The trithiols **1a** and **1b** dissolved in THF were added dropwise to acetonitrile solutions of $(PPh_4)_2[Fe_4S_4(SEt)_4]$[12] at r.t., and the solutions were slowly evacuated to give the clusters $(PPh_4)_2[Fe_4S_4(SEt)(TempS_3)]$ (**4a**) and $(PPh_4)_2[Fe_4S_4(SEt)(TefpS_3)]$ (**4b**) as black powders in 90% and 87% yields, respectively (Scheme 2-2). In these reactions, thiolate exchange proceeded smoothly because of the higher acidity of the arenethiols in **1a**,**b**, the higher volatility of the leaving ethanethiol, and the entropy of the chelate effect.

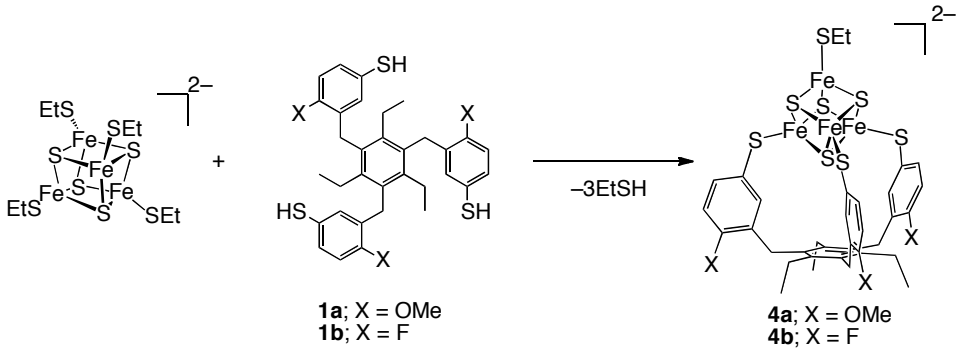

Scheme 2-2. Synthesis of **4a**,**b**.

Layering hexane and ether on the acetonitrile solutions of **4a**,**b** afforded black crystalline plate, allowing their molecular structures to be elucidated by X-ray analysis (Figure 2-3). The tridentate ligands are coordinated to the [4Fe-4S] cores at three irons, and the unique iron sites are occupied by ethanethiolate. The metric parameters of the cubane cores in Table 2-1 resemble those of other reported $[4Fe\text{-}4S]^{2+}$ clusters coordinated by four thiolates such as $[Fe_4S_4(SCH_2C_6H_5)_4]^{2-}$.[12-15] Although in cluster **4a** the Fe-Fe bonds around the unique Fe1 site could be slightly longer than the other Fe-Fe bonds, a similar short/long Fe-Fe bond alternation is often observed, as in $(NEt_4)_2[Fe_4S_4(SCH_2C_6H_5)_4]$ for example,[12] and the geometry of the unique irons of **4a**,**b** is unexceptional. Thus, these tridentate ligands are able

to hold an [4Fe-4S] cluster core without causing significant distortion. While the structures of **4a** and **4b** are alike, a significant difference exists between the Fe-S(thiolate) distances. The Fe1–S8 bond of **4b** is somewhat shorter than that of **4a**, whereas the Fe2–S5 and Fe3–S6 bonds of **4b** are significantly longer than the corresponding bonds of **4a**. These structural properties could be attributable to the electron-withdrawing nature of the fluorides in **4b**, which weaken the coordination of the $TefpS_3^{3-}$ ligand to the [4Fe-4S] core, and accordingly the ethanethiolate coordination would become stronger.

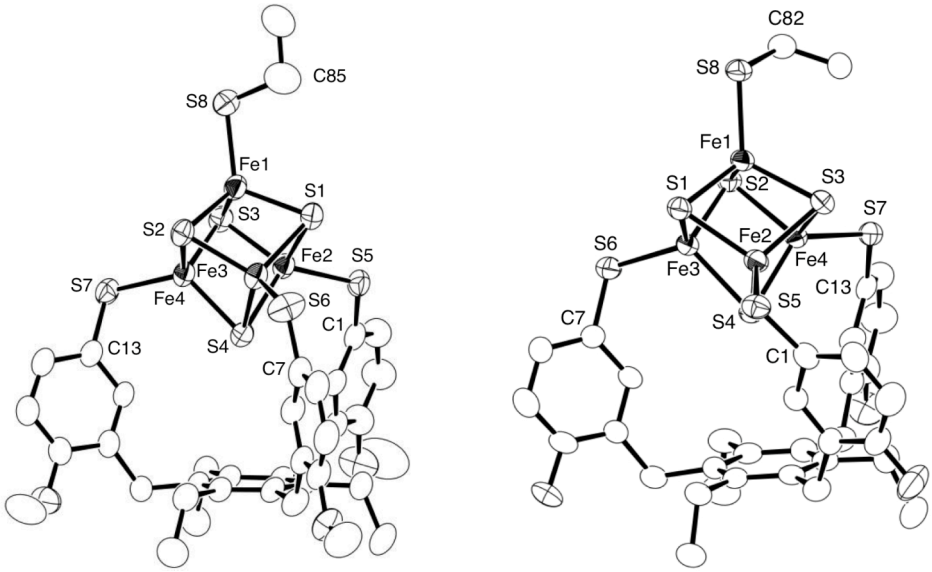

4a **4b**

Figure 2-3. Molecular structures of the anions of **4a** (left) and **4b** (right) with 50% thermal ellipsoids. Hydrogen atoms and the disordered CH_3 group of the ethanethiolate of **4a** are omitted for clarity.

2.2.3 Reaction of 4a,b with benzenethiol

When cluster **4a**,**b** were treated with 1 equiv benzenethiol in acetonitrile, thiolate exchange took place at the unique iron, and the benzenethiolate clusters $(PPh_4)_2[Fe_4S_4(SPh)(TempS_3)]$ (**5a**), $(PPh_4)_2[Fe_4S_4(SPh)(TefpS_3)]$ (**5b**) were obtained as black crystals in 46% and 74% yield, respectively (Scheme 2-3). The success of these site-selective

reactions are attributable to the chelate effect of the tridentate ligands, and in these particular cases, to the higher acidity of benzenethiol and the higher volatility of ethanethiol.

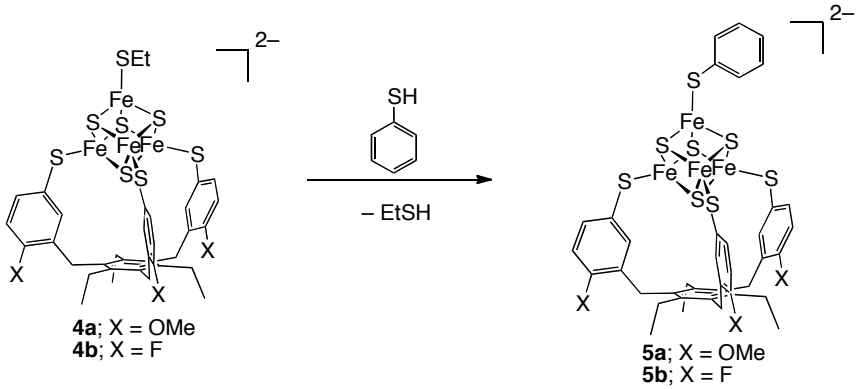

Scheme 2-3. Synthesis of **5a**,**b**.

The molecular structures of **5a**,**b** were analyzed by X-ray crystallography. As shown in Figure 2-4 and Table 2-1, the metrical parameters of these clusters are almost identical to those of **4a**,**b** and other common $[4Fe\text{-}4S]^{2+}$ clusters having four thiolates.[12-15] The parameters around the unique irons are also similar to those of the reported benzenethiolate cluster $[Fe_4S_4(SPh)_4]^{2-}$.[14]

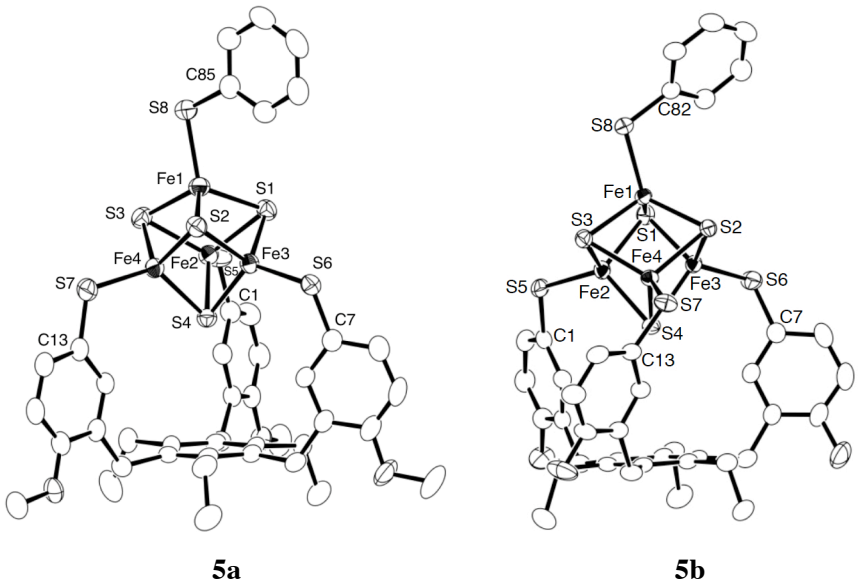

5a **5b**

Figure 2-4. Molecular structures of the anion of **5a**,**b** with 50% thermal ellipsoids. Hydrogen atoms are omitted for clarity.

Table 2-1. Selected bond distances (Å) and angles (deg) for **4a**,**b** and **5a**,**b**.

	4a	**4b**	**5a**	**5b**
Fe1-Fe2	2.7399(10)	2.7349(12)	2.7081(11)	2.7569(8)
Fe1-Fe3	2.7585(11)	2.7183(12)	2.7322(11)	2.7624(7)
Fe1-Fe4	2.7382(13)	2.7226(12)	2.7181(11)	2.6927(8)
Fe2-Fe3	2.6891(8)	2.7344(12)	2.7599(11)	2.7161(9)
Fe2-Fe4	2.7202(10)	2.7106(13)	2.7616(12)	2.7307(8)
Fe3-Fe4	2.7301(9)	2.7208(13)	2.7572(11)	2.7130(9)
Fe1-S1	2.2205(12)	2.2306(18)	2.2667(16)	2.2684(10)
Fe1-S2	2.3283(15)	2.3051(17)	2.2704(16)	2.2734(10)
Fe1-S3	2.3041(12)	2.3205(17)	2.2900(16)	2.3175(9)
Fe2-S1	2.3179(15)	2.3036(17)	2.3005(16)	2.3322(10)
Fe2-S3	2.2545(12)	2.2344(17)	2.2763(15)	2.2694(10)
Fe2-S4	2.3052(15)	2.3124(17)	2.2783(14)	2.2826(9)
Fe3-S1	2.323(2)	2.3106(18)	2.2818(15)	2.2880(10)
Fe3-S2	2.2577(12)	2.2262(17)	2.2776(15)	2.2646(9)
Fe3-S4	2.3060(13)	2.3157(17)	2.2967(15)	2.3066(9)
Fe4-S2	2.3164(12)	2.3100(17)	2.3026(16)	2.3112(9)
Fe4-S3	2.3045(14)	2.3038(17)	2.2729(15)	2.2943(9)
Fe4-S4	2.2400(11)	2.2444(17)	2.2769(14)	2.2728(9)
Fe1-S8	2.2586(18)	2.2483(18)	2.2668(16)	2.2906(9)
Fe2-S5	2.2493(12)	2.2675(18)	2.2578(17)	2.2626(10)
Fe3-S6	2.2529(14)	2.2719(19)	2.2764(15)	2.2768(10)
Fe4-S7	2.2706(15)	2.2740(18)	2.2512(17)	2.2503(9)
Fe1-S8-C82	–	104.0(3)	–	108.17(10)
Fe1-S8-C85	105.5(3)	–	106.29(19)	–
Fe2-S5-C1	111.78(16)	100.9(2)	114.20(17)	114.99(10)
Fe3-S6-C7	120.70(13)	111.2(2)	114.99(18)	110.38(10)
Fe4-S7-C13	106.60(13)	108.3(2)	115.41(18)	102.46(10)

2.2.4 Redox properties of 4a,b and 5a,b

The redox behavior of clusters **4a**,**b** and **5a**,**b** were investigated by cyclic voltammetry in acetonitrile. The data are summarized in Table 2-2, and their CV spectra are representatively shown in Figure 2-5. Each cluster shows one reversible redox couple attributable to the $[4Fe\text{-}4S]^{2+}/[4Fe\text{-}4S]^{+}$ process.[16] Their half-wave potentials $E_{1/2}$ are in the range of reported values for $[4Fe\text{-}4S]^{2+}$ clusters having four thiolates.[2c,3c,17] The redox potentials reflect the electronic properties of the tridentate ligands. The $E_{1/2}$ values of the $TefpS_3^{3-}$ clusters **4b**,**5b** exhibited significantly more positive values compared to that of the corresponding $TempS_3^{3-}$ clusters **4a**,**5a**, in accord with the less electron-donating nature of the $TefpS_3^{3-}$ ligand and with their observed structural differences. The substituents on the unique iron sites also affect the potential; the benzenethiolate clusters **5a**,**b** exhibit more positive $E_{1/2}$ values than the ethanethiolate clusters **4a**,**b**. This trend is consistent with the positive potential shift of $[Fe_4S_4(SPh)_4]^{2-}$ by 0.32 V from that of $[Fe_4S_4(SEt)_4]^{2-}$.[17c] The CV of **4a** and **5a** in THF were also measured (Figure 2-6). Interestingly, both clusters show one oxidation wave and two reduction waves, which are attributable to the $[4Fe\text{-}4S]^{2+}/[4Fe\text{-}4S]^{3+}$, $[4Fe\text{-}4S]^{2+}/[4Fe\text{-}4S]^{+}$, and $[4Fe\text{-}4S]^{+}/[4Fe\text{-}4S]^{0}$ processes, though irreversible waves were observed at $E_{pa} = -2.18$ V. They are different from the CV in acetonitrile. The observation of multi-electron process in THF would be due to the stability of $[4Fe\text{-}4S]^{3+}$ and $[4Fe\text{-}4S]^{0}$ state in THF, and due to the less reactivity of THF. The potentials in THF are more negative than those in acetonitrile, resemble to CV of $[Fe_4S_4(SPh)_4]^{2-}$.[17b]

Table 2-2. Redox potentials of clusters **4a**,**b** and **5a**,**b**.[a]

	solvent	E_{pa} / V	E_{pc} / V	$E_{1/2}$ / V
4a	CH_3CN	–1.53	–1.45	–1.49
4b	CH_3CN	–1.47	–1.39	–1.43
5a	CH_3CN	–1.46	–1.39	–1.43
5b	CH_3CN	–1.39	–1.29	–1.35
4a	THF	–0.53	–0.39	–0.46
		–1.70	–1.56	–1.63
		–2.44	–2.27	–2.36
5a	THF	–0.45	–0.33	–0.39
		–1.64	–1.51	–1.58
		–2.39	–2.20	–2.30

[a] The data were recorded in 0.1 M *n*-Bu_4NPF_6 solution (CH_3CN or THF) with glassy carbon working electrode, a Pt counter electrode, and a $Ag/AgNO_3$ reference electrode. The scan rate was 0.1 Vs^{-1}.

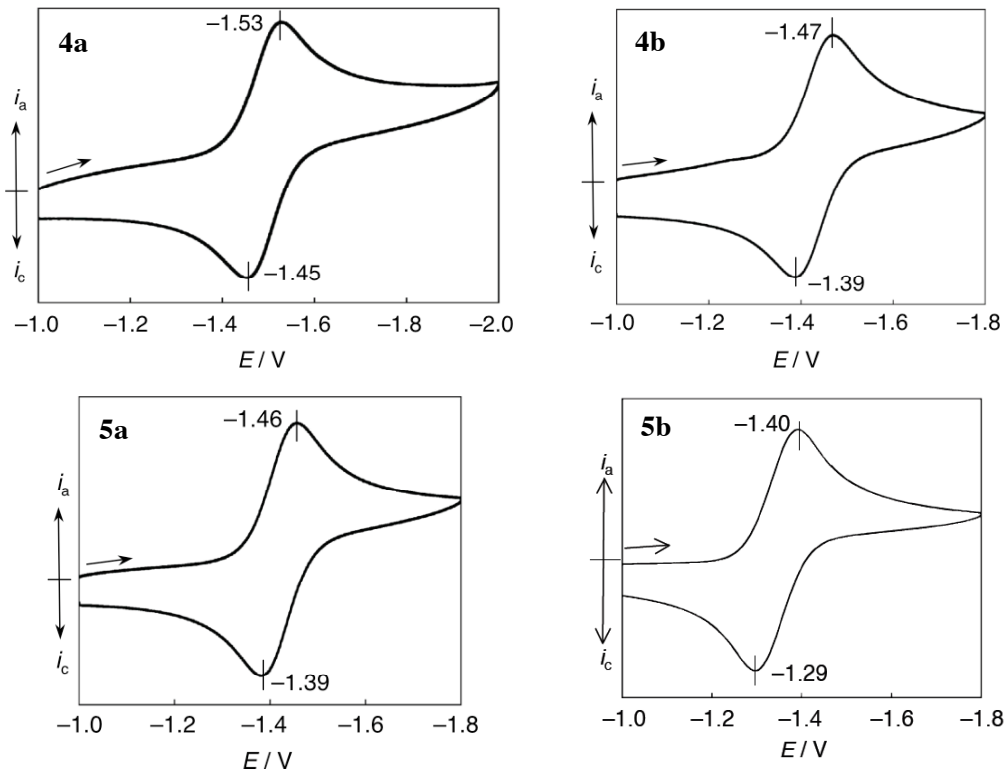

Figure 2-5. CV spectra of **4a**, **4b**, **5a**, and **5b** in acetonitrile.

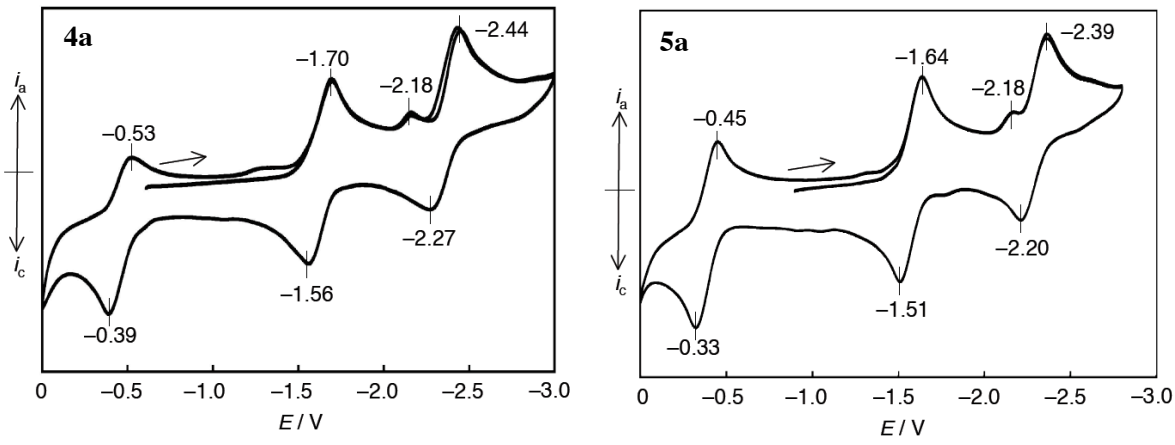

Figure 2-6. CV spectra of **4a** and **5b** in THF.

2.2.5 Reactions of 4a,b with H_2S

A [4Fe-4S] cluster with an HS^- ligand would provide a plausible active site model for the cluster included in the β-subunit of (*R*)-2-hydroxyisocaproyl-CoA dehydratase.[1g] Although a related hydrosulfide cluster $[Fe_4S_4(SH)(LS_3)]^{2-}$ has been reported by Holm,[3ce] its molecular structure has not been characterized. The author attempted the reaction of the ethanethiolate clusters **4a** and **4b** with 5 equiv of H_2S in acetonitrile respectively, and confirmed the formation of the hydrosulfide clusters $(PPh_4)_2[Fe_4S_4(SH)(TempS_3)]$ (**6a**) and $(PPh_4)_2[Fe_4S_4(SH)(TefpS_3)]$ (**6b**) by ESI-TOF-MS spectra (Scheme 2-4). However, upon removal of the solvent, the mass spectral signals of **6a**,**b** obviously became weak, and crystallization gave the sulfido-bridged double cubane clusters $(PPh_4)_4[\{Fe_4S_4(TempS_3)\}_2(\mu^2\text{-}S)]$ (**7a**) and $(PPh_4)_4[\{Fe_4S_4(TefpS_3)\}_2(\mu^2\text{-}S)]$ (**7b**) in 50% and 37% yields, respectively. Clusters **7a**,**b** can be formed via an intermolecular condensation of **6a**,**b** with release of the gaseous H_2S. This process is reversible, and thus addition of 5 equiv of H_2S to **7a** and **7b** in acetonitrile resulted in the formation of **6a** and **6b** respectively as detected by mass spectra.[18]

In order to isolate **6a**,**b**, the crude products obtained by the reactions of **4a**,**b** with H_2S

were treated with 5 equiv of H_2S in acetonitrile, followed by layering with hexane and ether. The hydrosulfide clusters **6a** and **6b** were obtained as crystalline black plates in 70% and 54% yields, respectively, and the structures were confirmed by X-ray analysis.

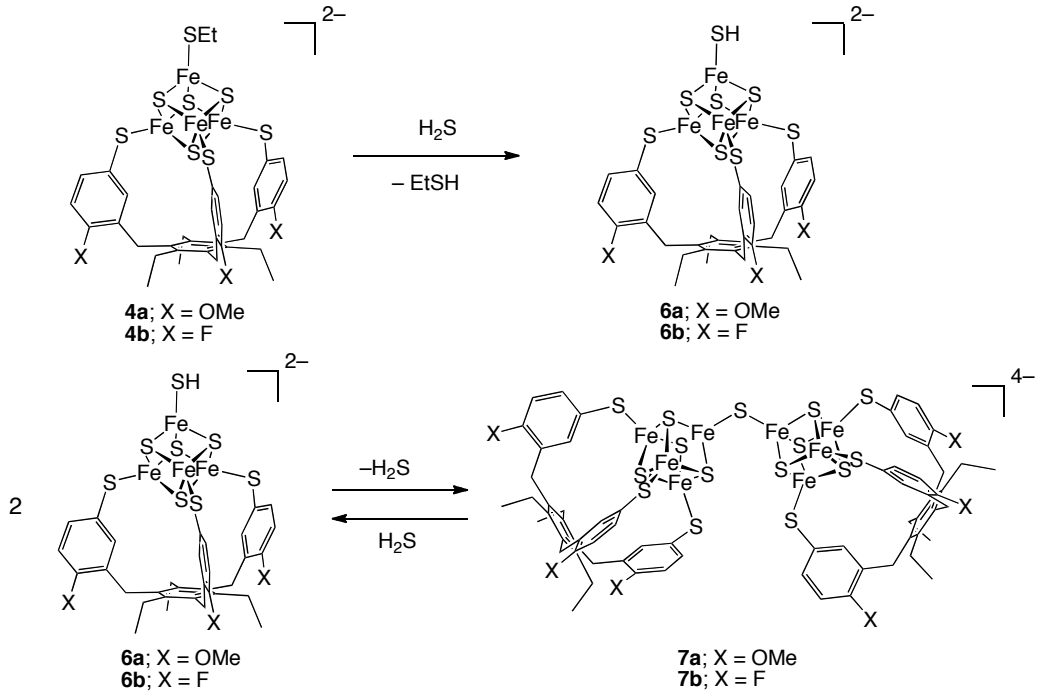

Scheme 2-4. Synthesis of **6a**,**b** and **7a**,**b**.

2.2.6 Molecular structures of 6a,b and 7a,b

The molecular structures of the hydrosulfide clusters **6a**,**b** and the double cubane clusters **7a**,**b** were analyzed by X-ray crystallography. As shown in Figures 2-7, 2-8, and Table 2-3, the [4Fe-4S] core structures are normal, and the metric parameters compare well with those of **4a**,**b** as well as typical common $[4Fe\text{-}4S]^{2+}$ clusters coordinated by four thiolates.[12-15] The Fe-S(H) bond distances in the hydrosulfide clusters **6a**,**b**, are also similar to those of $(PPh_4)_2[Fe_4S_4(SH)_4]$ (2.256(4), 2.269(5) Å).[15]

Clusters **6a** and **6b** can be considered good models of the [4Fe-4S] cluster in the β-subunit of (*R*)-2-hydroxyisocaproyl-CoA dehydratase, which is coordinated by three cysteine

thiolates and one sulfur ligand, a hydrosulfide or a sulfide. In the enzyme, the distance between the sulfur ligand S and the Fe is 2.3 Å, and this value is similar or slightly longer than the corresponding Fe-SH distances of **6a**,**b**. These data are consistent with the assignment of hydrosulfide as the sulfur ligand in the dehydratase as suggested by Dobbek *et al*.[1g]

Clusters **7a** and **7b** in Figure 2-8 are composed of the two [4Fe-4S] cluster cores bridged by a sulfide. A notable structural difference between **7a** and **7b** is the central μ-sulfide geometry. In cluster **7a**, the Fe1-S8-Fe1* bond is typically bent with 109.7(2)° as observed for the thiolate sulfurs of **4a** and **5a**, and this geometry is also found in the related double-cubane cluster $(n\text{-}Bu_4N)_2(PPh_4)_2[(Fe_4S_4Cl_3)_2(\mu^2\text{-}S)]$ and $(n\text{-}Bu_4N)_4[\{Fe_4S_4(SPy)_3\}_2(\mu^2\text{-}S)]$ reported by Coucouvanis *et al*.[19] However, the corresponding bond angle of **7b** is considerably wider, being close to linear, 161.7(2)°, and the Fe1-S8 bond is shorter by 0.06-0.07 Å from that of **7a**. These structural features are probably result from crystal packing. Acetonitrile molecules located near the $Fe_4S_4(TempS_3)$ units form hydrogen bond networks, stabilizing the crystal structure of **7b**.

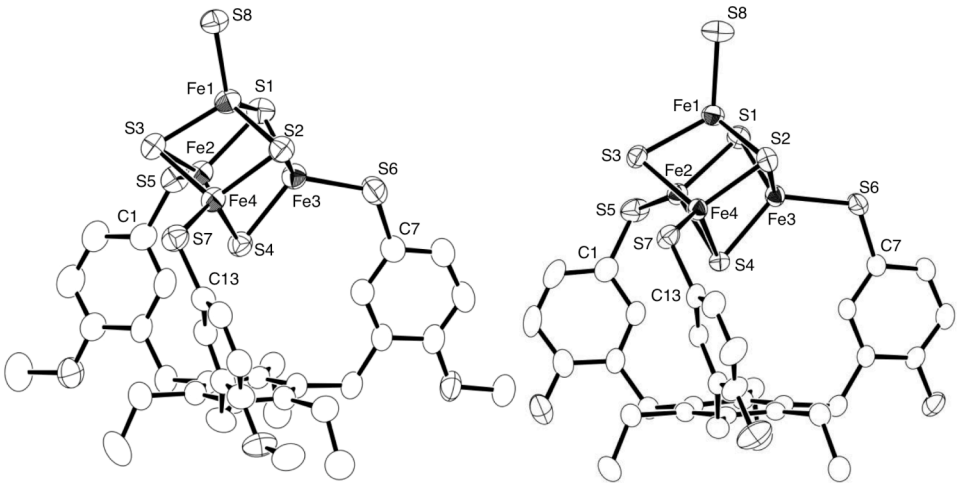

6a **6b**

Figure 2-7. Molecular structures of the anions of **6a**, **6b** with 50% thermal ellipsoids. Hydrogen atoms are omitted for clarity.

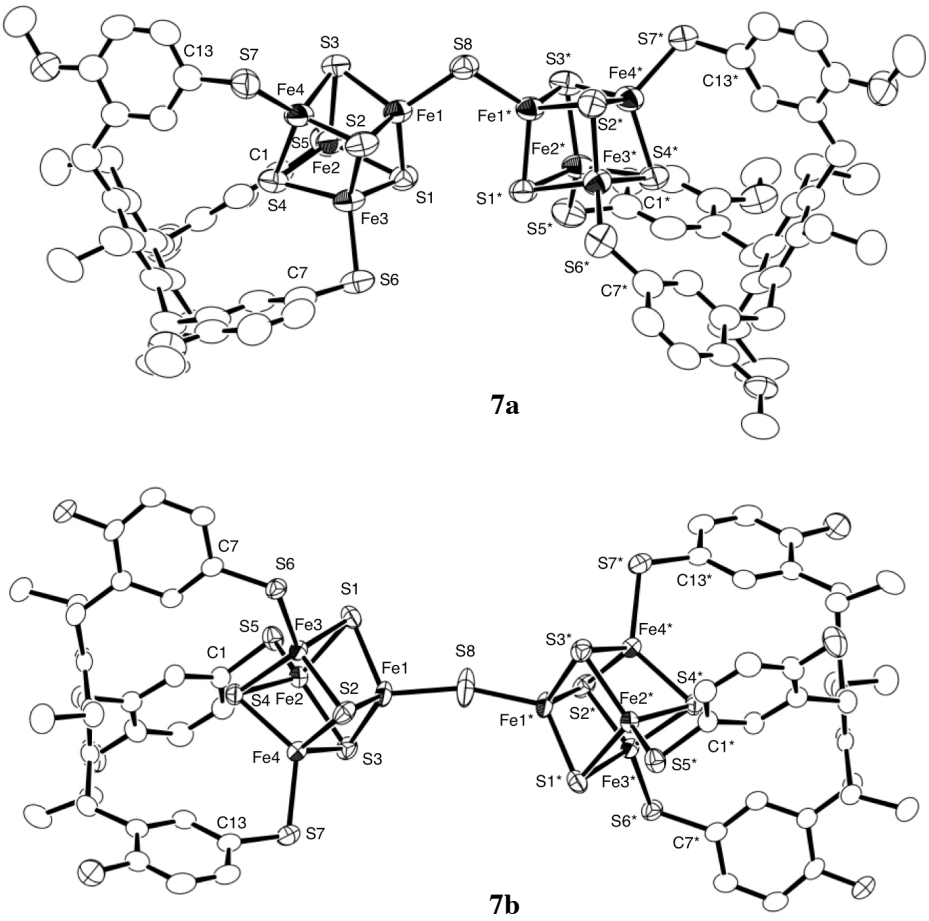

Figure 2-8. Molecular structures of the anions of **7a**, **7b** with 50% thermal ellipsoids. Hydrogen atoms and the disordered S8* of **7b** are omitted for clarity.

Table 2-3. Selected bond distances (Å) and angles (deg) of **6a**,**b**, and **7a**,**b**.

	6a	**6b**	**7a**	**7b**
Fe1-Fe2	2.7433(13)	2.7534(9)	2.8150(10)	2.7340(15)
Fe1-Fe3	2.7612(12)	2.7680(8)	2.7680(11)	2.7257(19)
Fe1-Fe4	2.7387(13)	2.7491(8)	2.7484(11)	2.7374(15)
Fe2-Fe3	2.6877(12)	2.7291(9)	2.7220(10)	2.7082(14)
Fe2-Fe4	2.7260(12)	2.7375(9)	2.7124(10)	2.7173(12)
Fe3-Fe4	2.7275(12)	2.7356(7)	2.7140(10)	2.7376(19)
Fe1-S1	2.2286(19)	2.2557(10)	2.2719(14)	2.2489(18)
Fe1-S2	2.3189(18)	2.3010(11)	2.2813(16)	2.2996(16)
Fe1-S3	2.3034(19)	2.2921(11)	2.3259(15)	2.3121(18)
Fe2-S1	2.3111(19)	2.2727(10)	2.3074(16)	2.3021(17)
Fe2-S3	2.2571(18)	2.2623(10)	2.2876(15)	2.2504(19)
Fe2-S4	2.3000(18)	2.3095(10)	2.2476(17)	2.3072(16)
Fe3-S1	2.3056(18)	2.2992(10)	2.2424(17)	2.3052(15)
Fe3-S2	2.2605(18)	2.2531(10)	2.2951(15)	2.2235(18)
Fe3-S4	2.2999(18)	2.2787(10)	2.3147(16)	2.3077(16)
Fe4-S2	2.3079(19)	2.2717(11)	2.3201(15)	2.2857(17)
Fe4-S3	2.2967(18)	2.3139(11)	2.2722(16)	2.3122(17)
Fe4-S4	2.2377(17)	2.2629(9)	2.2812(15)	2.2464(19)
Fe1-S8	2.2418(18)	2.2669(12)	2.2130(13)	2.135(9), 2.150(9)
Fe2-S5	2.2459(18)	2.2681(12)	2.2688(16)	2.2667(16)
Fe3-S6	2.245(3)	2.2775(11)	2.2679(17)	2.2744(17)
Fe4-S7	2.2611(19)	2.2683(9)	2.2653(17)	2.2618(17)
Fe1-S8-Fe1*	–	–	109.66(8)	161.7(3)
Fe1-S8-C85	–	–	–	–
Fe2-S5-C1	109.5(2)	101.57(13)	117.60(19)	101.19(15)
Fe3-S6-C7	121.6(3)	115.91(11)	103.95(19)	114.36(17)
Fe4-S7-C13	106.8(2)	109.36(10)	106.87(18)	107.52(12)

2.2.7 Redox properties of 6a,b and 7a,b

The redox potentials of clusters **6a**,**b** and **7a**,**b** recorded in acetonitrile are summarized in Table 2-4.[16] Their CV spectra are representatively shown in Figure 2-9. As was the case for the ethanethiolate clusters **4a**,**b**, the hydrosulfide clusters **6a**,**b** each show one reversible couple. The potentials $E_{1/2}$ of **6a** (–1.48 V) and **6b** (–1.40 V) also compare well with those of **4a** and **4b** respectively, indicating that the electron-donor properties of hydrosulfide and ethanethiolate are similar.

The double cubane clusters **7a** and **7b** exhibits two reversible redox couples (**7a**; $E_{1/2}$ = –1.66, –1.87 V, **7b**; $E_{1/2}$ = –1.55, –1.74 V) attributable to the couples of $\{[4Fe\text{-}4S]_2\}^{4+}/\{[4Fe\text{-}4S]_2\}^{3+}$ and $\{[4Fe\text{-}4S]_2\}^{3+}/\{[4Fe\text{-}4S]_2\}^{2+}$ states. The data show that there is an electronic interaction between the two intramolecular [4Fe-4S] cores. The first reduction of **7a** and **7b** occurs at a considerably more negative potential compared to those of **6a** and **6b**, probably due to the increased negative net charges on the [4Fe-4S] cores. These features are common to the similar μ-S double cubanes $\{[Fe_4S_4(LS_3)]_2(\mu\text{-}S)\}^{4-}$ reported by Holm *et al*.[3a,3c]

Table 2-4. Redox potentials of clusters **6a**,**b** and **7a**,**b**.[a]

	E_{pa} / V	E_{pc} / V	$E_{1/2}$ / V
6a	–1.53	–1.44	–1.48
6b	–1.43	–1.36	–1.40
7a	–1.69	–1.62	–1.66
	–1.92	–1.82	–1.87
7b	–1.58	–1.51	–1.55
	–1.78	–1.70	–1.74

[a] The data were recorded in 0.1 M n-Bu_4NPF_6 solution (CH_3CN) with glassy carbon working electrode and Pt counter electrode and $Ag/AgNO_3$ reference electrode. The scan rate was 0.1 Vs^{-1}.

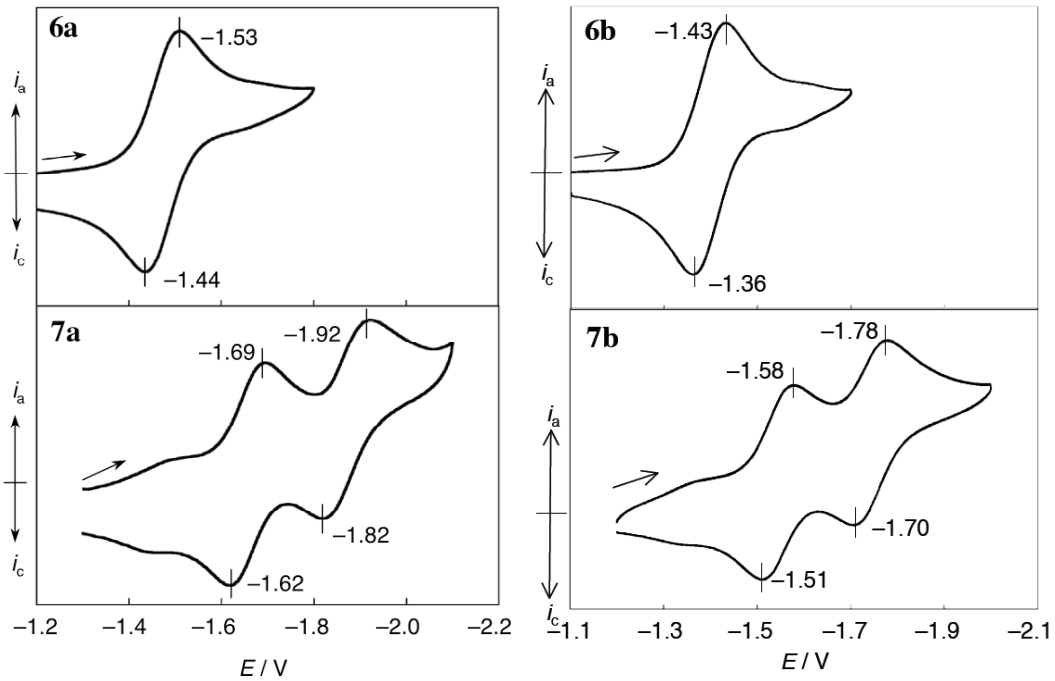

Figure 2-9. CV spectra of **6a**, **7a** and **6b**, **7b**.

2.3 Discussion

As indicated by the similar redox potentials of **6a**,**b** and **4a**,**b**, proteins with [4Fe-4S] clusters having a hydrosulfide or an ethanethiolate could function similarly in electron relay systems. This result begs the question why does the [4Fe-4S] cluster in the β-subunit of (*R*)-2-hydroxyisocaproyl-CoA dehydratase have a hydrosulfide ligand instead of the common cysteine thiolate. Because the β-subunit of the dehydratase is proposed to both donate an electron to the catalytic site in the α-subunit and accept an electron from it, the hydrosulfide cluster could have a tunable redox potential. Hydrogen bonding of the SH group would provide a possible tuning mechanism.[20] However, in this particular enzyme the hydrosulfide cluster in the β-subunit is located in a hydrophobic pocket and there is no hydrogen bonding

of the SH group with the protein matrix according to the crystal structure,[1g] and the role of the SH group is not clear, although the protein could change the conformation allowing hydrogen bonding.

2.4 Summary

The author has synthesized two new trithiols $Temp(SH)_3$ and $Tefp(SH)_3$, and demonstrated that they are suited for the production of [3:1] site-differentiated [4Fe-4S] clusters. Three such clusters, those with ethanethiolate, benzenethiolate, and hydrosulfide at the unique iron sites have been produced. As all these clusters were obtained as single crystals suitable for X-ray structural analysis, these tridentate ligands are useful for model studies of the various site-differentiated [4Fe-4S] clusters in organisms as demonstrated by the hydrosulfide clusters modeling that in the (*R*)-2-hydroxyisocaproyl-CoA dehydratase β-subunit.

2.5 Experimental Section

General:

All air-sensitive compounds were handled under an atmosphere of pure nitrogen gas using standard Schlenk techniques or glove boxes. Hexane, ether, acetonitrile, dichloromethane, THF, DMF, methanol, and ethanol were degassed and purified by the method described by Grubbs, in which the solvents were passed over columns of activated alumina and a copper catalyst supplied by Hansen & Co., Ltd. ^{1}H NMR spectra were acquired by using a JEOL ECA-600. NMR assignments were supported by additional 2D NMR experiments. Cyclic Voltammograms were recorded on a BAS-ALS-660B electron analyzer using a glassy carbon working electrode and 0.1 M (CH_3CN, CH_2Cl_2, DMF, DMSO) or 0.2 M (THF) *n*-Bu_4NPF_6 as the supporting electrolyte, and the potentials are referenced to the $Ag/AgNO_3$ electrode. Electrospray ionization time-of-flight mass spectrometry (ESI-TOF-MS) spectra were obtained from a Micromass LCT TOF-MS spectrometer. Elemental analyses were performed on a LECO-CHNS-932 elemental analyzer where the samples were sealed in silver capsules under nitrogen. 1,3,5-triethyl-2,4,6-triformylbenzene[7] and $(PPh_4)_2[Fe_4S_4(SEt_4)]$[12] were synthesized according to literature procedures.

Synthesis:

1,3,5-Tris(5-bromo-2-methoxyphenylhydroxymethyl)-2,4,6-triethylbenzene (2a): At –70 ºC, *n*-BuLi (1.7 M solution in hexane, 27 mL, 43 mmol) was added dropwise to 2,4-dibromoanisole (11 g, 43 mmol) in ether (90 mL). After stirring for 30 min, 1,3,5-triethyl-2,4,6-triformylbenzene (3.0 g, 12 mmol) in ether (20 mL) was added and the suspension was stirred for 12 h at r.t. The mixture was poured into aqueous HCl (ca. 1 M, 100 mL) and extracted with chloroform (400 mL). After drying over $MgSO_4$, the organic layer was concentrated, and ether (100 mL) was added to give **2a** (5.3 g, 6.5 mmol, 54% yield) as a

white powder. Anal. Calcd. for $C_{36}Br_3H_{29}O_6$: C, 53.55; H, 4.87. Found: C, 53.43; H, 5.18.

1,3,5-Tris(5-bromo-2-fluorophenylhydroxymethyl)-2,4,6-triethylbenzene (2b): At –70 ºC, lithium diisopropylamide (1.1 M solution in THF, 50 mL, 54 mmol) was added dropwise to 4-bromofluorobenzene (5.7 mL, 52 mmol) in THF (100 mL). After stirring for 30 min, 1,3,5-triethyl-2,4,6-triformylbenzene (4.0 g, 16 mmol) in THF (10 mL) was added, and the solution was stirred for 12 h at r.t. The mixture was treated as described for **2a** to give **2b** (8.5 g, 11 mmol, 70% yield) as white powder. Anal. Calcd. for $C_{33}Br_3H_{30}O_3F_3$: C, 51.39; H, 3.92. Found: C, 51.31; H, 3.46.

1,3,5-Tris(5-bromo-2-methoxybenzyl)-2,4,6-triethylbenzene (3a): At 0 ºC, triethylsilane (4.4 mL, 27 mmol) was added to a dichloromethane suspension (150 mL) of **2a** (6.1 g, 7.5 mmol). After stirring for 30 min, boron trifluoride etherate (3.4 mL, 27 mmol) was added at 0 ºC and stirred for 12 h at r.t. The mixture was poured into saturated aqueous $NaHCO_3$ (200 mL) and extracted with dichloromethane (250 mL). The organic layer was washed with aqueous HCl (ca. 1 M, 150 mL), dried over $MgSO_4$, and evaporated. The residue was recrystallized from dichloromethane and ethanol to give **3a** (4.5 g, 6.0 mmol) in 80% yield as a white crystalline powder. ^{1}H NMR ($CDCl_3$, δ); 7.24 (dd, arom, J = 2.5, 8.7 Hz, 3H), 6.71 (d, arom, J = 8.7 Hz, 3H), 6.64 (d, arom, J = 2.5 Hz, 3H), 3.96 (s, CH_2, 6H), 3.88 (s, OCH_3, 9H), 2.28 (q, CH_2CH$_3$, J = 7.5 Hz, 6H), 1.11 (t, CH$_2$CH_3, J = 7.5 Hz, 9H). Anal. Calcd. for $C_{36}Br_3H_{39}O_3$: C, 56.94; H, 5.18. Found: C, 57.13; H, 5.17.

1,3,5-Tris(5-bromo-2-fluorobenzyl)-2,4,6-triethylbenzene (3b): Compound **3b** was synthesized as described for **3a** from **2b** (3.0 g, 3.8 mmol) in 56% yield (1.57 g, 2.2 mmol). ^{1}H NMR ($CDCl_3$, δ); 7.26 (ddd, arom, $J_{H\text{-}F}$ = 4.5 Hz, J_1 = 2.5 Hz, J_2 = 9.0 Hz, 3H), 6.93 (dd,

arom, $J_{H\text{-}F}$ = 9.6 Hz, J = 9.0 Hz, 3H), 6.67 (dd, arom, $J_{H\text{-}F}$ = 6.9 Hz, J =2.5 Hz, 3H), 4.06(s, CH_2, 6H), 2.34 (q, CH_2CH$_3$, J = 7.6 Hz, 6H), 1.10 (t, CH$_2$CH_3, J = 7.6 Hz, 9H). Anal. Calc. for $C_{33}Br_3H_{30}F_3$: C, 54.80; H, 4.18. Found: C, 54.88; H, 4.26.

1,3,5-Triethyl-2,4,6-tris(5-mercapto-2-methoxybenzyl)benzene (Temp(SH)$_3$, 1a): At –70 ºC, *t*-BuLi (1.6 M solution in pentane, 10 mL, 16 mmol) was added dropwise to **3a** (1.9 g, 2.5 mmol) in THF (90 mL) and stirred for 30 min. After addition of elemental sulfur (810 mg, 25 mmol as 1/8 S_8) at –70 ˚C and stirring at r.t. for 5 h, the solution was treated with $LiAlH_4$ (934 mg, 25 mmol) and stirred for 30 min. The suspension was treated with water (20 mL) and aqueous HCl (ca. 1M, 30 mL), and evaporated to remove most THF. The mixture was poured into 1 M HCl (50 mL) and extracted with dichloromethane (250 mL). The organic layer was dried over $MgSO_4$ and evaporated to dryness. Reprecipitation from dichloromethane and hexane gave **1a** (0.91 mg, 1.5 mmol, 60% yield) as a white powder. ^{1}H NMR ($CDCl_3$, δ); 7.11 (dd, arom, J_1 = 2.1 Hz, J_2 = 8.3 Hz, 3H), 6.73 (d, arom, J = 8.3 Hz, 3H), 6.51 (d, arom, J = 2.1 Hz, 3H), 3.95 (s, CH_2, 6H), 3.88 (s, OCH_3, 9H), 3.57 (s, SH, 3H), 2.24 (q, CH_2CH$_3$, J = 7.3 Hz, 6H), 1.15 (t, CH$_2$CH_3, J = 7.3 Hz, 9H). Anal. Calc. for $C_{36}S_3H_{42}O_3$: C, 69.86; H, 6.84; S, 15.54. Found: C, 69.58; H, 6.81; S, 15.17.

1,3,5-Triethyl-2,4,6-tris(5-mercapto-2-fluorobenzyl)benzene (Tefp(SH)$_3$, 1b): Compound **1b** was synthesized as described for **1a** from **3b** (1.7 g, 2.3 mmol) in 38% yield (0.52 g, 0.89 mmol). ^{1}H NMR ($CDCl_3$, δ); 7.09 (ddd, arom, $J_{H\text{-}F}$ = 5.0 Hz, J_1 = 2.3 Hz, J_2 = 8.5 Hz, 3H), 6.93 (dd, arom, $J_{H\text{-}F}$= 9.3 Hz, J_1= 8.5 Hz, 3H), 6.48 (dd, arom, $J_{H\text{-}F}$ = 6.7 Hz, J_2 = 2.3 Hz, 3H), 4.04 (s, CH_2, 6H), 3.54 (s, SH, 3H), 2.31 (q, CH_2CH$_3$, J = 7.6 Hz, 6H), 1.15 (t, CH$_2$CH_3, J = 7.6 Hz, 9H). Anal. Calc. for $C_{33}S_3H_{33}F_3$: C, 68.01; H, 5.71; S, 16.51. Found: C, 68.26; H, 5.66; S, 16.22.

$(PPh_4)_2[Fe_4S_4(SEt)(TempS_3)]$ (4a): Compound **1a** (680 mg, 1.1 mmol) in THF (60 mL) was added to $(PPh_4)_2[Fe_4S_4(SEt)_4]$ (1.4 g, 1.1 mmol) in acetonitrile (100 mL). After stirring for 5 h, the reddish black solution was evaporated to dryness, and the residue was washed with THF and ether. The solid was extracted with acetonitrile (150 mL) and dried in vacuo, which gave **1a** as a black solid (1.4 g, 1.0 mmol, 90% yield). Single crystals of **1a** suited to X-ray analysis was obtained by layering hexane and ether onto the acetonitrile solution. ^{1}H NMR (600 MHz, CD_3CN, δ); 12.85 (br, SCH_2CH_3), 12.60 (br, SCH_2CH_3), 7.90 (t, $P(C_6H_5)_4$), 7.75-7.70 (m, $P(C_6H_5)_4$), 7.70-7.64 (m, $P(C_6H_5)_4$), 7.57 (s, arom), 6.23 (br, arom), 5.76 (br, arom), 3.97 (s, OCH_3), 3.41 (s, $ArCH_2Ar$), 2.34 (br, CH_2CH_3 and SCH_2CH_3), 1.14 (s, CH_2CH_3). Anal. Calc. for $C_{86}Fe_4S_8H_{84}O_3P_2 \bullet C_2H_3N$: C, 60.45; H, 5.02; N, 0.80; S, 14.67. Found: C, 60.61; H, 5.37; N, 0.99; S, 14.49. Cyclic voltammetry (acetonitrile, 0.1 Vs^{-1}); $E_{1/2}$= –1.49 V, E_{pc}'= –2.22 V,[16] (THF, 0.1 Vs^{-1}); $E_{1/2}$= –0.46, –1.63, –2.36 V. UV/Vis (CH_3CN): λ_{max} [nm] (ε [$M^{-1}cm^{-1}$]) = 439 (1.6×10^4), 298 (2.4×10^4) sh.

$(PPh_4)_2[Fe_4S_4(SEt)(TefpS_3)]$ (4b): Complex **4b** was synthesized as described for **4a** from $(PPh_4)_2[Fe_4S_4(SEt)_4]$ (930 mg, 0.73 mmol) and **1b** (425 mg, 0.73 mmol) in 87% yield (1.1 g, 0.063 mmol). ^{1}H NMR (600 MHz, CD_3CN, δ); 13.06 (br, SCH_2CH_3), 12.60 (br, SCH_2CH_3), 7.90 (t, $P(C_6H_5)_4$), 7.75-7.64 (m, $P(C_6H_5)_4$ and arom), 6.28 (br, arom), 5.69 (br, arom), 3.46 (s, $ArCH_2Ar$), 2.39 (br, CH_2CH_3), 2.32 (br, SCH_2CH_3), 1.15 (s, CH_2CH_3). Anal. Calc. for $C_{83}Fe_4S_8H_{75}P_2F_3$: C, 59.65; H, 4.52; S, 15.35. Found: C, 59.58; H, 4.56; S, 14.87. Cyclic voltammetry (acetonitrile, 0.1 Vs^{-1}); $E_{1/2}$= –1.43 V, E_{pc}'= –2.25 V.[16] UV/Vis (CH_3CN): λ_{max} [nm] (ε [$M^{-1}cm^{-1}$]) = 433 (2.0×10^4), 298 (2.8×10^4) sh.

$(PPh_4)_2[Fe_4S_4(SPh)(TempS_3)]$ (5a): Benzenethiol diluted in toluene (0.041 M, 1.5 mL, 0.065

mmol) was added to **4a** (101 mg, 0.059 mmol) in acetonitrile (20 mL), and the solution was stirred for 3.5 h. After removal of all the volatiles in vacuo, the residue was washed with hexane and extracted with DMF (1 mL) + acetonitrile (6 mL). The solution was layered with hexane and ether, which gave **5a** as black crystals (48 mg, 0.027 mmol, 46% yield). Anal. Calc. for $C_{90}Fe_4S_8H_{84}O_3P_2$: C, 61.58; H, 4.82; S, 14.61. Found: C, 61.74; H, 4.60; S, 14.17. Cyclic voltammetry (acetonitrile, 0.1 Vs^{-1}); $E_{1/2}$= –1.43 V, E_{pc}'= –2.23 V,[16] (THF, 0.1 Vs^{-1}); $E_{1/2}$= –0.39, –1.58, –2.30 V.

$(PPh_4)_2[Fe_4S_4(SPh)(TefpS_3)]$ (5b): Complex **5b** was synthesized as described for **5a** from **4b** (101 mg, 0.061 mmol) and benzenethiol diluted in toluene (0.2 M, 0.34 mL, 0.068 mmol) in 74% yield (78 mg, 0.045 mmol). ^{1}H NMR (600 MHz, CD_3CN, δ); 8.11 (br, SC_6H_5), 7.90 (t, $P(C_6H_5)_4$, 8H), 7.76-7.61 (m, $P(C_6H_5)_4$ and arom), 6.32 (br, arom), 5.98 (br, SC_6H_5), 5.68 (br, arom), 5.28 (br, SC_6H_5), 3.45 (s, $ArCH_2Ar$), 2.39 (br, CH_2CH_3), 1.15 (s, CH_2CH_3). Anal. Calc. for $C_{87}Fe_4S_8H_{75}P_2F_3$: C, 60.77; H, 4.40; S, 14.92. Found: C, 60.46; H, 4.18; S, 14.52. Cyclic voltammetry (acetonitrile, 0.1 Vs^{-1}); $E_{1/2}$= –1.35 V, E_{pc}'= –2.30 V. [16] UV/Vis (CH_3CN): λ_{max} [nm] (ε [$M^{-1}cm^{-1}$]) = 433 (2.0×10^4), 298 (2.8×10^4) sh.

$(PPh_4)_2[Fe_4S_4(SH)(TempS_3)]$ (6a): Using a gas-tight syringe, H_2S gas (20 mL) was injected to an acetonitrile solution (30 mL) of **4a** (300 mg, 0.18 mmol). After vigorous stirring for 5 min, a small amount of insoluble materials was filtered off. The solution was layered with hexane and ether, and the headspace was virtually filled with H_2S gas. Complex **6a** was obtained as crystalline black needles (210 mg, 0.12 mmol, 70% yield). Anal. Calc. for $C_{84}Fe_4S_8H_{80}O_3P_2$: C, 60.08; H, 4.80; S, 15.28. Found: C, 60.16; H, 5.04; S, 14.93. Cyclic voltammetry (acetonitrile, 0.1 Vs^{-1}); $E_{1/2}$= –1.48 V, E_{pc}'= –2.27 V.[16]

$(PPh_4)_2[Fe_4S_4(SH)(TefpS_3)]$ (6b): Complex **6b** was synthesized as described for **6a** from **4b** (90 mg, 0.054 mmol) in 54% yield 48 mg, 0.029 mmol). ^{1}H NMR (600 MHz, CD_3CN, δ); 7.90 (t, $P(C_6H_5)_4$), 7.76-7.64 (m, $P(C_6H_5)_4$ and arom), 6.36 (br, arom), 5.70 (br, arom), 3.46 (s, $ArCH_2Ar$), 2.39 (br, CH_2CH_3), 1.15 (s, CH_2CH_3), the proton of SH *was not assignable*. Anal. Calc. for $C_{81}Fe_4S_8H_{71}P_2F_3$: C, 59.20; H, 4.35; S, 15.61. Found: C, 59.58; H, 4.56; S, 15.78. Cyclic voltammetry (acetonitrile, 0.1 Vs^{-1}); $E_{1/2}$= –1.40 V, E_{pc}'= –2.28 V,[16] (DMF, 0.1 Vs^{-1}); $E_{1/2}$= –1.53 V, E_{pc}'= –2.30 V,[16] (DMSO, 0.1 Vs^{-1}); $E_{1/2}$= –1.43 V, E_{pc}'= –2.31 V,[16] (THF, 0.1 Vs^{-1}); $E_{1/2}$= –1.53, –2.28 V, E_{pa}'= –0.25 V. UV/Vis (CH_3CN): λ_{max} [nm] (ε [$M^{-1}cm^{-1}$]) = 454 (1.3×10^4) sh, 368 (1.8×10^4) sh, 295 (2.4×10^4) sh.

$(PPh_4)_4[\{Fe_4S_4(TempS_3)\}_2S]$ (7a): Using a gas-tight syringe, H_2S gas (6 mL) was injected to an acetonitrile solution (5 mL) of **4a** (90 mg, 0.053 mmol). After stirring for 5 min, all the volatiles were removed in vacuo, and the residue was extracted with acetonitrile (6 mL) and layered with hexane and ether. Cluster **7a** was obtained as crystalline black needles (44 mg, 0.013 mmol, 50% yield). Anal. Calc. for $C_{168}Fe_8S_{15}H_{158}O_6P_4 \bullet C_6H_9N_3$: C, 60.61; H, 4.88; N, 1.22; S, 13.95. Found: C, 60.41; H, 4.80; N, 0.80; S, 13.22. Cyclic voltammetry (acetonitrile, 0.1 Vs^{-1}); $E_{1/2}$= –1.66, –1.87 V, E_{pc}'= –2.31 V.[16]

$(PPh_4)_4[\{Fe_4S_4(TefpS_3)\}_2S]$ (7b): Complex **7b** was synthesized as described for **7a** from **4b** (100 mg, 0.060 mmol) in 37% yield (36 mg, 0.011 mmol). Anal. Calc. for $C_{162}Fe_8S_{15}H_{140}P_4F_6$: C, 59.82; H, 4.33; S, 14.79. Found: C, 59.36; H, 4.75; S, 14.33. Cyclic voltammetry (acetonitrile, 0.1 Vs^{-1}); $E_{1/2}$= –1.55, –1.74 V, E_{pc}'= –2.24 V.[16]

Crystal-Structure Determination:

Crystal data and refinement parameters for the clusters reported herein are summarized in

Table 5. Single crystals were mounted on a loop using oil (Paraton, Hampton Research Corp.). Diffraction data were collected at –100 ºC under a cold nitrogen stream on a Rigaku Micromax-007 with a Saturn 70 CCD area detector (for **4b**), or on a Rigaku FR-E with a Saturn 70 CCD detector (for **1b**, **4a**, **5a**, **6a**, **6b**, **7a** and **7b**) using graphite-monochromated MoKα radiation (λ = 0.710690 Å). Using an oscillation range of 0.5˚, 1080 data images were collected for **4a**, **6a**, **6b**, **7a**, and **7b**, while 720 images were measured for **1b**, **4b**, and **5a**. The data were integrated and corrected for absorption using the Rigaku/MSC CrystalClear program package. The structures were solved by a direct method (SHELXS97) and were refined by full-matrix least-squares on F^2 by the Rigaku/MSC CrystalStructure program package. Anisotropic refinement was applied to all non-hydrogen atoms except for disordered atoms and some crystal solvents. All the hydrogen atoms were put at the calculated positions. The ethanethiolate group of **4a** was disordered over two positions. The μ^2-S atom of **7b** was disordered over two positions in a 1:1 ratio. In **5a**, two DMF molecules are disordered over two positions in a 1:1 ratio. A phenyl group of PPh_4^+ of **6a** is disordered over two positions. An acetonitrile molecule of **6b** is disordered over two positions in a 1:1 ratio. Three acetonitriles of **7a** are disordered.

Table 2-5. Crystal data of **1b**, **4a**,**b**, **5a**,**b**, **6a**,**b**, and **7a**,**b**.

	1b	**4a**•CH_3CN	**4b**•1.5(CH_3CN)	**5a**•3(DMF)	**5b**•4(DMF)
fomula	$C_{33}H_{33}F_3S_3$	$C_{86}Fe_4S_8H_{84}O_3P_2$ •C_2H_3N	$C_{83}Fe_4S_8H_{75}P_2F_3$ •$C_3H_{4.5}N_{1.5}$	$C_{90}Fe_4S_8H_{84}O_3P_2$ •$C_9H_{21}N_3O_3$	$C_{87}Fe_4S_8H_{75}F_3P_2$ •$C_{12}H_{28}N_4O_4$
formula wt	582.80	1748.48	1732.89	1974.75	2011.74
crystal system	trigonal	monoclinic	orthorhombic	monoclinic	monoclinic
space group	$P3_1c$ (#159)	$C2/c$ (#15)	$Aea2$ (#41)	$P2_1/n$ (#14)	$C2$ (#5)
a/Å	13.5211(10)	50.557(3)	48.534(10)	14.829(3)	23.603(7)
b/Å	–	14.4362(5)	23.221(5)	27.288(5)	14.374(4)
c/Å	9.2218(9)	27.1283(13)	14.421(3)	24.211(5)	28.272(8)
α/deg	–	–	–	–	–
β/deg	–	120.1810(13)	–	90.188(3)	91.031(6)
γ/deg	–	–	–	–	–
V/Å^3	1460.1(2)	17116(2)	16242(6)	9797(4)	9590(5)
Z	2	8	8	4	4
D_{calc}/g cm^{-1}	1.326	1.357	1.417	1.339	1.393
μ/cm^{-1}	2.944	9.443	9.97	8.36	8.586
F(000)	612.00	7264.00	7160.00	4120.00	4184.00
$2\theta_{max}$/deg	54.9	55.0	54.9	55.0	54.9
no. of rflns (all)	11897	86671	51359	80311	38382
indep. rflns (R_{int})	2159 (0.052)	19388 (0.035)	14637 (0.054)	22445 (0.057)	20058 (0.0335)
no. of params	123	949	940	1048	1105
$R1$[a]	0.0423	0.0712	0.0520	0.0768	0.0343
w$R2$[b]	0.0971	0.2324	0.1381	0.2499	0.0928
GOF[c]	1.045	1.089	1.101	1.071	1.062

Table 2-5 (cont)

	6a•2(CH_3CN)(Et_2O)	**6b**•1.5(CH_3CN)	0.5{**7a**•3(CH_3CN)}	0.5{**7b**•4(CH_3CN)}
fomula	$C_{84}Fe_4S_8H_{80}O_3P_2$ •$C_4H_6N_2$•$C_4H_{10}O$	$C_{81}Fe_4S_8H_{71}P_2F_3$ •$C_3H_{4.5}N_{1.5}$	$C_{84}Fe_4S_{7.5}H_{79}O_3P_2$ •$C_3H_{4.5}N_{1.5}$	$C_{81}Fe_4S_{7.5}H_{70}P_2F_3$ •$C_4H_6N_2$
formula wt	1835.60	1703.83	1723.91	1708.33
crystal system	monoclinic	triclinic	monoclinic	triclinic
space group	$P2_1/n$ (#14)	P-1 (#2)	$C2/c$ (#15)	P-1 (#2)
a/Å	16.1342(10)	12.448(3)	32.971(2)	13.642(2)
b/Å	14.3608(7)	13.505(3)	13.9980(5)	13.875(6)
c/Å	39.525(3)	24.912(5)	37.190(2)	24.724(8)
α/deg	–	86.084(9)	–	75.28(5)
β/deg	92.482(4)	77.153(7)	96.552(2)	77.52(4)
γ/deg	–	74.801(6)	–	61.37(4)
V/Å^3	9149.4(10)	3940(2)	17052(2)	3948(3)
Z	4	2	8	2
D_{calc}/g cm^{-1}	1.332	1.436	1.343	1.437
μ/cm^{-1}	8.878	10.262	9.352	10.117
F(000)	3824.00	1756.00	7152.00	1762.00
$2\theta_{max}$/deg	50.1	55.0	55.0	50.1
no. of rflns (all)	76151	48504	86175	40715
indep. rflns (R_{int})	16124 (0.071)	17987 (0.037)	19527 (0.072)	13719 (0.038)
no. of params	960	934	950	937
$R1$[a]	0.0759	0.0515	0.0727	0.0435
w$R2$[b]	0.2375	0.1466	0.2433	0.1085
GOF[c]	1.072	1.085	1.031	1.071

[a] $R1 = \Sigma ||F_o| - |F_c|| / \Sigma |F_o|$ ($I > 2\sigma(I)$). [b] $wR2 = \{[\Sigma w(|F_o| - |F_c|)^2 / \Sigma wF_o^2]\}^{1/2}$ (all data). [c] GOF = $[\Sigma w(|F_o| - |F_c|)^2/(N_o - N_v)]^{1/2}$ (N_o = number of observations, N_v = number of variables).

References for Chapter 2

[1] a) A. Messerchmidt, R. Huber, T. Poulos, K. Wiehardt, *Handbook of Metalloproteins vol. 1,* John Wiley & Sons, Chichester, UK, **2001**, pp471–485; b) A. Messerchmidt, R. Huber, T. Poulos, K. Wiehardt, *Handbook of Metalloproteins vol. 2,* John Wiley & Sons, Chichester, UK, **2001**, 738–751, 880–896; c) M. G. Bertero, R. A. Rothery, M. Palak, C. Hou, D. Lim, F. Blasco, J. H. Weiner, N. C. Strynadka, J. *Nature Structural Biology* **2003**, *10*, 681–687; d) L. A. Sazanov, P. Hinchliffe, *Science* **2006**, *311*, 1430–1436; e) T. Gräwert, I. Span, W. Eisenreich, F. Rohdich, J. Eppinger, A. Bacher, M. Groll, *Proc. Natl. Acad. Sci.* **2010**, *107*, 1077–1081; f) A. Messerchmidt, *Handbook of Metalloproteins vol. 4,* John Wiley & Sons, Chichester, UK, **2011**, pp172–182, 397–412; g) S. H. Knauer, W. Buckel, H. Dobbek, *J. Am. Chem. Soc.* **2011**, *133*, 4342–4347.

[2] a) T. D. P. Stack, R. H. Holm, *J. Am. Chem. Soc.* **1987**, *109,* 2546–2547; b) T. D. P. Stack, R. H. Holm, *J. Am. Chem. Soc.* **1988**, *110*, 2484–2494; c) C. Zhou, R. H. Holm, *Inorg. Chem.* **1997**, *36,* 4066–4077; d) P. V. Rao, S. Bhaduri, J. Jiang, D. Hong, R. H. Holm, *J. Am. Chem. Soc.* **2005**, *127*, 1933–1945; e) R. Panda, C. P. Berlinguette, Y. Zhang, R. H. Holm, *J. Am. Chem. Soc.* **2005**, *127*, 11092–11101; f) J. Sun, C. Tessier, R. H. Holm, *Inorg. Chem.* **2007**, *46*, 2691–2699.

[3] a) T. D. P. Stack, M. J. Carney, R. H. Holm, *J. Am. Chem. Soc.* **1989**, *111,* 1670–1676; b) S. Ciurli, M. Carrié, J. A. Weigel, M. J. Carney, T. D. P. Stack, G. C. Papaefthymiou, R. H. Holm, *J. Am. Chem. Soc.* **1990**, *112,* 2654–2664; c) J. A. Weigel, R. H. Holm, *J. Am. Chem. Soc.* **1991**, *113,* 4184–4191; d) H. Y. Liu, B. Scharbert, R. H. Holm, *J. Am. Chem. Soc.* **1991**, *113,* 9529–9539; e) L. Cai, R. H. Holm, *J. Am. Chem. Soc.* **1994**, *116*, 7177–7188; f) C. Zhou, L. Cai, R. H. Holm, *Inorg. Chem.* **1996**, *35,* 2767–2772; g) P. V. Rao, R. H. Holm, *Chem. Rev.* **2004**, *104*, 527–559.

[4] C. Walsdorff, W. Saak, S. Pohl, *J. Chem. Soc., Dalton Trans.* **1997**, 1857–1861.

[5] a) M. A. Whitener, G. Peng, R. H. Holm, *Inorg. Chem.* **1991**, *30*, 2411–2417; b) G. P. F. van Strijdonck, J. A. E. H. van Haare, J. G. M. van der Linden, J. J. Steggerda, R. J. M. Nolte, *Inorg. Chem.* **1994**, *33*, 999–1000; c) G. P. F. van Strijdonck, J. A. E. H. van Haare, P. J. M. Hönen, R. C. G. M. van den Schoor, M. C. Feiters, J. G. M. van der Linden, J. J. Steggerda, R. J. M. Nolte, *J. Chem. Soc., Dalton Trans.* **1997**, 449–461; d) D. J. Evans, G. Garcia, G. J. Leigh, M. S. Newton, M. D. Santana, *J. Chem. Soc., Dalton Trans.* **1992**, 3229–3234; e) J. E. Barclay, M. I. Diaz, D. J. Evans, G. Garcia, M. D. Santana, M. C. Torralba, *Inorg. Chim. Acta* **1997**, *258*, 211–219; f) G. P. F. van Strijdonck, P. T. J. H. ten Have, M. C. Feiters, J. G. M. van der Linden, J. .J. Steggerda, R. J. M. Nolte, *Chem. Ber./Recueil* **1997**, *130,* 1151–1157; g) C. Tard, X. Liu, S. K. Ibrahim, M. Bruschi, L. D. Gioia, S. C. Davies, X. Yang, L.-S. Wang, G. Sawers, C. J. Pickett, *Nature* **2005**, *433*, 610–613; h) E. P. L. van der Geer, G. van Koten, R. J. M. K. Gebbink, B. Hessen, *Inorg. Chem.* **2008**, *47*, 2849–2857; i) D. L. Gerlach, D. Coucouvanis, N. Lehnert, *Eur. J. Inorg. Chem.* **2013**, 3883–3890.

[6] D. D. MacNicol, P. R. Mallinson, C. D. Robertson, *J. Chem. Soc., Chem. Commun.* **1985**, 1649–1651.

[7] M. Martin, G. Gasparini, M. Graziani, L. J. Prins, P. Scrimin, *Eur. J. Org. Chem.* **2010**,

3858–3866.

[8] M. Dąbrowski, J. Kubicka, S. Luliński, J. Serwatowski, *Tetrahedron* **2005**, *61*, 6590–6595.

[9] A. J. Bridges, A. Lee, E. C. Maduakor, C. E. Schwartz, *Tetrahedron Lett*. **1992**, *33*, 7495–7498.

[10] Y.-Q. Long, X.-H. Jiang, R. Dayam, T. Sanchez, R. Shoemaker, S. Sei, N. Neamati, *J. Med. Chem*. **2004**, *47,* 2561–2573.

[11] S. Ohta, Y. Ohki, Y. Ikagawa, R. Suizu, K. Tatsumi, *J. Organomet. Chem*. **2007**, *692*, 4792–4799.

[12] B. A. Averill, T. Herskovitz, R. H. Holm, J. A. Ibers, *J. Am. Chem. Soc*. **1973**, *95*, 3523–3534.

[13] P. K. Mascharak, K. S. Hagen, J. T. Spence, R. H. Holm, *Inorg. Chim.* Acta **1983**, *80*, 157–170; b) N. Ueyama, T. Sugawara, M. Fuji, A. Nakamura, N. Yasuoka, *Chem. Lett*. **1985**, 175–178; c) T. J. Ollerenshaw, C. D. Garner, B. Odell, W. Clegg, *J. Chem. Soc., Dalton Trans*. **1985**, 2161–2165; d) H. Kambayashi, H. Nagao, K. Tanaka, M. Nakamoto, S.-M. Peng, *Inorg. Chim. Acta* **1993**, *209*, 143–149; e) R. Hauptmann, J. Schneider, M. Köckerling, G. Henkel, *Acta Cryst*. **1999**, *C55*, 190–192; f) L. M. L. Daku, J. Pécaut, A. Lenormand-Foucaut, B. Vieux-Melchior, P. Iveson, J. Jordanov, *Inorg. Chem*. **2003**, *42*, 6824–6850; g) A. Kern, C. Näther, F. Studt, F. Tuczek, *Inorg. Chem*. **2004**, *43*, 5003–5010.

[14] a) L. Que, Jr., M. A. Bobrik, J. A. Ibers, R. H. Holm, *J. Am. Chem. Soc*. **1974**, *96*, 4168–4178; b) L. Guodong, Z. Hongtu, H. Sheng-Zhi, T. C. W. Mak, *Acta Cryst*. **1987**, C*43*, 352–353; c) J. Gloux, P. Gloux, H. Hendriks, G. Rius, *J. Am. Chem. Soc*. **1987**, *109*, 3220–3224; d) P. Excoffon, J. Laugier, B. Lamotte, *Inorg. Chem*. **1991,** *30*, 3075–3081.

[15] A. Müller, N. H. Schladerbeck, H. Bögge, *J. Chem. Soc., Chem. Commun*. **1987**, 35–36.

[16] The clusters reported herein exhibited an additional irreversible reduction wave. The values are shown as E_{pc}' in the Experimental Section.

[17] a) B. V. DePamphilis, B. A. Averill, T. Herskovitz, L. Que, Jr., R. H. Holm, *J. Am. Chem. Soc*. **1974**, *96*, 4159–4167; b) H. L. Blonk, O. Kievit, E. K.-H. Roth, J. Jordanov, J. G. M. van der Linden, J. J. Steggerda, *Inorg. Chem*. **1991**, *30*, 3231–3234; c) C. Zhou, J. W. Raebiger, B. M. Segal, R. H. Holm, *Inorg. Chim. Acta* **2000**, *300–302*, 892–902.

[18] A similar conversion was reported by Holm *et al,* see; ref 3e.

[19] a) P. R. Challen, S.-M. Koo, W. R. Dunham, D. Coucouvanis, *J. Am. Chem. Soc*. **1990**, *112,* 2455–2456; b) D. L. Gerlach, D. Coucouvanis, J. Kampf, N. Lehnert, *Eur. J. Inorg. Chem*. **2013**, 5253–5264

[20] The author measured CV spectra of **6b** in THF, DMF, and DMSO, and the data were compared with those in acetonitrile. However, the potential shifts were very similar to those observed for the ethanethiolate cluster **4b**, and therefore the hydrogen bonding effect toward the redox properties of **6b** have not been elucidated.

Chapter 3

[3:1] Site-Differentiated [4Fe-4S] Clusters Having One Carboxylate and Three Thiolates

3.1 Introduction

[3:1] Site-differentiated [4Fe-4S] clusters carrying one non-cysteine ligand have been reported and attracted much attention, described as chapter 1.[1-6] Carboxylates are the representative ligands, and those structures included in various proteins have also been demonstrated crystallographically. The aspartate coordination is known in ferredoxin from *Pyrococcus furiosus* (*Pf*)[2] and in dark operative protochlorophyllide oxidoreductase (DPOR) from *Rhodobacter capsulatus*,[3] and those clusters function as electron transfer mediator. Aconitase, catalyzing isomerization of citrate into isocitrate,[4] also contains a cluster of this type, and the structure with a unique iron coordinated by isocitrate was analyzed. Similar carboxylate coordination is also reported for isoprenoid biosynthesis protein (IspG) from *Aquifex aeolicus*,[5] and for radical-SAM superfamily enzymes such as biotin synthase and pyruvate formate-lyase, in which the clusters are chelated by SAM (S-adenosylmethionine) at the carboxylate and the amine have been elucidated (Chart 3-1).[6]

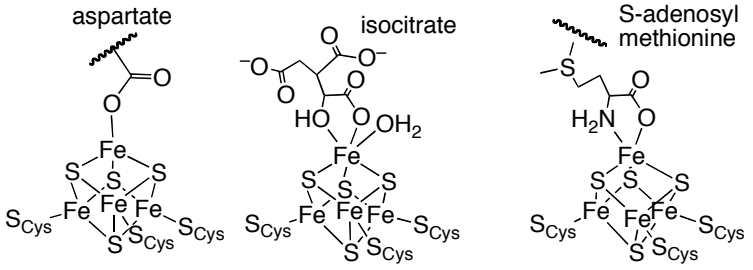

Chart 3-1

On the other hand, synthetic [4Fe-4S] clusters having both carboxylate and thiolate were first reported by Holm *et al* earlier than the structural elucidation of those proteins. They

synthesized a series of clusters formulated as $[Fe_4S_4(SR)_{4-n}(OCOR')_n]^{2-}$ (n = 1-4).[7] Later, Holm *et al*[8] and Nolte *et al*[9] respectively synthesized the clusters having one carboxylate and three thiolates by taking advantages of tridentate thiolate ligands, and their redox properties were analyzed. However, their structural details were not elucidated, although Holm *et al* suggested the η^2-coordination geometry for the acetate at the unique iron site according to the IR spectra.[8]

In chapter 2, the author reported the design and preparation of new trithiols $Temp(SH)_3$ (**1a**) and $Tefp(SH)_3$ (**1b**) suited for the production of [3:1] site-differentiated [4Fe-4S] clusters, and the author demonstrated their usefulness for model studies of the various site-differentiated [4Fe-4S] clusters in organisms via synthesis of these clusters having ethanethiolate, benzenethiolate, and hydrosulfide at the unique iron sites. All these clusters were obtained as single crystals suitable for X-ray structural analysis. In this chapter, the author reports the synthesis of the model clusters having a tridentate thiolate $TempS_3^{3-}$and a carboxylate.

3.2 Results and Discussion

3.2.1 Synthesis of carboxylate coordinated [3:1] site-differentiated [4Fe-4S] clusters

The synthesis of the carboxylate clusters were examined by the reaction of the ethanethiolate adduct $[PPh_4]_2[Fe_4S_4(SEt)(TempS_3)]$ (**4a**) with carboxylic acids. Addition of 4.5 equiv acetic acid to **4a** in acetonitrile and successive slow evaporation allowed the removal of volatile ethanethiol to give the acetate cluster $[PPh_4]_2[Fe_4S_4(OCOCH_3)(TempS_3)]$ (**8**) in 67% yield (Scheme 3-1). ESI-MS spectra confirm the formulation, and the IR spectrum shows the two CO_2^- stretching bands at 1571 and 1373 cm^{-1}.

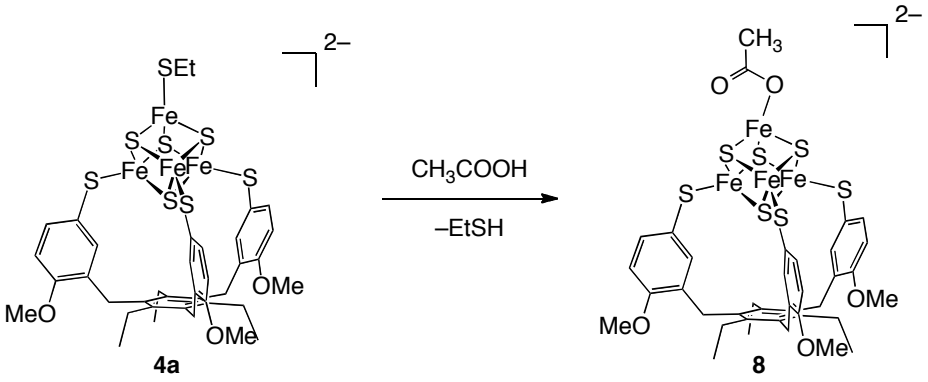

Scheme 3-1. Synthesis of the acetate cluster **8**.

Several other carboxylate clusters were also synthesized by a similar procedure (Scheme 3-2). Reactions with acrylic acid, propiolic acid, maleic acid, and benzoic acid gave the corresponding carboxylate adducts **9**-**12**, respectively. To synthesize the model clusters found for aconitase [4bf] and radical SAM enzymes,[6bcef] salicylic acid, anthranilic acid, and pyrrole-2-carboxylic acid were also reacted with **4a**, which gave the corresponding carboxylate adducts **13**-**15**. The CO_2^- stretching frequencies of cluster **8**-**10**, **12**-**15** analyzed by IR spectra are summarized in Table 3-1. The symmetric stretching bands were observed

between 1313 and 1406 cm^{-1}, while the asymmetric bands were found between 1557 and 1622 cm^{-1}. The spectra for **12** and **14** were also collected in acetonitrile solutions, in which the CO_2^- stretching frequencies were almost identical to those measured as KBr disks.

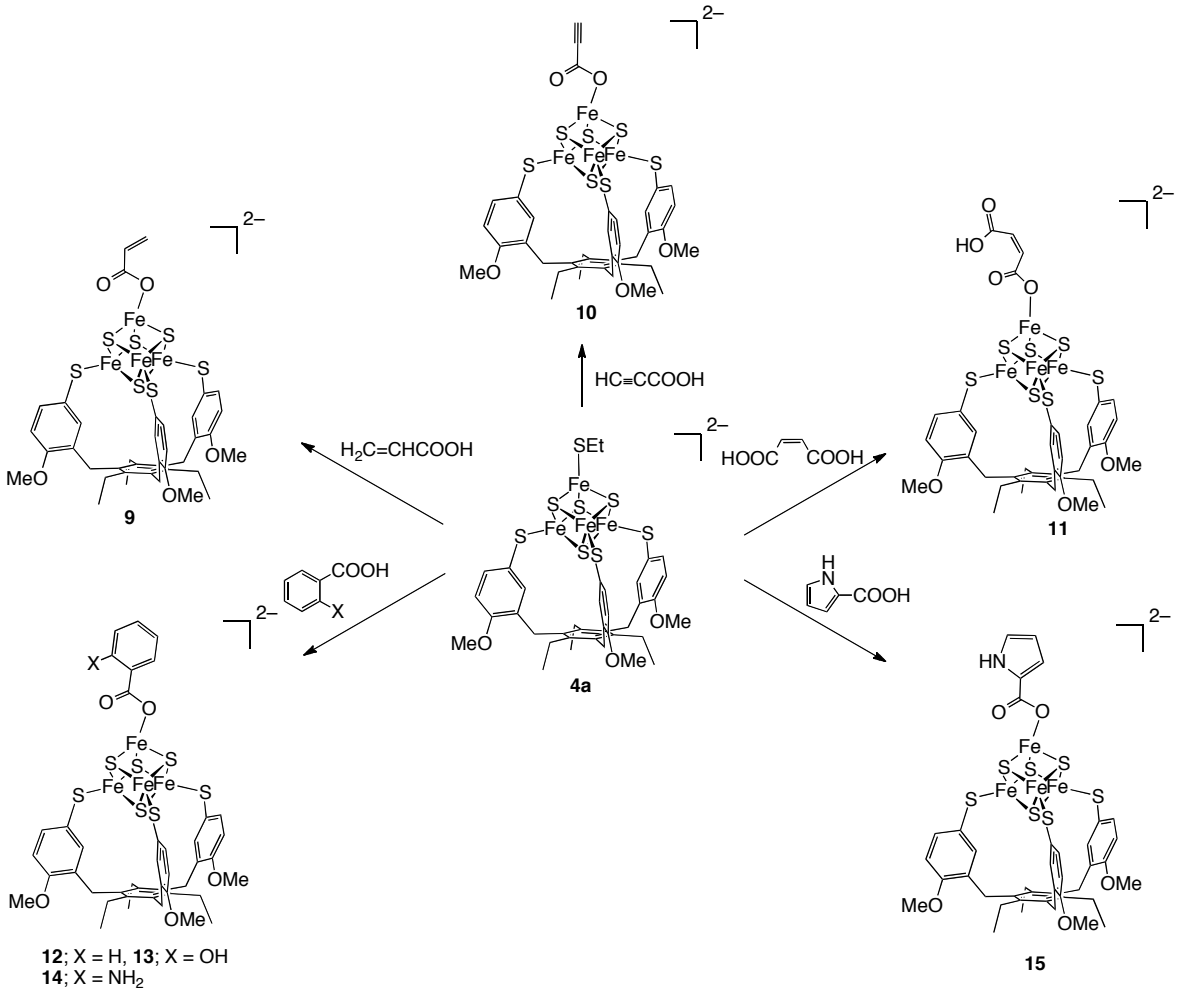

Scheme 3-2. Synthesis of **9**-**15**.

Table 3-1. The CO_2^- stretching frequencies of carboxylate ligands for **8**-**10**, **12**-**15** (KBr disk).

	$\nu(COO^-)/cm^{-1}$
8	1571, 1373
9	1557, 1406
10	1615, 1313
12	1622, 1322
13	1597, 1361
14	1612, 1340
15	1559, 1352

3.2.2 X-ray structural analysis of 8-15

The molecular structures of **8**-**15** were analyzed by X-ray crystallography. The molecular structures and the selected metric parameters of **8**, **10**, **11**, **13**, and **15** are shown in Figure 3-1 and Table 3-2, while the structural details of **9**,**12**,**14** are not discussed due to the insufficient quality of the crystals. Their tentative structures are also shown in Figure 3-1.

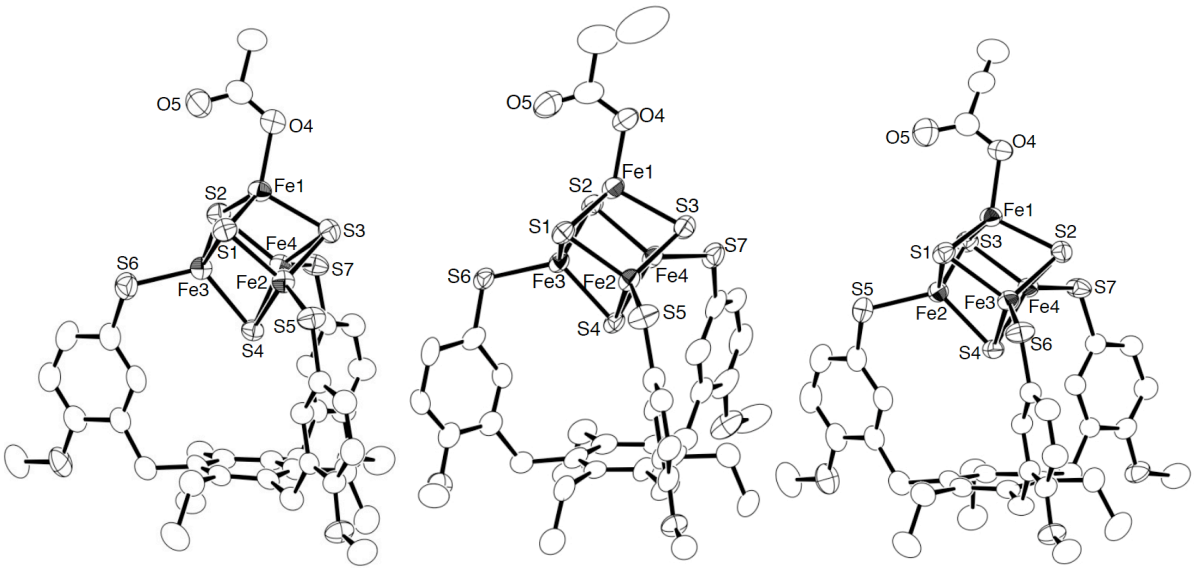

8 **9** **10**

Figure 3-1. Molecular structures of the anion of **8**, **10**, **11**, **13**, and **15** with 50% thermal ellipsoids, and those of **9**, **12**, and **14** with 30% thermal ellipsoids. Hydrogen atoms are omitted for clarity, except for H6A of **11**, H6A of **13**, and H1 of **15**.

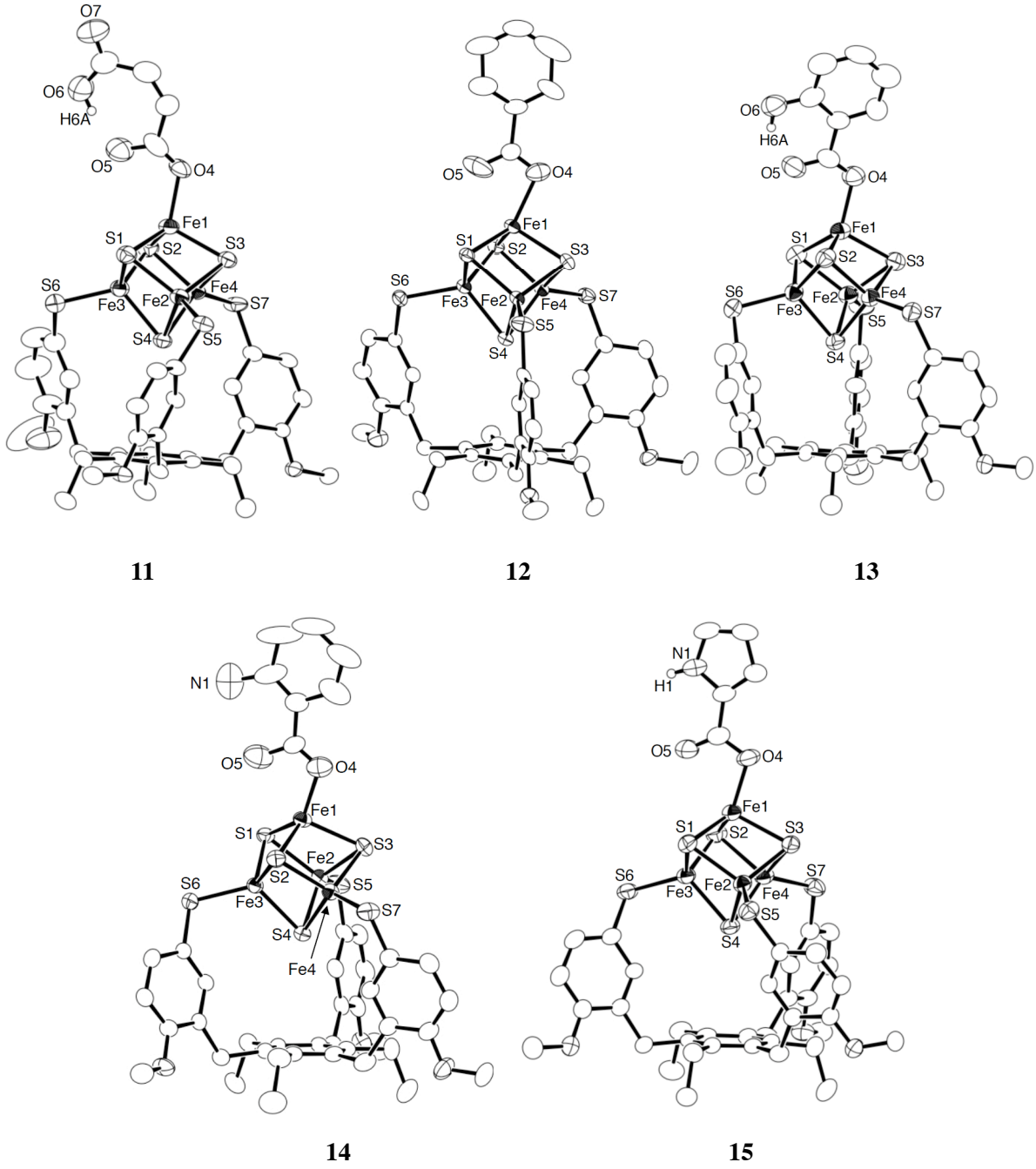

Figure 3-1. (cont)

As is evident in Figure 3-1, three irons of the [4Fe-4S] cores are capped by the tridentate $TempS_3^{3-}$, and the carboxylate ligands coordinate to the unique iron sites. Despite the uniqueness of the Fe1 sites due to the carboxylate coordination, the Fe-Fe and Fe-S distances around Fe1 are almost identical with those of other irons, and the metric parameters for

cubane cores also resemble those of the ethanethiolate cluster **4a**, described as chapter 2. The coordination mode of the carboxylates is notable. As summarized in Table 3-2, the Fe1-O4 distances are 1.94-2.02 Å, and 0.7-1.0 Å shorter than the Fe1-O5 distances with 2.65-3.12 Å. Although the Fe1-O5 distances are shorter than the sum of the van der Waals radii estimated as 3.5 Å,[10] their parameters are similar to the reported iron η^1-carboxylate complexes.[11] Thus, the carboxylate coordination to each unique iron would be regarded as η^1 via O4 rather than η^2. The O5 atoms of the carboxylates are commonly pointing the middle of the two S atoms of the cubane cores to avoid steric repulsion.

The difference of the two C-O bond distances of the carboxylate ligands is also notable. While the C85-O4 bonds regarded as single bonds are reasonably longer than the double bond-like C85-O5 bonds for **8**, **10**, and **15**, the C85-O4 bonds of **11** and **13** are shorter than the C85-O5 bonds, probably due to the hydrogen bonding interaction between the terminal carboxylic acid for **11** and the hydroxyl group for **13**. As for **15**, intermolecular hydrogen bonding were formed as shown in Figure 3-2 as indicated by the intermolecular N•••O distance of 2.845 (7) Å.[12] However, due to the low acidity of the pyrrole, long-short alternation for the carboxylate C–O bonds was not observed.

The S4…Fe1-O4 angles of **8, 10, 15** are 164.44(16), 164.58(9), 163.56(11)º, respectively. Their unique iron have distorted tetrahedral geometry, though that of cluster **4a** has tetrahedral and the S4…Fe1-S8 angle is 174.00º, which is supposed that the binding mode of these carboxylate ligands are close to asymmetric η^2, rather than η^1. However, Fe1-O5 distances are longer than their van der Waals radii, and therefore the distorted geometry would result from crystal packing. The S4-Fe1-O4 angles of **11**, **13** (**11**; 172.4(3), **13**; 167.48(19)º) are more linear than that of **8, 10, 15**, which also results from crystal packing.

Table 3-2. Selected interatomic distances (Å) and angles (deg) for **8**, **10**, **11**, **13**, and **15**.

	8	**10**	**11**	**13**	**15**
Fe1-Fe2	2.7745(13)	2.7259(7)	2.7427(18)	2.7632(15)	2.7663(10)
Fe1-Fe3	2.7395(13)	2.7603(7)	2.7301(18)	2.7447(15)	2.7362(11)
Fe1-Fe4	2.7356(13)	2.7277(8)	2.7514(17)	2.7708(14)	2.7550(9)
Fe2-Fe3	2.7384(13)	2.7406(7)	2.756(2)	2.7864(15)	2.7740(10)
Fe2-Fe4	2.7549(12)	2.7385(7)	2.7345(18)	2.7375(14)	2.7170(10)
Fe3-Fe4	2.7383(13)	2.7616(7)	2.7310(16)	2.7591(14)	2.7300(10)
Fe1-S1	2.2359(19)	2.2308(10)	2.258(3)	2.253(2)	2.2739(17)
Fe1-S2	2.2987(18)	2.3030(10)	2.294(3)	2.278(2)	2.2953(16)
Fe1-S3	2.3138(18)	2.3060(10)	2.310(2)	2.297(2)	2.3400(12)
Fe2-S1	2.3148(18)	2.3211(10)	2.301(2)	2.306(2)	2.3095(12)
Fe2-S3	2.2453(19)	2.2310(10)	2.260(2)	2.243(2)	2.2624(16)
Fe2-S4	2.3075(17)	2.3034(10)	2.293(3)	2.2819(19)	2.2881(15)
Fe3-S1	2.3191(17)	2.3146(10)	2.301(3)	2.287(2)	2.3033(15)
Fe3-S2	2.2300(18)	2.2557(10)	2.267(3)	2.268(2)	2.2619(16)
Fe3-S4	2.3031(17)	2.3108(10)	2.294(2)	2.3120(19)	2.3010(12)
Fe4-S2	2.2960(18)	2.3132(10)	2.301(2)	2.306(2)	2.3085(13)
Fe4-S3	2.3095(17)	2.2985(10)	2.306(3)	2.280(2)	2.2864(16)
Fe4-S4	2.2399(18)	2.2405(10)	2.252(2)	2.2574(19)	2.2484(17)
Fe2-S5	2.269(2)	2.2487(12)	2.255(3)	2.269(2)	2.2713(15)
Fe3-S6	2.260(3)	2.2650(12)	2.257(3)	2.276(2)	2.2601(19)
Fe4-S7	2.2765(18)	2.2788(10)	2.261(2)	2.266(2)	2.2616(15)
Fe1-O4	1.944(5)	1.958(3)	2.020(7)	1.997(5)	1.974(5)
Fe1-O5	2.996(6)	3.120(4)	3.089(8)	2.883(6)	2.652(4)
O4-C85	1.279(9)	1.280(5)	1.140(14)	1.181(10)	1.288(6)
O5-C85	1.230(9)	1.223(5)	1.265(14)	1.252(11)	1.221(9)
O5-O6	–	–	2.497(12)	2.552(9)	–

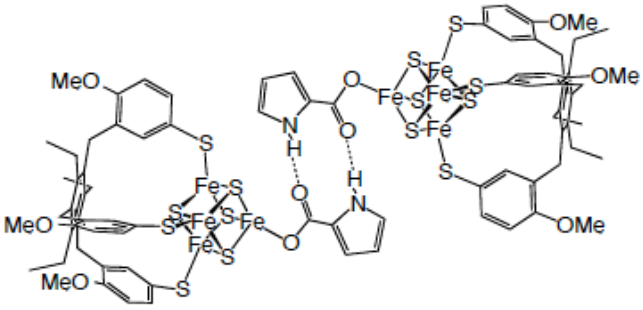

Figure 3-2. Intermolecular hydrogen bonding interaction of cluster **15**.

3.2.3 Structural comparison of the model clusters and those in metalloproteins

As is evident in the structures in Figure 3-1, the carboxylates used herein commonly coordinate to the iron at their carboxylate moieties exclusively in a η^1 manner. This coordination mode conforms to those observed for the [4Fe-4S] clusters in DPOR, *Pf* ferredoxin, and IspG (Chart 3-1).[2c,3d,5a] On the other hand, it is dissimilar to the chelate binding observed for aconitase or radical SAM superfamily enzymes,[4bf,6bcef] although the carboxylates of **9**, **10**, **13**, **14**, and **15** have additional auxiliaries potentially coordinatable to the iron such as alkene, alkyne, hydroxy group, amino group, and pyrrole. The reasons for the different coordination are not clear, but possible explanation is that the oxidation state of the [4Fe-4S] clusters in aconitase and radical SAM superfamily enzymes might be in the oxidized $[4Fe\text{-}4S]^{3+}$ state. Previously, the author's group reported the structure of the site-differentiated $[4Fe\text{-}4S]^{3+}$ cluster $[Fe_4S_4(SDmp)_3(thf)_3]$,[13] in which the unique iron site is coordinated by three THF oxygen atoms to assume an octahedral geometry, while the other three irons have monodentate bulky thiolates $DmpS^-$ (Dmp = 2,6 dimesitylphenyl). Another explanation is that the hydroxyl of citrate/isocitrate of aconitase and amine of SAM of radical SAM superfamily

enzymes might be more anionic through the hydrogen bonding network with the surrounding protein. Further model synthesis and structural elucidation is needed to elucidate the nature of the clusters in the enzymes.

3.2.4 Redox properties of 8-15

The cyclic voltammograms (CVs) of **8**-**15** recorded in 0.1 M NBu_4PF_6 acetonitrile solution have revealed the redox properties. As shown in Figure 3-3, cluster **8** displays one reversible $[Fe_4S_4]^{2+}/[Fe_4S_4]^{+}$ redox at $E_{1/2}$ = –1.40 V vs Ag/Ag^{+}. Clusters **9**, **12**, and **15** also show a similar redox waves at –1.43, –1.40, and –1.41 V, respectively (Table 3-3). These potentials are significantly positive compared to that of the ethanethiolate cluster **4a** observed at –1.49 V, and this positive shift is common to the similar [4Fe-4S] clusters having a tridentate thiolate and an acetate previously reported by Holm *et al*[8,14] and Nolte *et al*.[9,15]

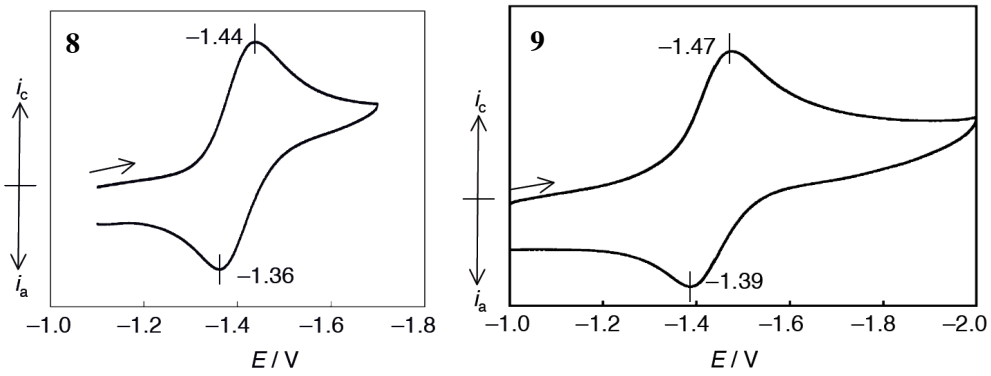

Figure 3-3. CV spectra of cluster **8**, **9**, **12**, and **15** in acetonitrile.

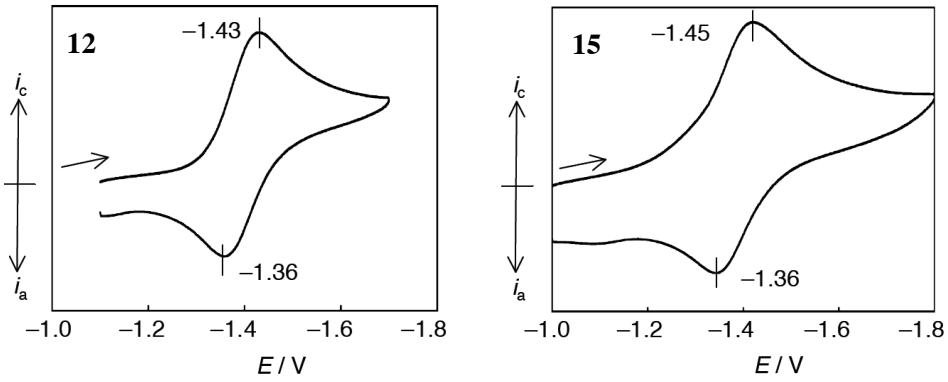

Figure 3-3. (cont)

However, the CV spectra of **10**, **11**, **13**, and **14** coordinated respectively by propiolate, maleate, salicylate, and anthranilate are rather complicated as shown in Figure 3-4. Cluster **14** appears to show the redox process at $E_{1/2}$ = –1.40 V, but the i_a for this reverse oxidation process appears smaller. In addition to this fact, a smaller reversible redox couple was observed at $E_{1/2}$ = –1.13 V. Similarly **11**, and **13** also shows two redox processes, although each of reversibility and relative intensity of the two reduction waves vary. When the CV of **14** was recorded in the presence of excess $(NEt_4)(OCOC_6H_4NH_2)$, the reversibility of the negative redox process was significantly improved, and concomitantly the smaller redox couple at $E_{1/2}$ = –1.13 V had disappeared. The same spectral change was also observed for **13**. This result indicates that for **14** the redox at $E_{1/2}$ = –1.40 V is assignable to that of the carboxylate cluster **14**, and that the carboxylate ligand dissociates from the cluster upon reduction. In the case of **11** and **13**, a similar carboxylate-dissociation would have occurred, which could result in the complex CV spectra. For the case of **11**, **13** and **14**, the facile dissociation of the carboxylate ligands would partly attributable to the intramolecular hydrogen bondings that stabilize the dissociated carboxylates, although the reason for the

irreversibility of **10** has not been clear. The species that gave a redox process at around $E_{1/2}$ = –1.13 V was not characterized, but this potentials suggests the formation of a cluster having a charge-neutral ligand in addition to the tridentate thiolate.[16] A plausible structure could be the acetonitrile adduct.

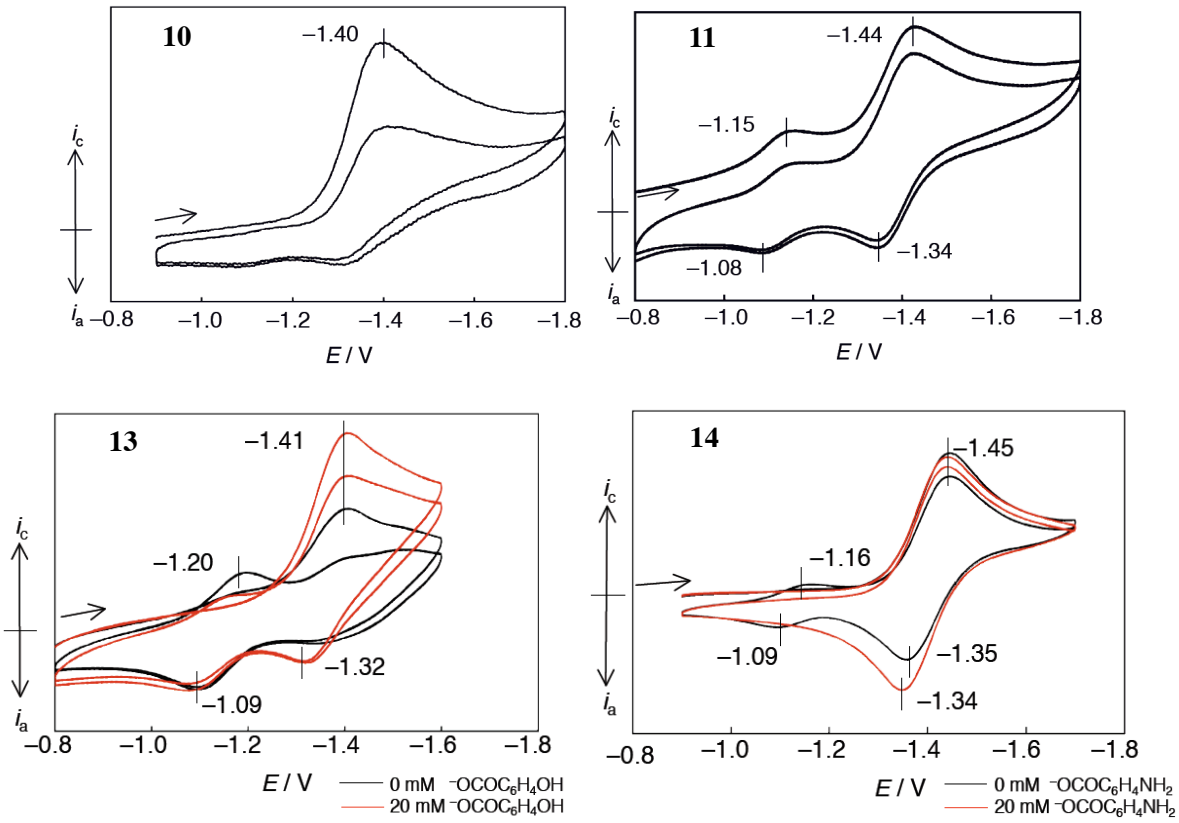

Figure 3-4. CV spectra of cluster **10**, **11**, **13**, and **14**.

When the author collected the CV data for **14** in THF, the reversibility for the $[Fe_4S_4]^{2+}/[Fe_4S_4]^{+}$ redox was considerably improved, and became reversible in CH_2Cl_2. The results suggest that the dissociation of the carboxylate ligands is promoted in the polar and highly coordinating solvent.

Previously, Nakamura an co-workers reported the effect of the hydrogen bonding

interation toward the thiolate ligand S for the [4Fe-4S] clusters having four thiolates ligands.[17] In their case, the significant positive shift for the $[Fe_4S_4]^{2+}/[Fe_4S_4]^{+}$ redox potential was observed via the hydrogen bonding interaction because the donation from the thiolate ligands became weaker. Similarly, the coordination of the carboxylate became weaker in the author's case, although the redox potentials of **13**, **14** are similar to the value of **12**.

Table 3-3. Redox potentials of cluster **8**-**15**[a].

	E_{pc} / V	E_{pa} / V	$E_{1/2}$ / V
8	–1.44	–1.36	–1.40
9	–1.47	–1.39	–1.43
10	–1.40	–	–
11	–1.44	–1.34	–1.39
	–1.15	–1.08	–1.12
12	–1.43	–1.36	–1.40
13	–1.41	–	–
	–1.20	–1.09	–1.15
13 with 20 mM			
$(NEt_4)(OCOC_6H_4OH)$	–1.41	–1.32,	–1.37
	–	–1.09	–
14	–1.45	–1.35	–1.40
	–1.16	–1.09	–1.13
14 with 20 mM			
$(NEt_4)(OCOC_6H_4NH_2)$	–1.45	–1.34	–1.40
15	–1.45	–1.36	–1.41

[a] The data were recorded in 0.1 M *n*-Bu_4NPF_6 solution (CH_3CN) with glassy carbon working electrode, a Pt counter electrode, and a $Ag/AgNO_3$ reference electrode. The scan rate was 0.1 Vs^{-1}.

3.2.5 Redox properties of the model clusters and those in metalloproteins

The redox potentials of the carboxylate clusters **8**-**15** exhibit a significant positive shift from that of the thiolate cluster **4a**, and thus the carboxylate clusters function as a better electron acceptor. This redox property conforms to the arrangement of the [4Fe-4S] clusters in the electron transfer systems included in DPOR,[3] where the electron flows from the all-cysteine [4Fe-4S] cluster to the active site through the aspartate [4Fe-4S] cluster shown in Chart 3-1.[18] A similar electron relay is also included in formaldehyde oxidoreductase (FOR) with *Pf* ferredoxin,[2] in which electron flows in an opposite direction from active site to cysteine cluster, and further to aspartate cluster.[19]

It is also notable that the reduction potential of WT *Pf* ferredoxin at E_m = –368 mV showed a 58 mV negative shift upon mutation of aspartate to cysteine coordinated to the unique iron site of the cluster.[2b] The shift of the potential is similar to the values for the model clusters (ΔE = 60-120 mV). It was also reported that no activity was found for the D36C DPOR mutant,[3d] which contains an all-cysteine cluster instead of the aspartate cluster (Chart 3-1). A conceivable reason is that the electron transfer is blocked between the two [4Fe-4S] clusters according to this work.

3.3 Summary

The author synthesized a series of [4Fe-4S] clusters coordinated by three thiolates and one carboxylate. The model studies provided us with various important pieces of information. An important achievement is that the carboxylate coordination geometry was confirmed by X-ray structural analysis, in which the carboxylates would be commonly coordinated to the unique iron site in η^1 rather than η^2 manner, and it conforms to similar protein structures. Because the CO_2^- stretching frequencies from KBr disk and acetonitrile solution are almost identical, the coordination mode would be retained even in the solution. Another achievement resides in the redox potentials for the $[4Fe\text{-}4S]^{2+/1+}$ process. The positively shifted potential of the carboxylate clusters conforms to the arrangement of the thiolate and carboxylate clusters in the electron relay systems.

3.4 Experimental Section

General:

All compounds were handled under an atmosphere of pure nitrogen using standard Schlenk techniques or glove boxes. Hexane, ether, THF, acetonitrile, dichloromethane, DMF were degassed and purified by the method described by Grubbs, in which the solvents were passed over columns of activated alumina and a copper catalyst supplied by Hansen & Co. Ltd.. ^{1}H NMR spectra were acquired by using a JEOL ECA-600. NMR assignments were supported by additional 2D NMR experiments. Cyclic Voltammograms were recorded on a BAS-ALS-660A electron analyzer using a glassy carbon working electrode and 0.1 M (CH_3CN, CH_2Cl_2) or 0.2 M (THF) *n*-Bu_4NPF_6 as the supporting electrolyte, in which the potentials are referred to the $Ag/AgNO_3$ electrode. Electrospray ionization time-of-flight mass spectrometry (ESI-TOF-MS) spectra were obtained from a Micromass LCT TOF-MS spectrometer or Bruker microTOF II-NUT. Infrared spectra were recorded with a JASCO FT/IR-410. UV/Vis spectra were recorded in 10-mm quartz glass cells with a JASCO V560 spectrometer. Elemental analyses were performed on a LECO-CHNS-932 elemental analyzer or Elementar Analysensysteme GmbH varioMICRO where the samples were sealed in tin or silver capsules under nitrogen. $(PPh_4)_2[Fe_4S_4(SEt)(TempS_3)]$ (**4a**) was synthesized according to chapter 2.

Synthesis:

$(PPh_4)_2[Fe_4S_4(OCOCH_3)(TempS_3)]$ (8): Acetic acid in acetonitrile (0.17 M, 2.3 mL, 0.40 mmol) was added to **4a** (150 mg, 0.088 mmol) in acetonitrile (30 mL), and stirred for 4 h. After removal of all the volatiles in vacuo very slowly, the residue was washed by ether and

THF mixture solvent and extracted by acetonitrile (15 mL). Removal of solvent in vacuo gave **8** as black powder (100 mg, 0.059 mmol, 67% yield). Layering hexane and ether on acetonitrile solution of **8** gave black plate crystals. Anal. Calc. for $C_{86}Fe_4S_7H_{82}O_5P_2•C_2H_3N•C_{1.5}H_{3.5}$: C, 60.80; H, 5.05; N, 0.79; S, 12.70. Found: C, 61.15; H, 5.25; N, 0.84; S, 12.31. ^{1}H NMR (CD_3CN, δ); 7.89 (s, $P(C_6H_5)_4$), 7.72-7.58 (m, arom + $P(C_6H_5)_4$), 6.30 (br, arom), 5.55 (br, arom), 4.58 (s, $OCOCH_3$), 3.99 (s, OCH_3), 3.37 (s, CH_2), 2.32 (br, CH_2CH_3), 1.11 (t, CH_2CH_3, 9H). Cyclic voltammetry (CH_3CN, 0.1 V/s); $E_{1/2}$ = –1.40 V, (THF, 0.1 V/s); $E_{1/2}$ = –1.54. UV/Vis (CH_3CN); λ_{max} [nm] (ε [$cm^{-1}•M^{-1}$]) = 456 (1.2 x 10^4), 299 (2.0 x 10^4) sh. IR (KBr); $\nu(COO^-)$ = 1571, 1373 cm^{-1}.

$(PPh_4)_2[Fe_4S_4(OCOCH=CH_2)(TempS_3)]$ (9): Cluster **9** was synthesized as described for **8** from **4a** (91 mg, 0.053 mmol) and acrylic acid (0.26 M, 0.22 mL, 0.057 mmol) in 38% yield as black micro crystal (35 mg, 0.020 mmol). Anal. Calc. for $C_{87}Fe_4S_7H_{82}O_5P_2$: C, 60.85; H, 4.81; S, 13.07. Found: C, 60.95; H, 4.85; S, 12.97. ^{1}H NMR (CD_3CN, δ); 8.23 (br, $OCOCH=CH_2$), 7.90 (s, $P(C_6H_5)_4$), 7.72-7.65 (m, arom + $P(C_6H_5)_4$), 6.32 (br, arom), 6.02 (br, $OCOCH=CH_2$), 5.66 (br, $OCOCH=CH_2$), 5.55 (br, arom), 3.99 (s, OCH_3), 3.37 (s, CH_2), 2.32 (br, CH_2CH_3), 1.12 (t, CH_2CH_3). Cyclic voltammetry (CH_3CN, 0.1 V/s); $E_{1/2}$ = –1.43 V. UV/Vis (CH_3CN); λ_{max} [nm] (ε [$cm^{-1}•M^{-1}$]) = 466 (9.4 x 10^3), 361 (1.1 x 10^4) sh., 294 (1.9 x 10^4) sh. IR (KBr); $\nu(COO^-)$ = 1557, 1406 cm^{-1}.

$(PPh_4)_2[Fe_4S_4(OCOC\equiv CH)(TempS_3)]$ (10): Cluster **10** was synthesized as described for **8** from **4a** (160 mg, 0.093 mmol) and propiolic acid (0.16 M, 1.2 mL, 0.19 mmol) in 80% yield as crystals (128 mg, 0.075 mmol). Anal. Calc. for $C_{87}Fe_4S_7H_{80}O_5P_2•C_2H_3N•C_{1.5}H_{3.5}$: C, 61.14;

H, 4.90; N, 0.79; S, 12.62. Found: C, 61.53; H, 5.16; N, 0.81; S, 11.72. Cyclic voltammetry (CH_3CN, 0.1 V/s); E_{pc} = –1.40 V. IR (KBr); $\nu(COO^-)$ = 1615, 1313 cm^{-1}, ν (C≡C) = 2091 cm^{-1}.

$(PPh_4)_2[Fe_4S_4(OCOCH{=}CH(cis\text{-}COOH))(TempS_3)]$ (11): Cluster **11** was synthesized as described for **8** from **4a** (150 mg, 0.088 mmol) and maleic acid (0.018 M, 5.0 mL, 0.090 mmol) in 15% yield as crystals (24 mg, 0.014 mmol), except for using acetonitrile and DMF solution of **5** in crystallization. Anal. Calc. for $C_{88}Fe_4S_7H_{82}O_7P_2$: C, 60.01; H, 4.69; S, 12.74. Found: C, 60.08; H, 5.18; S, 12.89. ^{1}H NMR (CD_3CN, δ); 7.90 (s, P(C_6H_5)$_4$), 7.72-7.65 (m, arom + P(C_6H_5)$_4$), 6.34 (br, arom), 5.60 (br, arom), 3.99 (s, OCH_3), 3.37 (s, CH_2), 2.32 (br, CH_2CH$_3$), 1.13 (s, CH$_2$CH_3), the protons of carboxylate ligand *were not assignable*. Cyclic voltammetry (CH_3CN, 0.1 V/s); $E_{1/2}$ = –1.12, –1.39 V. UV/Vis (CH_3CN); λ_{max} [nm] (ε [cm^{-1}•M^{-1}]) = 472 (1.4 x 10^4), 363 (1.7 x 10^4) sh, 288 (2.5 x 10^4).

$(PPh_4)_2[Fe_4S_4(OCOC_6H_5)(TempS_3)]$ (12): Cluster **12** was synthesized as described for **8** from **4a** (95 mg, 0.056 mmol) and benzoic acid (0.046 M, 1.5 mL, 0.069 mmol) in 38% yield as black micro crystals (38 mg, 0.022 mmol). Anal. Calc. for $C_{91}Fe_4S_7H_{84}O_5P_2$: C, 61.84; H, 4.79; S, 12.70. Found: C, 61.60; H, 4.90; S, 12.60. ^{1}H NMR (CD_3CN, δ); 8.13 (br, OCOC$_6H_5$), 7.90 (t, P(C_6H_5)$_4$), 7.72-7.64 (m, arom + P(C_6H_5)$_4$), 7.57 (br, OCOC$_6H_5$), 7.27 (br, OCOC$_6H_5$), 6.33 (br, arom), 5.59 (br, arom), 4.00 (s, OCH_3), 3.38 (s, CH_2), 2.32 (br, CH_2CH$_3$), 1.13 (s, CH$_2$CH_3). Cyclic voltammetry (CH_3CN, 0.1 V/s); $E_{1/2}$ = –1.40 V, (THF, 0.5 V/s); $E_{1/2}$ = –0.31, –1.53 V attributable to the $[Fe_4S_4]^{2+}/[Fe_4S_4]^{3+}$ and $[Fe_4S_4]^{2+}/[Fe_4S_4]^{+}$ processes, (CH_2Cl_2, 0.1 V/s); $E_{1/2}$ = –0.24, –1.48 V attributable to the $[Fe_4S_4]^{2+}/[Fe_4S_4]^{3+}$ and $[Fe_4S_4]^{2+}/[Fe_4S_4]^{+}$

processes. UV/Vis (CH_3CN); λ_{max} [nm] (ε [cm^{-1}•M^{-1}]) = 462 (1.1 x 10^4), 354 (1.4 x 10^4) sh, 297 (2.1 x 10^4) sh. IR (KBr); $\nu(COO^-)$ = 1622, 1322 cm^{-1}.

$[PPh_4]_2[Fe_4S_4(OCOC_6H_4(o\text{-}OH))(TempS_3)]$ (13): Cluster **13** was synthesized as described for **8** from **4a** (100 mg, 0.059 mmol) and salicylic acid (0.012 M, 5.0 mL, 0.059 mmol) in 65% yield as black crystals (68 mg, 0.038 mmol). Anal. Calc. for $C_{91}Fe_4S_7H_{84}O_6P_2$: C, 61.29; H, 4.75; S, 12.59. Found: C, 61.01; H, 4.84; S, 12.42. ^{1}H NMR (CD_3CN, δ); 8.07 (br, $OCOC_6H_4OH$), 7.88 (t, $P(C_6H_5)_4$), 7.80-7.63 (m, arom + $P(C_6H_5)_4$), 7.13 (br, $OCOC_6H_4OH$), 6.93 (br, $OCOC_6H_4OH$), 6.35 (br, arom), 5.58 (br, arom), 4.00 (s, OCH_3), 3.41 (s, CH_2), 2.33 (br, CH_2CH_3), 1.11 (s, CH_2CH_3), some protons of carboxylate ligand *were not assignable*. Cyclic voltammetry (CH_3CN, 0.1 V/s); $E_{1/2}$ = –1.15 V, E_{pc} = –1.41 V, (the presence of 20 mM (NEt_4)($OCOC_6H_4OH$) in CH_3CN, 0.1 V/s); $E_{1/2}$ = –1.37 V, E_{pa} = –1.09 V. UV/Vis (CH_3CN); λ_{max} [nm] (ε [cm^{-1}•M^{-1}]) = 461 (1.1 x 10^4), 296 (2.3 x 10^4). IR (KBr); $\nu(COO^-)$ = 1597, 1361 cm^{-1}.

$(PPh_4)_2[Fe_4S_4(OCOC_6H_4(o\text{-}NH_2))(TempS_3)]$ (14): Cluster **14** was synthesized as described for **8** from **4a** (100 mg, 0.059 mmol) and anthranilic acid (0.055 M acetonitrile solution, 1.3 mL, 0.072 mmol) in 47% yield as black crystalline powder (49 mg, 0.028 mmol). Anal. Calc. for $C_{91}Fe_4S_7H_{85}O_5NP_2$: C, 61.32; H, 4.81; N, 0.79; S, 12.59. Found: C, 61.04; H, 5.00; N, 1.17; S, 12.38. ^{1}H NMR (CD_3CN, δ); 8.10 (br, $OCOC_6H_4NH_2$), 7.90 (t, $P(C_6H_5)_4$), 7.72-7.64 (m, arom + $P(C_6H_5)_4$), 6.94 (br, $OCOC_6H_4NH_2$), 6.72 (br, $OCOC_6H_4NH_2$), 6.33 (br, arom), 6.13 (br, $OCOC_6H_4NH_2$), 5.58 (br, arom), 4.00 (s, OCH_3), 3.37 (s, CH_2), 2.32 (br, CH_2CH_3), 1.11 (t, CH_2CH_3), some protons of carboxylate ligand *were not assignable*. Cyclic

voltammetry (CH_3CN, 0.1 V/s); $E_{1/2}$ = –1.13, –1.40 V, (the presence of 20 mM $(NEt_4)(OCOC_6H_4NH_2)$ in CH_3CN, 0.1 V/s); $E_{1/2}$ = –1.40 V, (THF, 0.1 V/s); $E_{1/2}$ = –0.40, –1.57 V attributable to the $[Fe_4S_4]^{2+}/[Fe_4S_4]^{3+}$ and $[Fe_4S_4]^{2+}/[Fe_4S_4]^{+}$ processes, (CH_2Cl_2, 0.1 V/s); $E_{1/2}$ = –0.26, –1.48 V attributable to the $[Fe_4S_4]^{2+}/[Fe_4S_4]^{3+}$ and $[Fe_4S_4]^{2+}/[Fe_4S_4]^{+}$ processes. UV/Vis (CH_3CN); λ_{max} [nm] (ε [cm^{-1}•M^{-1}]) = 458 (1.6 x 10^4), 295 (3.1 x 10^4) . IR (KBr); $\nu(COO^-)$ = 1612, 1340 cm^{-1}.

$(PPh_4)_2[Fe_4S_4(OCO(NC_4H_4))(TempS_3)]$ (15): Cluster **15** was synthesized as described for **8** from **4a** (82 mg, 0.048 mmol) and pyrrole-2-carboxylic acid (0.035 M acetonitrile solution, 1.65 mL, 0.058 mmol) in 33% yield as black crystalline powder (28 mg, 0.016 mmol). Anal. Calc. for $C_{89}Fe_4S_7H_{83}O_5NP_2$: C, 60.86; H, 4.76; N, 0.80; S, 12.78. Found: C, 60.37; H, 4.65; N, 0.99; S, 12.32. ^{1}H NMR (CD_3CN, δ); 7.88 (s, $P(C_6H_5)_4$), 7.70-7.63 (m, arom + $P(C_6H_5)_4$), 6.54 (br, $OCOC_4H_3NH$), 6.46 (br, $OCOC_4H_3NH$), 6.32 (br, arom), 6.28 (br, $OCOC_4H_3NH$), 5.55 (br, arom), 3.99 (s, OCH_3), 3.37 (s, CH_2), 2.32 (br, CH_2CH_3), 1.11 (s, CH_2CH_3), one proton of carboxylate ligand *was not assignable*. Cyclic voltammetry (CH_3CN, 0.1 V/s); $E_{1/2}$ = –1.41 V. UV/Vis (CH_3CN); λ_{max} [nm] (ε [cm^{-1}•M^{-1}]) = 457 (1.5 x 10^4), 361 (2.0 x 10^4) sh, 295 (3.5 x 10^4) sh. IR (KBr); $\nu(COO^-)$ = 1559, 1352 cm^{-1}.

Crystal-Structure Determination:

Crystal data and refinement parameters for **8**, **10**, **11**, **13**, and **15** are summarized in Table 3-4. Preliminary crystallographic results for **9**, **12**, and **14** are also given in Table 3-4. Single crystals were mounted on a loop using oil (Paraton, Hampton Research Corp.). Diffraction data were collected at –100 ºC under a cold nitrogen stream on a Rigaku Micromax-007

instrument with a Saturn 70 CCD area detector (for **10**), or on a Rigaku FR-E instrument with a Saturn 70 CCD detector (for **8**, **11**, **13**, and **15**) using graphite-monochromated MoKa radiation (λ = 0.710690 Å). Using an oscillation range of 0.5º, 1080 data images were collected for **10**, while 720 images were measured for **8**, **11**, **13**, and **15**. The data were integrated and corrected for absorption using the Rigaku/MSC CrystalClear program package. The structures were solved by a direct method (SIR92 for **10**, **11**; SIR97 for **13**; SHELXS97 for **8**, **15**) and were refined by full-matrix least squares on F^2 by the Rigaku/MSC CrystalStructure program package. Anisotropic refinement was applied to all non-hydrogen atoms except for disordered atoms and several crystal solvents. All the hydrogen atoms were put at the calculated positions, especially using HFIX147 method for H6A atom of **11** and **13**. In **11**, a phenyl group of PPh_4^+ is disordered over two positions in a 1:1 ratio and an anisole group of tridentate thiolate is disordered. An acetonitrile molecules of **8** and **15** are disordered over two positions in a 2:1 and 1:1 ratio, respectively.

Table 3-4. Crystal data of **8**-**15**.

	8•(CH_3CN)•0.25(C_6H_{14})	**9**	**10**•(CH_3CN)•0.25(C_6H_{14})	**11**•2(DMF)
Fomula	$C_{86}Fe_4S_7H_{82}O_5P_2$•$C_2H_3N$ •$C_{1.5}H_{3.5}$	$C_{87}Fe_4S_7H_{82}O_5P_2$	$C_{87}Fe_4S_7H_{80}O_5P_2$•$C_2H_3N$ •$C_{1.5}H_{3.5}$	$C_{88}Fe_4S_7H_{82}O_7P_2$ •$C_6H_{14}O_2N_2$
Weight	1767.94	1727.36	1777.94	1907.56
Crystal system	monoclinic	monoclinic	monoclinic	monoclinic
Space group	$P2_1/c$ (#14)	$P2_1/n$ (#14)	$P2_1/c$ (#14)	$P2_1/n$ (#14)
a/Å	21.157(3)	14.688(5)	21.208(3)	21.004(5)
b/Å	14.060(2)	22.975(7)	14.108(2)	12.963(3)
c/Å	28.020(4)	23.931(8)	28.139(4)	34.035(8)
β/deg	91.294(2)	94.274(5)	90.578(3)	105.483(4)
V/Å^3	8333(2)	8053(5)	8419(2)	8931(4)
Z	4	4	4	4
D_{calc}/g cm^{-1}	1.409	1.416	1.403	1.419
μ/cm^{-1}	9.482	9.786	9.390	8.940
F(000)	3674.00	3560.00	3690.00	3968.00
$2\theta_{max}$/deg	55.0	50.7	55.0	50.0
no. of rflns (all) indep. rflns	58477	55359	101389	58300
(R_{int})	18769	14668	19266	15753
no. of params	980	961	1007	1045
$R1$ [a]	0.0781	0.1490	0.0553	0.1105
w$R2$ [b]	0.02678	0.2143	0.1647	0.3278
GOF[c]	1.067	1.037	1.186	1.049

[a] $R1 = ||F_o|-|F_c|| / \Sigma|F_o|$ ($I>2\sigma(I)$). [b] $wR2=\{[\Sigma w(|F_o|-|F_c|)^2/\Sigma wF_o^2]\}^{1/2}$ (all data). [c] GOF = $[\Sigma w(|F_o|-|F_c|)^2/(N_o-N_v))^{1/2}$ (N_o = number of observations, N_v = number of variables).

Table 3-4. (cont)

	12•2(CH_3CN)•(Et_2O)	**14**•(CH_3CN)•0.5(Et_2O)	**13**	**15**•(CH_3CN)
Fomula	$C_{91}Fe_4S_7H_{84}O_5P_2$ •$C_4H_6N_2$•$C_4H_{10}O$	$C_{91}Fe_4S_7H_{85}O_5P_2$•$C_2H_3N$ •$C_2H_5O_{0.5}$	$C_{91}Fe_4S_7H_{84}O_6P_2$	$C_{89}Fe_4S_7H_{83}O_5NP_2$ •C_2H_3N
Weight	1777.94	1860.55	1783.42	1797.45
Crystal system	orthorhombic	orthorhombic	monoclinic	monoclinic
Space group	$P2_12_12_1$ (#19)	$P2_12_12_1$ (#19)	$P2_1/n$ (#14)	$P2_1/c$ (#14)
a/Å	14.145(3)	14.1845(13)	13.033(2)	30.000(4)
b/Å	17.344(4)	17.371(2)	25.109(4)	13.037(2)
c/Å	37.459(8)	37.424(3)	25.071(4)	23.319(3)
β/deg	–	–	91.042(4)	111.7250(10)
V/Å^3	9190(4)	9221(2)	8203(2)	8473(2)
Z	4	4	4	4
D_{calc}/g cm^{-1}	1.390	1.340	1.444	1.409
μ/cm^{-1}	8.671	8.613	9.646	9.343
F(000)	4008.00	3868.00	3696.00	3728.00
$2\theta_{max}$/deg	50.8	50.7	55.0	55.0
no. of rflns (all)	55774	63189	66980	67501
indep. rflns (R_{int})	16654	16796	18411	19364
no. of params	1041	1035	998	997
$R1$ [a]	0.0731	0.0655	0.0866	0.0721
w$R2$ [b]	0.2058	0.1911	0.2866	0.2410
GOF[c]	1.081	1.090	1.049	1.059

[a] $R1 = ||F_o|-|F_c|| / \Sigma|F_o|$ ($I>2\sigma(I)$). [b] $wR2=\{[\Sigma w(|F_o|-|F_c|)^2/\Sigma wF_o^2]\}^{1/2}$ (all data). [c] GOF = $[\Sigma w(|F_o|-|F_c|)^2/(N_o-N_v))^{1/2}$ (N_o = number of observations, N_v = number of variables).

References for Chapter 3

[1] a) A. Messerchmidt, R. Huber, T. Poulos, K. Wiehardt, *Handbook of Metalloproteins vol. 1,* John Wiley & Sons, Chichester, UK, **2001**, pp471–485; b) A. Messerchmidt, R. Huber, T. Poulos, K. Wiehardt, *Handbook of Metalloproteins vol. 2,* John Wiley & Sons, Chichester, UK, **2001**, 738–751, 880–896; c) M. G. Bertero, R. A. Rothery, M. Palak, C. Hou, D. Lim, F. Blasco, J. H. Weiner, N. C. J. Strynadka, *Nature Structural Biology* **2003**, *10*, 681–687; d) L. A. Sazanov, P. Hinchliffe, *Science* **2006***, 311*, 1430–1436; e) T. Gräwert, I. Span, W. Eisenreich, F. Rohdich, J. Eppinger, A. Bacher, M. Groll, *Proc. Natl. Acad. Sci.* **2010**, *107*, 1077–1081; f) A. Messerchmidt, *Handbook of Metalloproteins vol. 4,* John Wiley & Sons, Chichester, UK, **2011**, pp172–182, 397–412; g) S. H. Knauer, W. Buckel, H. Dobbek, *J. Am. Chem. Soc.* **2011**, *133*, 4342–4347.

[2] a) Z. H. Zhou, M. W. W. Adams, *Biochemistry* **1997**, *36,* 10892–10900; b) P. S. Brereton, M. F. J. M. Verhagen, Z. H. Zhou, M. W. W. Adams, *Biochemistry* **1998,** *37,* 7351-7362; c) Y. Hu, S. Faham, R. Roy, M. W. W. Adams, D. C. Rees, *J. Mol. Biol.* **1999**, *286*, 899–914; d) A. Messerchmidt, R. Huber, T. Poulos, K. Wiehardt, *Handbook of Metalloproteins vol. 2,* John Wiley & Sons, Chichester, UK, **2001**, pp1086-1096.

[3] a) Y. Fujita, C. E. Bauer, *J. Biol. Chem.* **2000**, *275*, 23583–23588; b) R. Sarma, B. M. Barney, T. L. Hamilton, A. Jones, L. C. Seefeldt, J. W. Peters, *Biochemistry* **2008**, *47*, 13004–13015; c) J. Nomata, T. Ogawa, M. Kitashima, K. Inoue, Y. Fujita, *FEBS Lett.* **2008**, *582*, 1346–1350; d) N. Muraki, J. Nomata, K. Ebata, T. Mizoguchi, T. Shiba, H. Tamiaki, G. Kurisu, Y. Fujita, *Nature* **2010**, *465*, 110-115.

[4] a) A. H. Robbins, C. D. Stout, *Proc. Natl. Acad. Sci. USA* **1989**, *86*, 3639–3643; b) H. Lauble, M. C. Kennedy, H. Beinert, C. D. Stout, *J. Mol. Biol.* **1994**, *237*, 437–451; c) H. Lauble, M. C. Kennedy, H. Beinert, C. D. Stout, *Biochemistry* **1992**, *31*, 2135–2748; d) H. Lauble, C. D. Stout, *Proteins: Structure, Function, and Genetics* **1995**, *22*, 1–11; e) H. Beinert, M. C. Kennedy, C. D. Stout, *Chem. Rev.* **1996**, *96*, 2335–2373; f) S. J. Lloyd, H. Lauble, G. S. Prasad, C. D. Stout, *Protein Sci.* **1999** *8*, 2655–2662.

[5] a) M. Lee, T. Gräwert, F. Quitterer, F. Rohdich, J. Eppinger, W. Eisenreich, A. Bacher, M. Groll, *J. Mol. Biol.* **2010**, *404*, 600–610; b) W. Wang, J. Li, K. Wang, C. Huang, Y. Zhang, E. Oldfield, *Proc. Natl. Acad. Sci.* **2010**, *107*, 11189–11193; c) Y. Xiao, R. L. Nyland II, C. L. F. Meyers, P. Liu, *Chem. Commun.* **2010**, *46*, 7220–7222; d) W. Xu, N. S. Lees, D. Adedeji, J. Wiesner, H. Jomaa, B. M. Hoffman, E. C. Duin, *J. Am. Chem. Soc.* **2010**, *132*, 14509–14520.

[6] a) H. J. Sofia, G. Chen, B. G. Hetzler, J. F. Reyes-Spindola, N. E. Miller, *Nucleic Acids Research*, **2001**, *29*, 1097–1106; b) F. Berkovitch, Y. Nicolet, J. T. Wan, J. T. Jarrett, C. L. Drennan, *Science* **2004***, 303*, 76–79; c) P. Hänzelmann, H. Schindelin, *Proc. Natl. Acad, Sci. USA* **2004**, *101*,

12870–12875; d) C. J. Walsby, D. Ortillo, J. Yang, M. R. Nnyepi, W. E. Broderick, B. M. Hoffman, J. B. Broderick, *Inorg. Chem.* **2005**, *44*, 727–741; e) B. W. Lepore, F. J. Ruzicka, P. A. Frey, D. Ringe, *Proc. Natl. Acad, Sci. USA*, **2005**, *102*, 13819–13824; f) J. L. Vey, J. Yang, M. Li, W. E. Broderick, J. B. Broderick, C. L. Drennan, *Proc. Natl. Acad, Sci. USA* **2008**, *105*, 16137–16141; g) F. Yan, J. M. LaMarre, R. Röhrich, J. Wiesner, H. Jomaa, A. S. Mankin, D. G. Fujimori, *J. Am. Chem. Soc.* **2010**, *132*, 3953–3964; h) J. L. Vey, C. L. Drennan, *Chem. Rev.* **2011**, *111*, 2487–2506.

[7] a) R. W. Johnson, R. H. Holm, *J. Am. Chem. Soc.* **1978**, *100*, 5338–5344; b) D. J. Evans, *Inorg. Chim. Acta* **1993**, *203*, 253–256; c) Y.-J. Fu, X. Yang, X.-B. Wang, L.-S. Wang, *Inorg. Chem.* **2004**, *43*, 3647–3655.

[8] J. A. Weigel, R. H. Holm, *J. Am. Chem. Soc.* **1991**, *113*, 4184–4191.

[9] G. P. F. van Strijdonck, P. T. J. H. ten Have, M. C. Feiters, J. G. M. van der Linden, J. J. Steggerda, R. J. M. Nolte, *Chem. Ber./Recueil* **1997**, *130,* 1151–1157.

[10] S. Nag, K. Banerjee, D. Datta, *New J. Chem.* **2007**, *31*, 832–834.

[11] a) S. Ménage, L. Que Jr. *Inorg. Chem.* **1990,** *29,* 4293-4297; b) J. R. Hagadorn, L. Que Jr. W. B. Tolman, *Inorg. Chem.* **2000**, *39,* 6086–6090; c) D. Lee, S. J. Lippard, *Inorg. Chim. Acta* **2002**, *341*, 1–11.

[12] A similar intermolecular hydrogen bonding interaction for zinc pyrrole-2-carboxylate was reported, see T. A. Zevaco, H. Görls, E. Dinjus, *Polyhedron* **1998**, *17*, 2199–2206.

[13] Y. Ohki, K. Tanifuji, N. Yamada, M. Imada, T. Tajima, K. Tatsumi, *Proc. Natl. Acad. Sci.* **2011**, *108*, 12635–12640.

[14] C. Zhou, R. H. Holm, *Inorg. Chem.* **1997**, *36,* 4066–4077.

[15] G. P. F. van Strijdonck, J. A. E. H. van Haare, J. G. M. van der Linden, J. J. Steggerda, R. J. M. Nolte, *Inorg. Chem.* **1994**, *33*, 999–1000.

[16] Holm *et al* reported that the redox potentials of [4Fe-4S] clusters having a tridentate ligand and a neutral ligands such as imidazole, pyridine, and phosphine shows ca 20 mV positive shift relative to the value of the acetate cluster, see ref 14.

[17] R. Ohno, N. Ueyama, A. Nakamura, *Inorg. Chem.* **1991**, *30*, 4887–4891.

[18] The theoretical analysis showed the redox potential $[4Fe\text{-}4S]^{2-/3-}$ of four cysteines coordinated [4Fe-4S] cluster has more positive than that of one aspartate and three cysteine coordinated [4Fe-4S] cluster in DMF, which is different from results of our models, see Y. Takano, Y. Yonezawa, Y. Fujita, G. Kurisu, H. Nakamura, *Chem. Phys. Lett.* **2011**, *503*, 296–300.

[19] The theoretical study showed similar results, see K. P. Jensen, B.-L. Ooi, H. E. M. Christensen, *Inorg. Chem.* **2007**, 46, 8710–8716.

Chapter 4

[3:1] Site-Differentiated [4Fe-4S] Cluster Having One Imidazole and Three Thiolates

4.1 Introduction

The [3:1] site-differentiated [4Fe-4S] clusters, which have three cysteine thiolates and one other ligand, have been discovered in some metalloproteins.[1-6] One type of [3:1] site-differentiated clusters have one histidine imidazole, which are found in [NiFe] hydrogenase from *Desulfovibrio gigas* (*Dg*) and *Desulfovibrio fructosovorans* (*Df*),[2] [FeFe] hydrogenase from *Clostridium pasteurianum*,[3] membrane-bound nitrate reductase A from *Escherichia coli*,[4] dihydronicotinamide adenine dinucleotide (NADH)-ubiquinone oxidoreductase from *Thermus thermophilus*,[5] and 4-hydroxybutyryl-CoA dehydratase from the γ-aminobutyrate-fermenting *Clostridium aminobutyricum*.[6]

In order to understand roles of the imidazole ligands, synthesis of the [4Fe-4S] clusters coordinated by three thiolates and one imidazole have been studied.[7-9] Holm *et al* prepared the site-differentiated cluster $[Fe_4S_4Cl(LS_3)]^{2-}$ by using the tridentate thiolate LS_3^{3-}, and replaced the chloride with 2-methylimidazole and 4-methylimidazole. These clusters were prepared in situ, characterized by ^{1}H NMR spectra, and analyzed by cyclic voltammograms.[8] Recently the author's group have developed a new synthetic route to such site-differentiated clusters, using the all-ferric $[Fe_4S_4\{N(SiMe_3)_2\}_4]$ and its one-electron reduced form as precursors. Thus, the author's group obtained $[Fe_4S_4(SDmp)_3(Me_4Im)]^-$ and its one-electron reduced form $[Fe_4S_4(SDmp)_3(Me_4Im)]^{2-}$ by introducing the bulky thiolate $DmpS^-$ (Dmp = 2,6-dimesitylphenyl, Me_4Im = tetramethylimidazole), and the molecular structures and redox properties were elucidated.[9] The author has also conducted the synthesis of site-differentiated [4Fe-4S] clusters by using the newly designed tripodal trithiol $Temp(SH)_3$ (**1a**) to expand the scope, and have reported a series of site-differentiated [4Fe-4S] clusters as indicated by chapter 2 and 3. Although the use of tripodal trithiol follows the Holm's strategy, the new ligands have advantage in that they can be prepared easily in short steps, and in that they tend to give crystalline [4Fe-4S] clusters suitable for X-ray structural analysis. In this chapter, the

author reports the synthesis of the [4Fe-4S] clusters having one tetramethylimidazole and 1-methylimidazole, and also those carrying 2-methylimidazole and 4-methylimidazole that serve as better histidine models with leaving protons on the imidazole N atoms. Their molecular structures and redox properties have been investigated.

4.2 Results

4.2.1 Synthesis of imidazole coordinated [3:1] site-differentiated clusters

In chapter 2, the author has reported that site-selective substitution of the ethanethiolate ligand of $(PPh_4)_2[Fe_4S_4(SEt)(TempS_3)]$ (**4a**) was achieved by treatment with benzenethiol and hydrogen sulfide to give the corresponding adducts respectively with concomitant release of ethanethiol. The synthesis of the clusters having one carboxylate ligand $(PPh_4)_2[Fe_4S_4(OCOR)(TempS_3)]$ (R = Me, $CH{=}CH_2$, Ph, and so on) that serve as models of the [4Fe-4S] clusters having a carboxylate in organisms was also achieved by a similar procedure, described as chapter 3. However, this method was not applicable to the synthesis of those having imidazole derivatives at the unique iron site due to their much less acidity. Therefore, the ethanethiolate ligand of **4a** should have been substituted by a better leaving group, and thus the synthesis of the triflate adduct was examined as was also reported by Holm *et al*.[10] When cluster **4a** was treated with $(NEt_3H)(OTf)$ in acetonitrile, complete consumption of **4a** was indicated by ESI-MS spectra, and the formation of a single product was confirmed by ^{1}H NMR spectra. These results indicate the formation of the triflate cluster $(PPh_4)_2[Fe_4S_4(OTf)(TempS_3)]$ (**16**), although the isolation and full-characterization has not

been achieved.[11]

When the triflate cluster **16** was prepared accordingly and was reacted with tetramethylimidazole in acetonitrile, the imidazole adduct $(PPh_4)[Fe_4S_4(Me_4Im)(TempS_3)]$ (**17**) was formed as confirmed by ESI-MS spectra. Crystallization from acetonitrile/hexane/ether gave **17** in 50% yield as black crystals. The reactions with 1-methylimidazole, 2-methylimidazole, and 4-methylimidazole also proceeded similarly, and the corresponding imidazole adducts $(PPh_4)[Fe_4S_4(1\text{-}MeH_3Im)(TempS_3)]$ (**18**, 1-MeH_3Im = 1-methylimidazole), $(PPh_4)[Fe_4S_4(2\text{-}MeH_3Im)(TempS_3)]$ (**19**, 2-MeH_3Im = 2-mehylimidazole), and $(PPh_4)[Fe_4S_4(4\text{-}MeH_3Im)(TempS_3)]$ (**20**, 4-MeH_3Im = 4-methylimidazole) were obtained. . Due to the less solubility of **18**, **19**, and toward acetonitrile, these clusters were dissolved into a mixture of acetonitrile and DMF, and crystallized by layering hexane and ether onto it.

In the reaction with 4-methylimidazole, a trace amount of $(PPh_4)_3[\{Fe_4S_4(TempS_3)\}_2(MeH_2Im)]$ (**21**) was obtained as crystals along with **20**, which was also characterized by X-ray structural analysis, shown in Figure 4-1.

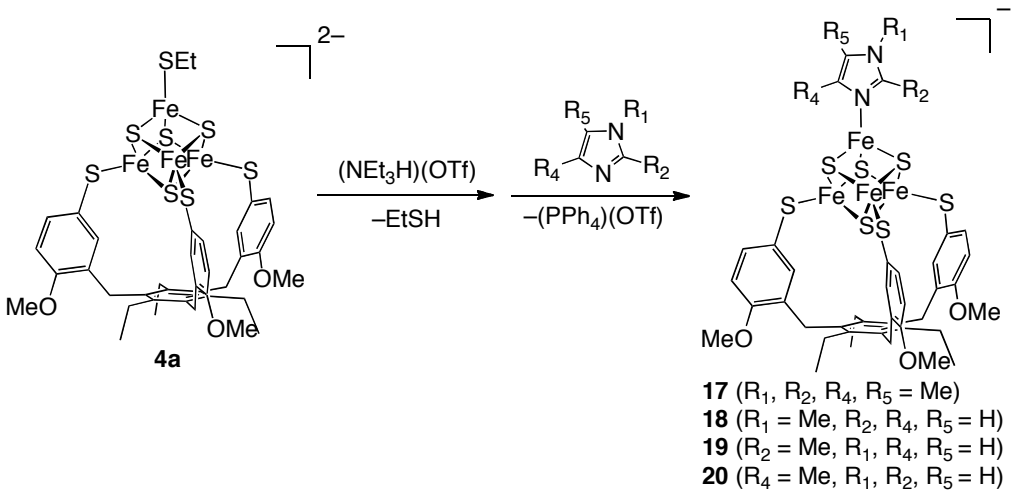

Scheme 4-1. Synthesis of **17-20**.

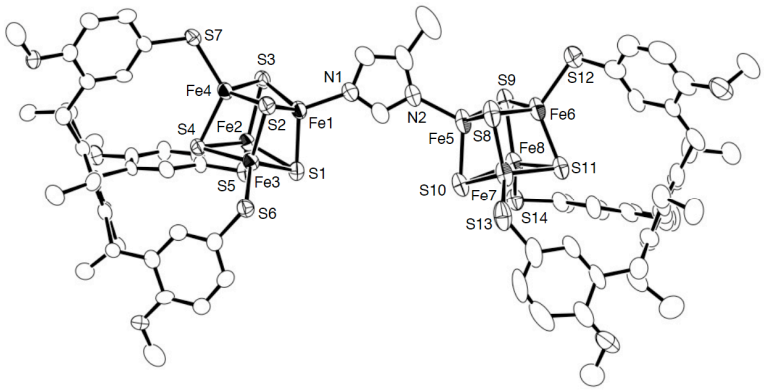

Figure 4-1. Molecular structures of the anion of **21** with 30% thermal ellipsoids. Hydrogen atoms are omitted for clarity.

4.2.2 X-ray crystallography

The molecular structures of **17**-**20** were analyzed by single crystal X-ray structural analysis. The selected bond lengths and angles are collected in Table 4-1. As shown in Figure 4-2, their [4Fe-4S] cores are capped by the tridentate thiolate $TempS_3^{3-}$ at the three irons as is observed for **4a**, and the unique irons are coordinated by the respective imidazole derivatives at the N atoms. Although the reaction with 4-methylimidazole could have afforded 5-methylimidazole adduct as an isomer, 4-methyl-isomer **20** was obtained as a single isomer.[12] The metric parameters of the [4Fe-4S] cores such as Fe-Fe and Fe-S distances, especially those around the unique irons, are unexceptional and similar to those of **4a**, although the unique irons are coordinated by charge-neutral imidazoles. A notable feature for **19**,**20** is that these particular clusters form a dimeric structure through intermolecular hydrogen bondings between the imidazole NH proton and the thiolate sulfur of $TempS_3^{3-}$ ligand as shown in Figure 3, in which the N•••S distances for **19** and **20** are 3.258 (3) and 3.403 (7) Å, respectively (Figure 4-3).

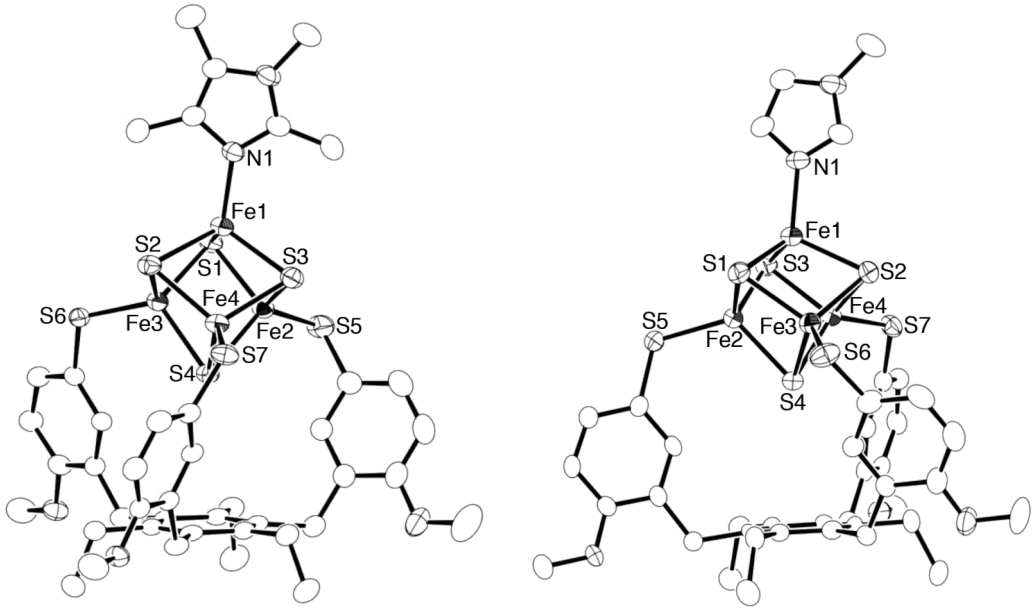

17

18

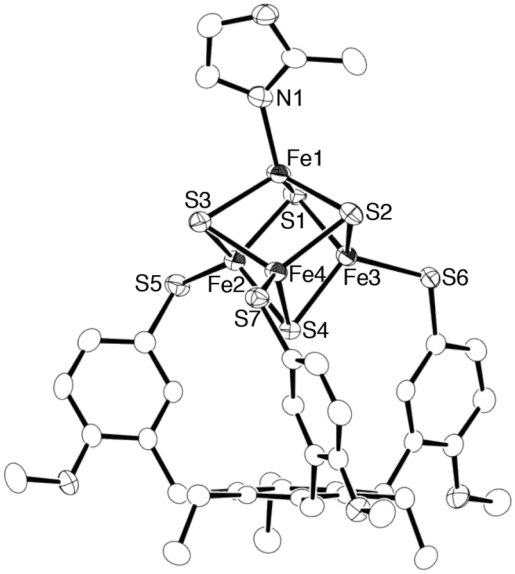

19

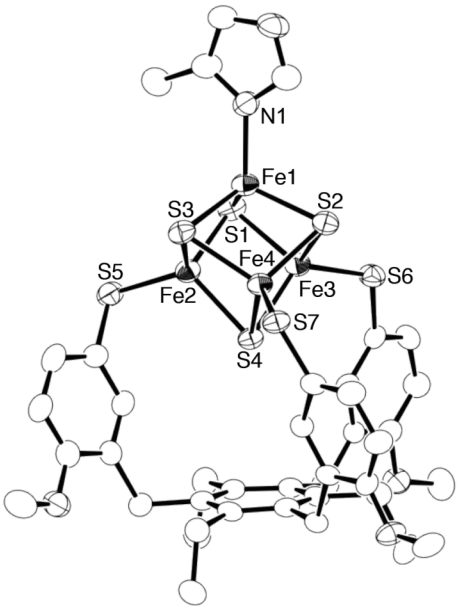

20

Figure 4-2. Molecular structures of the anion of **17**-**20** with 50% thermal ellipsoids. Hydrogen atoms are omitted for clarity.

Table 4-1. Selected bond lengthes of cluster **17**-**20**

	17	**18**	**19**	**20**
Fe1-Fe2	2.7232(6)	2.7153(12)	2.7165(7)	2.6989(14)
Fe1-Fe3	2.7710(7)	2.6941(13)	2.7398(8)	2.7109(12)
Fe1-Fe4	2.7453(6)	2.7084(13)	2.6723(9)	2.7562(14)
Fe2-Fe3	2.7245(6)	2.7691(13)	2.7568(8)	2.7366(15)
Fe2-Fe4	2.7517(6)	2.7248(12)	2.7227(8)	2.7365(13)
Fe3-Fe4	2.7253(6)	2.7352(13)	2.7116(8)	2.7303(14)
Fe1-S1	2.2343(9)	2.2219(19)	2.2267(10)	2.2653(17)
Fe1-S2	2.3095(9)	2.2850(18)	2.3053(10)	2.2650(19)
Fe1-S3	2.3118(9)	2.2996(19)	2.3058(9)	2.287(3)
Fe2-S1	2.3139(8)	2.3181(19)	2.3218(10)	2.288(3)
Fe2-S3	2.2484(10)	2.2464(19)	2.2480(10)	2.2913(17)
Fe2-S4	2.3045(9)	2.2921(17)	2.3085(9)	2.2829(16)
Fe3-S1	2.3240(9)	2.3069(18)	2.3261(9)	2.2925(18)
Fe3-S2	2.2346(9)	2.2559(18)	2.2428(10)	2.2833(17)
Fe3-S4	2.3018(8)	2.3092(17)	2.2998(9)	2.2732(19)
Fe4-S2	2.3024(9)	2.3097(19)	2.3096(9)	2.288(2)
Fe4-S3	2.3068(10)	2.3023(19)	2.3093(9)	2.3017(18)
Fe4-S4	2.2299(9)	2.2314(17)	2.2168(9)	2.2563(15)
Fe1-N1	2.032(3)	2.017(6)	2.020(3)	2.028(5)
Fe2-S5	2.2534(9)	2.2529(17)	2.2500(10)	2.2451(19)
Fe3-S6	2.2548(9)	2.250(2)	2.2538(10)	2.237(2)
Fe4-S7	2.2603(9)	2.2517(18)	2.2575(9)	2.2706(18)

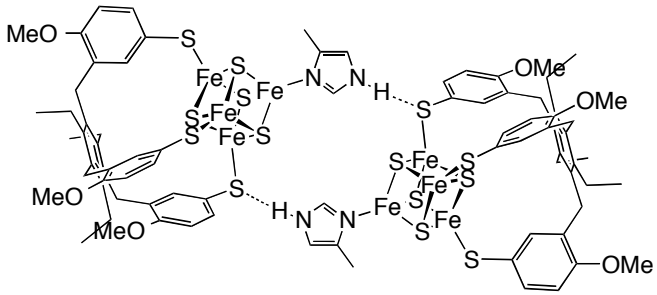

Figure 4-3. Interaction of two molecular of **20**.

4.2.3 Redox behavior of 17-20

The cyclic voltammograms (CV) of **17**-**20** were measured in acetonitrile using $Ag/AgNO_3$ reference electrode (Table 4-2). The spectrum of **17** recorded with 0.1 V/s scan rate shows one pseudo-reversible wave (E_{pc} = –1.25 V, E_{pa} = –1.09 V) along with one smaller reversible wave at $E_{1/2}$ = –1.74 V (Figure 4-4 right). Because the related clusters having carboxylates such as maleate, salicylate, and anthranilate at the unique iron site also shows a similar pseudo-reversible couple due to the dissociation of the carboxylate ligand, described as chapter 3, cluster **17** would release the tetramethylimidazole ligand upon reduction, and indeed it was confirmed by measuring the CV of **17** in the presence of tetramethylimidazole. In a 20 mM acetonitrile solution of tetramethylimidazole, cluster **17** gave the new oxidation peak at E_{pa} = –1.19 V in addition to the original oxidation peak, while the E_{pc} value showed a significant negative shift. Concomitantly, the reversible small redox couple at $E_{1/2}$ = –1.74 V had disappeared. This spectral change became obvious according to increase of the imidazole concentration, and eventually in 120 mM solution of tetramethylimidazole the redox couple became reversible and the potential converged at $E_{1/2}$ = –1.23 V.[13,14] Accordingly, the redox potential for $[Fe_4S_4]^{2+}/[Fe_4S_4]^{+}$ of **17** would be assigned to $E_{1/2}$ = –1.23 V, while the redox wave observed in the absence of tetramethylimidazole would be attributable to a mixture of **17** and the cluster generated by dissociation of the imidazole, which may have acetonitrile instead, and the weak redox couple at $E_{1/2}$ = –1.74 V would be attributable to the $[Fe_4S_4]^{+}/[Fe_4S_4]^{0}$ redox of the latter cluster.

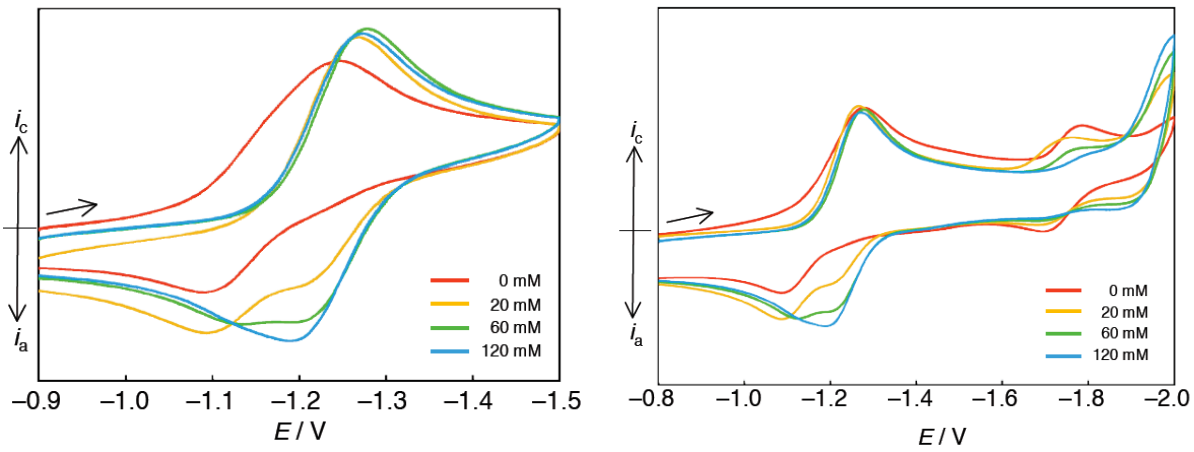

Figure 4-4. CV spectra of **17** with 0.1 V/s in the presence of 0 mM (red line), 20 mM (orange line), 60 mM (green line), and 120 mM (blue line) tetramethylimidazole.

A scan-rate dependent CV analysis also support this assignment. As shown above, the CV of **17** in a 20 mM tetramethylimidazole with 0.1 V/s shows the two oxidation processes at E_{pa} = –1.09 and –1.19 V. When the scan rate was increased up to 0.5 V/s, the wave at –1.19 V became dominant, and $E_{1/2}$ was –1.23 V (Figure 4-5), in which the dissociation of tetramethylimidazole would be negligible. On the other hand, the wave at –1.09 V became dominant at a lower scan rate of 0.02 V/s, in which the species generated by tetramethylimidazole dissociation upon reduction would be dominant.

The dissociation of the imidazole ligand was prevented in CH_2Cl_2 according to the CV spectra. The redox couple of **17** was observed at $E_{1/2}$ = –1.33 V with good reversibility, and the spectrum did not vary upon addition of tetramethylimidazole, probably due to the less polarity and weaker coordinating property of CH_2Cl_2 compared to those of acetonitrile.

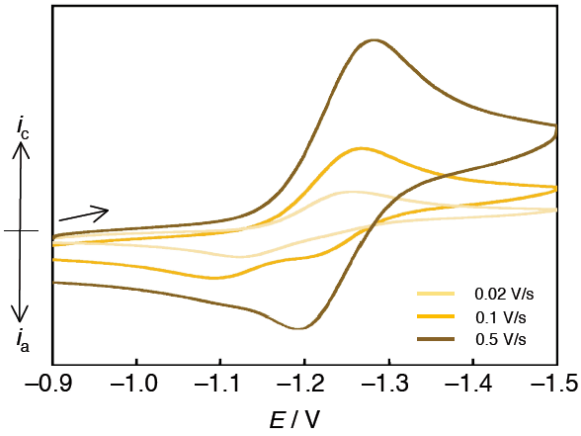

Figure 4-5. CV spectra of **17** in the presence of 10 mM tetramethylimidazole with 0.02 V/s (light yellow), 0.1 V/s (yellow), 0.5 V/s (dark yellow).

It is notable that the redox potential of **17** ($E_{1/2}$ = –1.23 V) is considerably positive compared to that of **1** ($E_{1/2}$ = –1.49 V) and those having carboxylates due to the charge neutral imidazole ligand coordination. Holm *et al* also reported the CV of [4Fe-4S] clusters carrying an imidazole and tridentate thiolate LS_3^{3-},[8] which have reduction potential at –1.02 to –1.04 V vs Ag/Ag^+. However the CV was measured under the condition of $[Fe_4S_4Cl(LS_3)]^{2-}$ with $NaBF_4$ and excess imidazoles, which indicates the chloride-dissociation/ imidazole-coordination behavior, different from the CV result of cluster **17** as indicating imidazole dissociation/re-coordination system.

The CV of **18**, **19** and **20** were similarly investigated (shown in Figure 4-6, 4-7, 4-8, Table 4-2). As observed for **17**, each cluster shows one pseudo-reversible and one weaker reversible redox couples without an external addition of imidazoles (**18**; $E_{1/2}$ = –1.10, –1.71 V, **19**; $E_{1/2}$ = –1.11, –1.69 V, **20**; $E_{1/2}$ = –1.13, –1.74 V), indicating that the dissociation of the imidazole ligands are commonly occurred in acetonitrile. Addition of the respective imidazoles resulted in a similar negative shift of the pseudo-reversible couples, and concomitantly the weaker couples at $E_{1/2}$ = –1.71 for **18**, –1.69 for **19**, and –1.74 V for **20** had disappeared. The redox pontentials of **18**, **19**, **20** in the presence of 120 mM imidazole were shifted to $E_{1/2}$ = –1.17,

–1.16, –1.20 V, respectively. To observe the redox behavior of non-dissociated imidazole cluster, the CV of **20** in CH_2Cl_2 was examined to measure. However, the CV in CH_2Cl_2 could not be measured because **20** are not stable in CH_2Cl_2 solution.

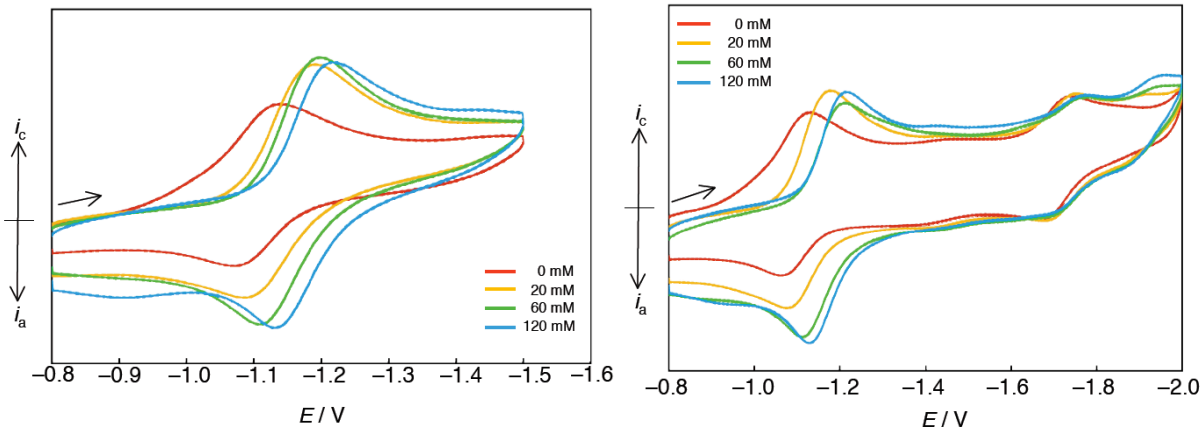

Figure 4-6. CV spectra of **18** with 0.1 V/s in the presence of 0 mM (red line), 20 mM (orange line), 60 mM (green line), and 120 mM (blue line) 1-methylimidazole.

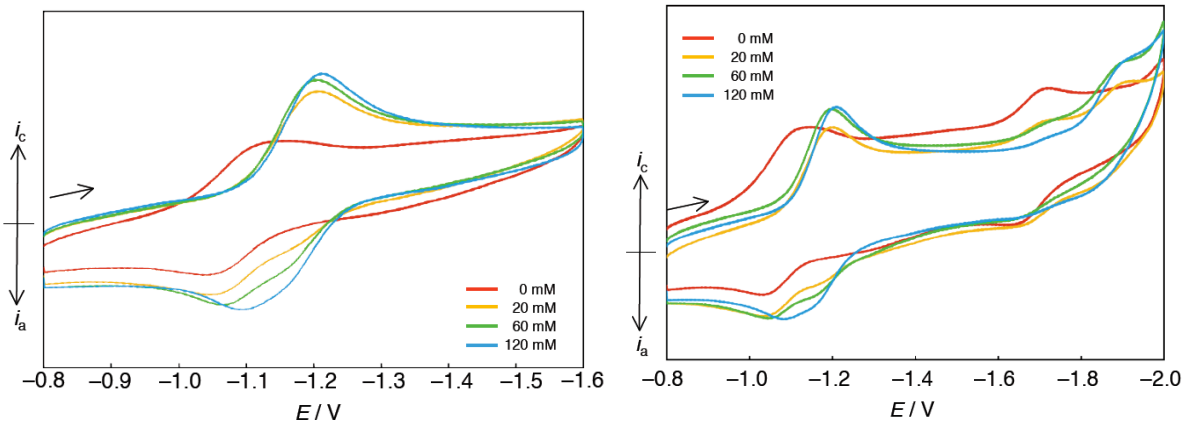

Figure 4-7. CV spectra of **19** with 0.1 V/s in the presence of 0 mM (red line), 20 mM (orange line), 60 mM (green line), and 120 mM (blue line) 2-methylimidazole.

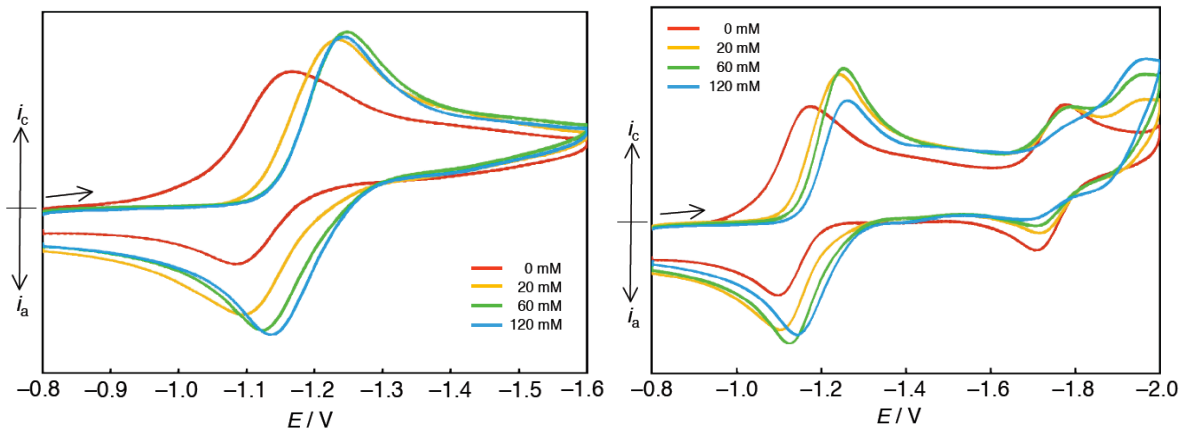

Figure 4-8. CV spectra of **20** with 0.1 V/s in the presence of 0 mM (red line), 20 mM (orange line), 60 mM (green line), and 120 mM (blue line) 4-methylimidazole.

When the CV of **20** was recorded by adding the 1,8-bis(dimethylamino)naphthalene as a proton sponge, the potential for $[Fe_4S_4]^{2+}/[Fe_4S_4]^{+}$ redox shifted negatively (Figure 4-9). The reason of negative shift would be that the imidazole ligand becomes anionic imidazolate ligand after the proton is extracted with the base. This result indicates that the interaction of the proton of imidazole with base gives the more negative reduction potential for [4Fe-4S] clusters. By the way, the CV of **18** did not change by the addition of proton sponge.

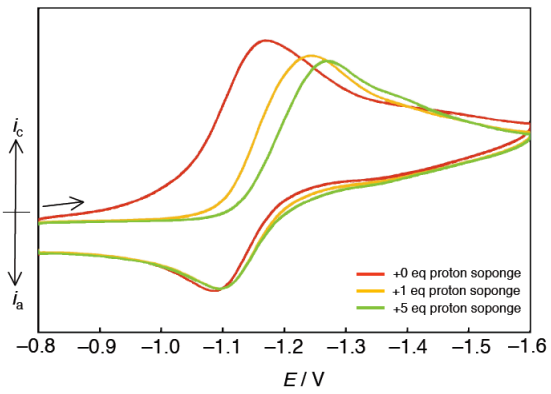

Figure 4-9. CV spectra of **20** with 0.1 V/s in the addition of 0 equiv (red line), 1 equiv (orange line), and 5 equiv (yellow-green line) proton sponge.

Table 4-2. Redox properties of **17-20** with or without excess imidazoles.[a]

	E_{pc} / V	E_{pa} / V	$E_{1/2}$ / V
17	–1.25	–	–
	–	–1.09	–
	–1.79	–1.69	–1.74
17 with 120 mM tetramethylimidazole	–1.27	–1.19	–1.23
18	–1.14	–1.06	–1.10
	–1.75	–1.66	–1.71
18 with 120 mM 1-methylimidazole	–1.24	–1.13	–1.17
19	–1.14	–1.04	–1.09
	–1.73	–1.65	–1.69
19 with 120 mM 2-methylimidazole	–1.21	–1.11	–1.16
20	–1.17	–1.08	–1.13
	–1.78	–1.70	–1.74
20 with 120 mM 4-methylimidazole	–1.25	–1.14	–1.20

[a] The data were recorded in 0.1 M *n*-Bu_4NPF_6 solution (CH_3CN) with glassy carbon working electrode, a Pt counter electrode, and a $Ag/AgNO_3$ reference electrode. The scan rate was 0.1 Vs^{-1}.

4.3 Discussion

The structural analysis and redox behavior of **17**-**20** provide us important information on the [4Fe-4S] cluster in organisms carrying a histidine imidazole and three cysteine thiolates. The geometry and metric parameters around the unique iron and those around the other three irons are alike, which suggests the delocalization of the d-electrons over the four irons irrespective of the site-differentiation. The CV analysis also indicates that (i) the $[Fe_4S_4]^{2+}$ cluster having the imidazole ligand can be reduced at more positive potential than that carrying thiolate ligands, (ii) reduction of the $[Fe_4S_4]^{2+}$ cluster promotes the dissociation of the imidazole ligand on the unique iron and it would allow the coordination of the substrate or modulation of the redox potential in organisms, and (iii) the redox potential can be controlled through hydrogen bonding interaction of the proton on imidazole N-atom.

The study of H184C mutant *Df* [NiFe] hydrogenase was reported by Léger *et al*, on which histidine-ligated [4Fe-4S] cluster was lost and all cysteine coordinated cluster is evolved.[2e] The activity of mutant was very low, which was suggested that the electron transfer system changes from that of wild type protein. On the other hand, the redox potential of [4Fe-4S] clusters for H50C mutant of *E. coli* membrane-bound nitrate reductase A shows a shift of 500 mV from the value of that of wild type.[4c] The author's works recommend these difference of the redox potentials between four thiolates coordination and three thiolates and one imidazole coordination (ΔE = 260-320 mV). However a small potential shift was reported for *Dg* [NiFe] hydrogenase.[2d] *Dg* [NiFe] hydrogenase has two [4Fe-4S] clusters, one coordinated by a histidine three cysteines, and another having four cysteines, and their potential difference ΔE was reported as 50 mV. This value is considerably smaller than that for our models **4a** and **17**-**20** with ΔE = 260-320 mV. The reason for this difference is not clear, but the imidazole ligands of these enzymes could be coordinated as an anionic imidazolate.

4.4 Summary

In summary, we reported the synthesis of [4Fe-4S] cluster having a tridentate thiolate and an imidazole ligand, especially the first example of synthesis of the clusters having a 2-methylimidazole and a 4-methylimidazole that serve as better histidine models with leaving protons on the imidazole N atoms. Their redox behavior proposes that the imidazole ligand easily dissociate from the unique iron along reduction and that the redox potentials of imidazole-ligations are positive than that of all thiolate coordinated [4Fe-4S] cluster. These results provide important information to a histidine coordinated [4Fe-4S] clusters in metalloproteins.

4.5 Experimental Section

General:

All compounds were handled under an atmosphere of pure dinitrogen using standard Schlenk techniques or glove boxes. Hexane, ether, acetonitrile, DMF, THF were degassed and purified by the method described by Grubbs, in which the solvents were passed over columns of activated alumina and a copper catalyst supplied by Hansen & Co. Ltd. ^{1}H NMR spectra were acquired by using a JEOL ECA-600. NMR assignments were supported by additional 2D NMR experiments. Cyclic Voltammograms were recorded on a BAS-ALS-660B electron analyzer using a glassy carbon working electrode and 0.1 M *n*-Bu_4NPF_6 as the supporting electrolyte, in which the potentials are referred to the $Ag/AgNO_3$ electrode. Electrospray ionization time-of-flight mass spectrometry (ESI-TOF-MS) spectra were obtained from a Micromass LCT TOF-MS spectrometer or Bruker micrOTOF II-NUT. UV/Vis spectra were recorded in 10-mm quartz glass cells with a JASCO V560 spectrometer. Elemental analyses were performed on a LECO-CHNS-932 elemental analyzer or Elementar Analysensysteme GmbH varioMICRO where the samples were sealed in tin or silver capsules under nitrogen. $(PPh_4)_2[Fe_4S_4(SEt)(TempS_3)]$ (**4a**) was synthesized according to chapter 2.

Synthesis:

$(PPh_4)[Fe_4S_4(Me_4Im)(TempS_3)]$ (17): Triethylammoniumtriflate in acetonitrile (0.081 M, 0.95 mL, 0.077 mmol) was added to **4a** (86 mg, 0.050 mmol) in acetonitrile (15 mL), and the solution was stirred for 1 h. After removal of all the volatiles in vacuo, the residue was washed with ether, and added acetonitrile (15 mL), and tetramethylimidazole in acetonitrile (0.025 M, 3.0 mL, 0.075 mmol). After stirred for 6 h and removal of all the volatiles in vacuo, the residue was washed with THF and ether, and extracted with acetonitrile (5 mL). Layered hexane and ether on this solution, which gave **17** as black crystals (36 mg, 0.025 mmol, 50%

yield). Anal. Calc. for $C_{67}H_{71}N_2Fe_4O_3PS_7$: C, 56.23; H, 5.00; N, 1.96; S, 15.68. Found: C, 56.22; H, 5.04; N, 2.44; S, 15.00. ^{1}H NMR (CD_3CN, δ); 7.90 (t, P(C_6H_5)$_4$), 7.74-7.71 (m, P(C_6H_5)), 7.68 (s, arom), 7.67-7.65 (m, P(C_6H_5)$_4$), 7.66 (s, C_cH), 6.35 (br, arom), 5.75 (br, arom), 4.61 (br, CH_3 of imidazole), 4.33 (br, CH_3 of imidazole), 3.99 (s, OCH_3), 3.41 (s, CH_2), 2.83 (br, CH_3 of imidazole), 2.56 (br, CH_3 of imidazole), 2.33 (br, CH_2CH_3), 1.14 ppm (s, CH_2CH_3). Cyclic voltammetry (acetonitrile, 0.1 Vs^{-1}); $E_{1/2}$ = –1.17, –1.74 V (without excess tetramethylimidazole), –1.23 V (in 120 mM tetramethylimidazole).). Cyclic voltammetry (CH_2Cl_2, 0.1 Vs^{-1}); $E_{1/2}$ = –1.33 V. UV/Vis (CH_3CN); λ_{max} [nm] (ε [cm^{-1}•M^{-1}]) = 473 (1.1x10^4), 366 (1.3 x10^4) sh, 298 (2.0 x10^4) sh.

(PPh_4)[Fe_4S_4(1-MeH_3Im)($TempS_3$)] (18): Triethylammonium triflate in acetonitrile (0.081 M, 1.1 mL, 0.085 mmol) was added to **4a** (94 mg, 0.055 mmol) in acetonitrile (15 mL), and the solution was stirred for 1 h. After removal of all the volatiles in vacuo, the residue was washed with ether, and added acetonitrile (15 mL), and 1-methylimidazole in acetonitrile (0.060 M, 1.4 mL, 0.086 mmol). After stirred for 6 h and removal of all the volatiles in vacuo, the residue was washed with THF and ether, and extracted with DMF (1 mL) and acetonitrile (5 mL). Layered hexane and ether on this solution, which gave **18** as black crystals (24 mg, 0.017 mmol, 31% yield). Anal. Calc. for $C_{64}H_{65}N_2Fe_4O_3PS_7$•$(C_2H_3N)_{1.5}$: C, 55.48; H, 4.83; N, 3.38; S, 15.47. Found: C, 55.40; H, 5.00; N, 3.10; S, 15.17. ^{1}H NMR (CD_3CN, δ); 7.90 (t, P(C_6H_5)$_4$), 7.73-7.65 (m, P(C_6H_5)), 6.36 (br, arom), 5.67 (br, arom), 4.42 (br, CH_3 of imidazole), 3.99 (s, OCH_3), 3.40 (s, CH_2), 2.33 (br, CH_2CH_3), 1.14 ppm (s, CH_2CH_3), one aromatic proton of $TempS_3^{3-}$and three protons of 1-methylimidazole *were not assignable*. Cyclic voltammetry (acetonitrile, 0.1 Vs^{-1}); $E_{1/2}$ = –1.10, –1.71 V (without excess 1-methylimidazole), –1.17 V (in 120 mM 1-methylimidazole). UV/Vis (CH_3CN); λ_{max} [nm] (ε [cm^{-1}•M^{-1}]) = 473 (8.8 x 10^3), 365 (1.0 x 10^4) sh, 299 (1.5 x 10^4) sh.

(PPh_4)[Fe_4S_4(2-MeH_3Im)($TempS_3$)] (19): Cluster **19** was synthesized as described for **18** from **4a** (92 mg, 0.054 mmol), triethylammonium triflate (0.079 M, 0.81 mL, 0.064 mmol), and 2-methylimidazole (0.083 M, 1.0 mL, 0.083 mmol) in 47% yield as black crystals (35 mg, 0.025 mmol). Anal. Calc. for $C_{64}H_{65}N_2Fe_4O_3PS_7 \bullet C_2H_3N$: C, 55.43; H, 4.79; N, 2.94; S, 15.70. Found: C, 55.66; H, 5.02; N, 2.85; S, 15.34. ^{1}H NMR (DMF-d^7, δ); 8.0 (br, P(C_6H_5)$_4$), 7.90-7.88 (m, P(C_6H_5)), 7.75 (br, arom), 6.24 (br, arom), 5.59 (br, arom), 4.04 (s, OCH_3), 3.36 (s, CH_2), 2.35 (br, CH_2CH_3), 1.13 (s, CH_2CH_3). the protons of 2-methylimidazole *were not assignable*. Cyclic voltammetry (acetonitrile, 0.1 Vs^{-1}); $E_{1/2}$ = –1.09, –1.69 V (without excess 2-methylimidazole), –1.16 V (in 120 mM 2-methylimidazole). UV/Vis (DMF); λ_{max} [nm] (ε [$cm^{-1} \bullet M^{-1}$]) = 466 (1.1 x 10^4), 358 (1.5 x 10^4) sh, 299 (2.5 x 10^4) sh.

(PPh_4)[Fe_4S_4(4-MeH_3Im)($TempS_3$)] (20): Cluster **20** was synthesized as described for **18** from **4a** (92 mg, 0.054 mmol), triethylammonium triflate (0.059 M, 1.8 mL, 0.11 mmol), and 4-methylimidazole (0.073 M, 1.5 mL, 0.11 mmol) in 55% yield as black crystals (41 mg, 0.030 mmol). Anal. Calc. for $C_{64}H_{65}N_2Fe_4O_3PS_7 \bullet 0.5(C_4H_{10}O)$: C, 55.59; H, 4.95; N, 1.96; S, 15.74. Found: C, 55.57; H, 5.04; N, 2.25; S, 15.43. ^{1}H NMR (CD_3CN, δ); 7.90 (br, P(C_6H_5)$_4$), 7.73-7.66 (m, P(C_6H_5)), 7.68 (br, arom), 6.35 (br, arom), 5.69 (br, arom), 3.99 (s, OCH_3), 3.40 (s, CH_2), 2.33 (br, CH_2CH_3), 1.13 (s, CH_2CH_3), the protons of 4-methylimidazole *were not assignable*. Cyclic Voltammetry (acetonitrile, 0.1 Vs^{-1}); $E_{1/2}$ = –1.13, –1.74 V (without excess 4-methylimidazole), –1.20 V (in 120 mM 4-methylimidazole). UV/Vis (CH_3CN); λ_{max} [nm] (ε [$cm^{-1} \bullet M^{-1}$]) = 461 (1.2 x 10^4), 358 (1.4 x 10^4) sh, 292 (2.1 x 10^4) sh.

Crystal-Structure Determination:

Crystal data and refinement parameters for the cluster **17**, **18**, **19**, and **20** reported herein are summarized in Table 4-3. Preliminary crystallographic result for **21** is also given in Table 4-3. Single crystals were mounted on a loop using oil (Paraton, Hampton Research Corp.). Diffraction data were collected at –100 ºC under a cold nitrogen stream on a Rigaku FR-E instrument with a Saturn 70 CCD detector using graphite-monochromated MoKa radiation (λ = 0.710690 Å). Using an oscillation range of 0.3 for **17**, or 0.5º for **18**, **19**, and **20**, 1800 data images were collected for **17**, 1080 data images were collected for **19** and **20**, while 720 images were measured for **18**. The data were integrated and corrected for absorption using the Rigaku/MSC CrystalClear program package. The structures were solved by a direct method (SHELXS97) and were refined by fullmatrix least squares on F^2 by the Rigaku/MSC CrystalStructure program package. Anisotropic refinement was applied to all non-hydrogen atoms except for some crystal solvents. All the hydrogen atoms were put at the calculated positions.

Table 4-3. Crystal data of **17**, **18**, **19**, **20**, and **21**.

	17•3.5(CH_3CN)	**18**•1.5(CH_3CN)	**19**•(CH_3CN)	**20**•0.5(Et_2O)	**21**•(CH_3CN)•2(Et_2O)
	$C_{67}Fe_4S_7H_{71}O_3$	$C_{64}Fe_4S_7H_{65}O_3$	$C_{64}Fe_4S_7H_{65}O_3$	$C_{64}Fe_4S_7H_{65}O_3$	$C_{148}Fe_8S_{14}H_{143}O_6N_2P_3$
Fomula	N_2P•$C_7H_{10.5}N_{3.5}$	N_2P•$C_3H_{4.5}N_{1.5}$	N_2P•C_2H_3N	N_2P•$C_2H_5O_{0.5}$	•C_2H_3N•$C_8H_{20}O$
Weight	1574.77	1450.59	1430.06	1426.07	3223.60
Crystal system	monoclinic	monoclinic	monoclinic	triclinic	triclinic
Space group	$P2_1/c$ (#14)	$P2_1/c$ (#14)	$P2_1/c$ (#14)	P-1 (#2)	P-1 (#2)
a/Å	13.8151(5)	13.834(2)	13.929(3)	12.036(2)	13.257(3)
b/Å	13.0110(4)	12.910(2)	12.910(3)	13.012(3)	17.398(4)
c/Å	41.870(2)	37.042(6)	36.305(8)	23.036(5)	35.901(11)
α/deg	–		–	85.460(8)	86.010(13)
β/deg	95.729(2)	91.663(3)	91.883(3)	74.830(6)	88.815(12)
γ/deg	–		–	79.525(8)	68.620(9)
V/Å^3	7488.5(5)	6613(2)	6525(3)	3422.1(13)	7692(4)
Z	4	4	4	2	2
D_{calc}/g cm^{-1}	1.397	1.457	1.456	1.384	1.392
μ/cm^{-1}	10.248	11.528	11.669	11.124	10.090
F(000)	3276.00	3004.00	2960.00	1478.00	3352.00
$2\theta_{max}$/deg	55.0	55.0	55.0	55.0	50.0
no. of rflns (all)	74088	53240	66159	42438	51338
indep. rflns (R_{int})	17097	14871	14921	15116	26502
no. of params	850	766	757	750	1775
$R1$ [a]	0.0448	0.0661	0.0463	0.0888	0.1383
w$R2$ [b]	0.1161	0.1955	0.1224	0.2836	0.4245
GOF[c]	1.113	1.091	1.104	1.067	1.077

[a] $R1 = ||F_o|-|F_c|| / \Sigma|F_o|$ ($I>2\sigma(I)$). [b] $wR2=\{[\Sigma w(|F_o|-|F_c|)^2/\Sigma wF_o^2]\}^{1/2}$ (all data). [c] GOF = $[\Sigma w(|F_o|-|F_c|)^2/((N_o-N_v))^{1/2}$ (N_o = number of observations, N_v = number of variables).

References for Chapter 4

[1] a) H. Beinert, M. C. Kennedy, C. D. Stout, *Chem. Rev.* **1996,** *96*, 2335–2373; b) A. Messerchmidt, R. Huber, T. Poulos, K. Wiehardt, *Handbook of Metalloproteins vol. 1,* John Wiley & Sons, Chichester, UK, **2001**, pp471–485; c) A. Messerchmidt, R. Huber, T. Poulos, K. Wiehardt, *Handbook of Metalloproteins vol. 2,* John Wiley & Sons, Chichester, UK, **2001**, 1086-1096; *10*, 681–687; d) F. Berkovitch, Y. Nicolet, J. T. Wan, J. T. Jarrett, C. L. Drennan, *Science* **2004***, 303*, 76–79; e) P. Hänzelmann, H. Schindelin, *Proc. Natl. Acad, Sci. USA* **2004**, *101*, 12870–12875; d) B. W. Lepore, F. J. Ruzicka, P. A. Frey, D. Ringe, *Proc. Natl. Acad, Sci. USA*, **2005**, *102*, 13819–13824; f) J. L. Vey, J. Yang, M. Li, W. E. Broderick, J. B. Broderick, C. L. Drennan, *Proc. Natl. Acad, Sci. USA* **2008**, *105*, 16137–16141; g) T. Gräwert, I. Span, W. Eisenreich, F. Rohdich, J. Eppinger, A. Bacher, M. Groll, *Proc. Natl. Acad. Sci.* **2010**, *107*, 1077–1081; h) N. Muraki, J. Nomata, K. Ebata, T. Mizoguchi, T. Shiba, H. Tamiaki, G. Kurisu, Y. Fujita, *Nature* **2010**, *465*, 110–115; i) M. Lee, T. Gräwert, F. Quitterer, F. Rohdich, J. Eppinger, W. Eisenreich, A. Bacher, M. Groll, *J. Mol. Biol.* **2010**, *404*, 600–610; f) A. Messerchmidt, *Handbook of Metalloproteins vol. 4,* John Wiley & Sons, Chichester, UK, **2011**, 397–412; j) S. H. Knauer, W. Buckel, H. Dobbek, *J. Am. Chem. Soc.* **2011**, *133*, 4342–4347.

[2] a) M. Teixeira, I. Moura, A. V. Xavier, J. J. G. Moura, J. LeGall, D. V. DerVartanian, H. D. Peck, Jr., B.-H. Huynh, *J. Biol. Chem.* **1989**, *264*, 16435–16450; b) A. Volbeda. M.-H. Charon, C. Piras, E. C. Hatchikian, M. Frey, J. C. Fontecilla-Camps, *Nature*, **1995**, *373*, 580–587; c) A. Volbeda, E. Garcin, C. Piras, A. L. de Lacey, V. M. Fernandez, E. C. Hatchikian, M. Frey, J. C. Fontecilla-Camps**,** *J. Am. Chem. Soc.* **1996**, *118,* 12989–12996; d) A. Messerchmidt, R. Huber, T. Poulos, K. Wiehardt, *Handbook of Metalloproteins vol. 2,* John Wiley & Sons, Chichester, UK, **2001**, pp880-896; e) S. Dementin, V. Belle, P. Bertrand, B. Guigliarelli, G. Adryanczyk-Perrier, A. L. De Lacey, V. M. Fernandez, M. Rousset, C. Léger, *J. Am. Chem. Soc.* **2006**, 128, 5209–5218; f) S. Dementin, B. Burlat, V. Fourmond, F. Leroux, P.-P. Liebgott, A. A. Hamdan, C. Léger, M. Rousset, B. Guigliarelli, P. Bertrand, *J. Am. Chem. Soc.* **2011**, *133*, 10211–10221.

[3] a) J. W. Peters, W. N. Lanzilotta, B. J. Lemon, L. C. Seefeldt, *Science* **1998**, *282*, 1853–1858; b) Y. Nicolet, C. Piras, P. Legrand, C. E. Hatchikian, J. C. Fontecilla-Camps, *Structure* **1999**, *7*, 13–23; c) A. Messerchmidt, R. Huber, T. Poulos, K. Wiehardt, *Handbook of Metalloproteins vol. 2,* John Wiley & Sons, Chichester, UK, **2001**, 738–751; d) J. C. Fontecilla-Camps, A. Volbeda, C. Cavazza, Y. Nicolet, *Chem. Rev.* **2007**, *107*, 4273–4303; e) C. Tard, C. J. Pickett, *Chem. Rev.* **2009**, *109,* 2245–2274.

[4] a) A. Magalon, M. Asso, B. Guigliarelli, R. A. Rothery, P. Bertrand, G. Giordano, F. Blasco, *Biochemistry* **1998**, *37*, 7363–7370; b) M. G Bertero, R. A Rothery, M. Palak, C. Hou, D. Lim, F. Blasco, J. H. Weiner, N. C. J. Strynadka, *Nature Structural Biology* **2003**, *10*, 681–687; c) R. A. Rothery, M. G. Bertero, T. Spreter, N. Bouromand, N. C. J. Strynadka, J. H. Weiner, *J. Biol. Chem.* **2010**, *285*, 8801–8807; d) A. Messerchmidt, *Handbook of Metalloproteins vol. 5,* John Wiley & Sons, Chichester, UK, **2011**, pp524–532.

[5] a) L. A. Sazanov, P. Hinchliffe, *Science* **2006**, *311*, 1430–1436; b) A. Messerchmidt, *Handbook of Metalloproteins vol. 4*, John Wiley & Sons, Chichester, UK, **2011**, pp47–61; c) H. R. Bridges, E. Bill, J. Hirst, *Biochemistry* **2012**, *51*, 149−158.

[6]a) U. Müh, I. Çinkaya, S. P. J. Albracht, W. Buckel, *Biochemistry* **1996**, *35,* 11710–11718; b) B. M. Martins, H. Dobbek, I. Çinkaya, W. Buckel, A. Messerschmidt, *Proc. Natl. Acad. Sci. USA* **2004**, *101*, 15645–15649; c) A. Messerchmidt, *Handbook of Metalloproteins vol. 4*, John Wiley & Sons, Chichester, UK, **2011**, 172–182.

[7] J. E. Barclay, M. I. Diaz, D. J. Evans, G. Garcia, M. D. Santana, M. C. Torralba, *Inorg. Chim. Acta* **1997**, *258*, 211-219.

[8] C. Zhou, R. H. Holm**,** *Inorg. Chem.* **1997,** *36,* 4066 – 4077.

[9] Y. Ohki, K. Tanifuji, N. Yamada, M. Imada, T. Tajima, K. Tatsumi, *Proc. Natl. Acad. Sci. USA*, **2011**, *108*, 12635–12640.

[10] J. Zhou, R. H. Holm, *J. Am. Chem. Soc.* **1995**, *117*, 11353 – 11354.

[11] ^{1}H NMR of cluster **16** (CD_3CN, *d*); 7.91 (m, $P(C_6H_5)_4$), 7.73-7.66 (m, $P(C_6H_5)_4$), 7.61 (s, arom), 6.20 (br, arom), 5.75 (br, arom), 3.98 (s, OCH_3), 3.39 (s, CH_2), 2.33 (br, CH_2CH_3), 1.13 ppm (s, CH_2CH_3).

[12] a) M. F. Hoq, C. R. Johnson, S. Paden, R. E. Shepherd, *Inorg. Chem.* **1983**, *22,* 2693-2700, b) W. W. Henderson, R. E. Shepherd, J. Abolaf, *Inorg. Chem.* **1986**, *25,* 3157-3163.

[13] The spectrum in 200 mM solution of tetramethylimidazole was not changed from that in 120 mM solution.

[14] indicated for the related cluster reported by ref 8

Chapter 5

Synthesis of Reduced [4Fe-4S]$^{+}$ Clsuter Having a Tridentate Thiolate Ligand

5.1. Introduction

In chapter 2, 3, and 4, the author described the synthesis, the crystal structures, and the redox properties of [3:1] site-differentiated $[4Fe\text{-}4S]^{2+}$ clusters using tridentate thiolate $TempS_3^{3-}$ or $TefpS_3^{3-}$. Usual [4Fe-4S] clusters including [3:1] site-differentiated type in metalloproteins have a redox coupling of $[4Fe\text{-}4S]^{2+}/[4Fe\text{-}4S]^{+}$,[1,2] and therefore the author focused on the synthesis of $[4Fe\text{-}4S]^{+}$ cluster. The synthetic $[4Fe\text{-}4S]^{+}$ clusters having four thiolates were reported by Holm *et al* in 1978. Compared with diamagnetic $[4Fe\text{-}4S]^{2+}$ clusters, their paramagnetic properties are interesting and were investigated by electron spin resonance spectroscopy (ESR) and magnetic susceptibility.[3] Afterward, four hydrosulfides, chlorides, phosphines and cyanides coordination were synthesized.[4] Although the [3:1] site-differentiated clusters such as three phosphines and one thiolate coordinated cluster were also synthesized,[5] the synthesis of [3:1] site-differentiated $[4Fe\text{-}4S]^{+}$ clusters as model of the clusters in metalloproteines has not been achieved. Therefore, the synthesis of them and investigation of their properties are attracted much attention.

Herein, the author described the synthesis, crystal structure, and magnetic properties of [3:1] site-differentiated $[4Fe\text{-}4S]^{+}$ clusters carrying the tridentate thiolate $TefpS_3^{3-}$ and benzenethiolate, via the synthesis and the reaction of chloride coordinated cluster $[Fe_4S_4(Cl)(TefpS_3)]^{2-}$ and edge-bridged double cubane cluster $[\{Fe_4S_4(TefpS_3)\}_2]^{4-}$.

5.2 Results and Discussion

5.2.1 Synthesis, Structure, and Redox Property of $(PPh_4)_2[Fe_4S_4(Cl)(TefpS_3)]$ (22)

The [4Fe-4S] cluster having a chloride and a tridentate thiolate ligand LS_3^{3-} was synthesized by Holm *et al*.[6] They reported the reaction of chloride cluster with ionic compound such as sodium phenolate and sodium benzenethiolate and with sodium tetrafluoroborate and neutral compound such as phosphine and imidazole which gave a lot of [3:1] site-differentiated [4Fe-4S] clusters, though almost all of these clusters were not gotten crystal structures.[7] Introduction of chloride ligand on unique iron is useful for synthesis of various [4Fe-4S] clusters, and therefore the author examined to synthesize chloride-ligated [4Fe-4S] cluster having the tridentate thiolate $TefpS_3^{3-}$.

When 1 equiv of acetonitrile solution of benzoyl chloride was added to $(PPh_4)_2[Fe_4S_4(SEt)(TefpS_3)]$ (**4b**) in acetonitrile at –40 ºC, immediately the chloride coordinated [4Fe-4S] cluster $(PPh_4)_2[Fe_4S_4(Cl)(TefpS_3)]$ (**22**) was formed. Layering hexane and ether on acetonitrile solution of **22** gave black crystals. The crystal structure and some metric parameter were shown in Figure 5-1 and Table 5-1. The unique iron site is occupied by the chloride, while other irons are coordinated by tridentate thiolate $TefpS_3^{3-}$. The metric parameters of the cubane core resemble those of **4b** and $[Fe_4S_4(Cl)(LS_3)]^{2-}$ reported by Holm *et al*.[6]

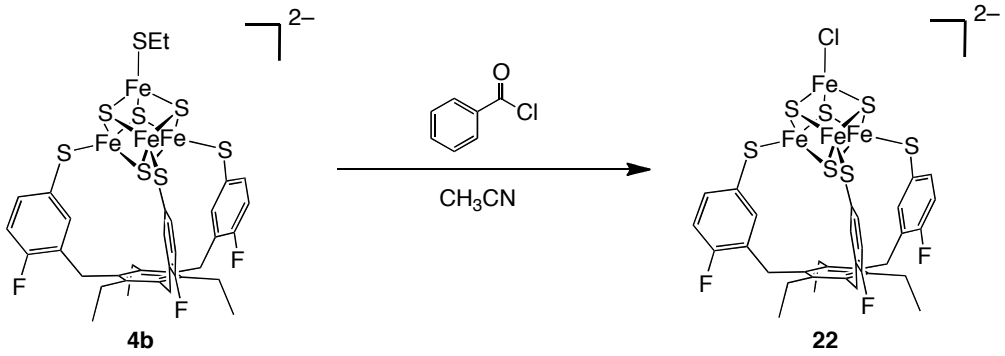

Scheme 5-1. Synthesis of **22**.

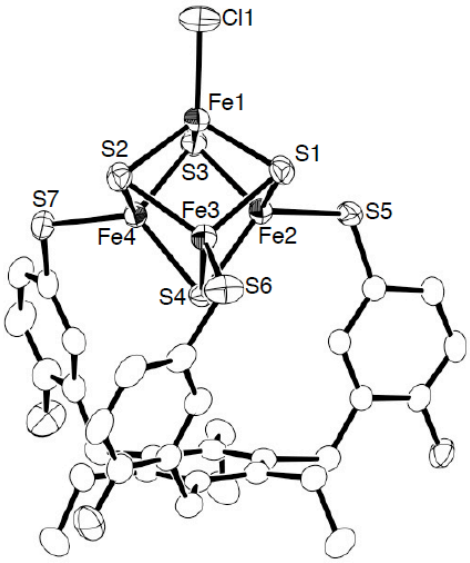

Figure 5-1. Molecular structure of the anion of **22** with 50% thermal ellipsoids. Hydrogen atoms are omitted for clarity.

Table 5-1. Selected bond distances (Å) for **22**.

Fe1-Fe2	2.7760(7)	Fe1-S1	2.2695(9)
Fe1-Fe3	2.7609(8)	Fe1-S2	2.2862(10)
Fe1-Fe4	2.7549(7)	Fe1-S3	2.3015(11)
Fe2-Fe3	2.7304(8)	Fe2-S1	2.2904(10)
Fe2-Fe4	2.7370(6)	Fe2-S3	2.2649(10)
Fe3-Fe4	2.7433(7)	Fe2-S4	2.2712(9)
		Fe3-S1	2.2583(9)
Fe1-Cl1	2.2124(12)	Fe3-S2	2.2714(9)
Fe2-S5	2.2746(10)	Fe3-S4	2.3055(9)
Fe3-S6	2.2652(12)	Fe4-S2	2.3073(10)
Fe4-S7	2.2672(8)	Fe4-S3	2.2596(10)
		Fe4-S4	2.2742(9)

The redox behavior of cluster **22** was investigated by cyclic voltammetry in acetonitrile using $Ag/AgNO_3$ reference electrode, shown in Figure 5-2. The cluster has one reversible redox wave at $E_{1/2}$ = –1.32 V attributable to the $[4Fe\text{-}4S]^{2+}/[4Fe\text{-}4S]^{+}$ process. This redox potential is a little positive from ethanethiolate coordinated cluster **4b**, similar to the potentials of $[Fe_4S_4(Cl)(LS_3)]^{2-}$ ($E_{1/2}$ = –1.23 V) and $[Fe_4S_4(SEt)(LS_3)]^{2-}$ ($E_{1/2}$ = –1.35 V vs

$Ag/AgNO_3$) in acetonitrile.[7f] It could be resulted from electron-withdrawing of chloride ligand.

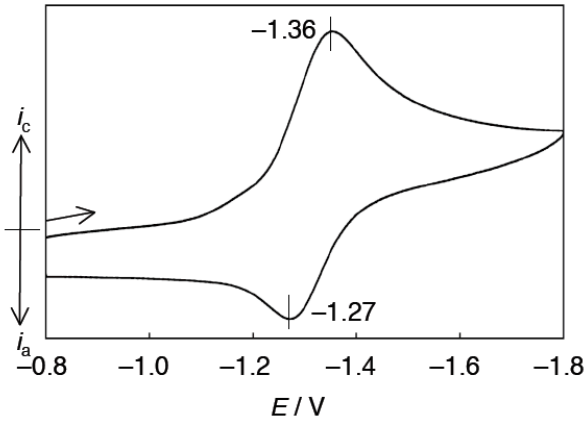

Figure 5-2. CV spectrum of **22**.

5.2.2 Synthesis, Structure, and Redox Property of $(PPh_4)_4[Fe_4S_4(TefpS_3)]_2$ (23)

On the way to search the ligand on unique iron introduced by the reaction of chloride-ligation except for Holm's works,[7] the author focused tetrahydroborate ligand. Previously, the two tetrahydroborate coordinated uranium complex was synthesized by the reaction of two chlorides coordinated complex with thallium tetrahydroborate.[8] Other works showed that the reaction of tetrahydroborate coordinated complexes with ethanol, phenol, acetic acid, and phenyl acetylene afford the ethoxido, phenolate, acetate, and phenylacetylide ligation.[9] Additionally, tetrahydroborate coordinated molybdenum-iron-sulfur cluster was reported by Coucouvanis *et al*. This structure consists of two $[MoFe_3S_4]$ cores bridged each other by each one Fe-S bonds and non-bridged irons have one tetrahydroborate in η^2 manner, respectively.[10] These reports provide that the tetrahydroborate coordinated cluster is also useful for introducing various ligands, and the structure of tetrahydroborate-ligation is attracted much attention. Therefore the author attempted the reaction of chloride cluster **22** with sodium tetrahydroborate for synthesis of tetrahydroborate coordinated cluster.

The chloride coordinated [4Fe-4S] cluster **22** was reacted with sodium tetrahydroborate in acetonitrile at –40ºC. After stirred for 3 h at –40ºC, measuring ESI-MS indicated the generation of tetrahydroborate coordinated $[Fe_4S_4(BH_4)(TefpS_3)]^{2-}$ or hydride coordinated $[Fe_4S_4(H)(TefpS_3)]^{2-}$.[11] The ^{1}H NMR spectrum shows the existence of one cluster, which is different from **22**,[12] and therefore the tetrahydroborate or hydride coordinated cluster was generated from this reaction. However, after stirred overnight at room temperature, their mass signals were disappeared. The crystallization indicated the formation of edge-bridged double cubane cluster $(PPh_4)_4[\{Fe_4S_4(TefpS_3)\}_2]$ (**23**) in 55% yield. The cluster **23** has two $[4Fe\text{-}4S]^+$ cores, which were reduced from $[4Fe\text{-}4S]^{2+}$ cluster **22**. Therefore, the reaction of **22** with sodium tetrahydroborate would proceed through the generation of $[Fe_4S_4(BH_4)(TefpS_3)]^{2-}$ or $[Fe_4S_4(H)(TefpS_3)]^{2-}$ and NaCl firstly, and then the reduction of [4Fe-4S] core with generation of H_2. The edge-bridged double cubane clusters were reported previously, such as $[Fe_8S_8(PCy_3)_6]$ and $[Fe_8S_8(P^iPr_3)_4(SSiPh_3)_2]$,[13] but **23** is the first example of having only thiolate ligands on six terminal irons.

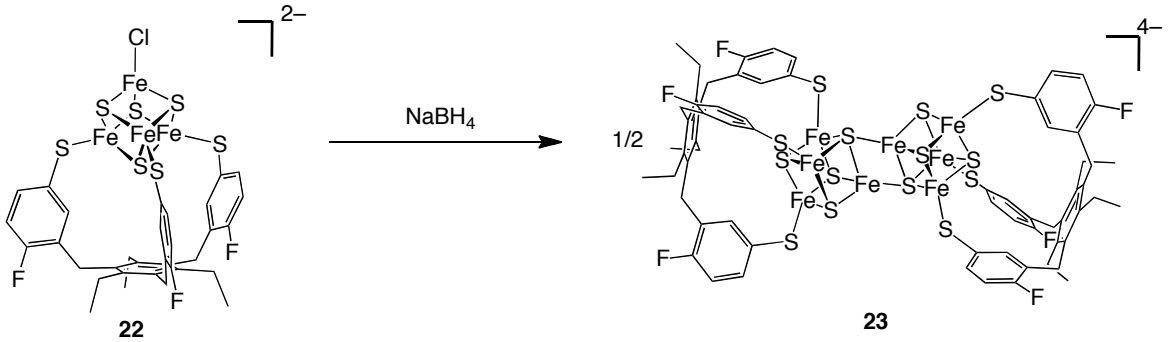

Scheme 4-2. Synthesis of **23**.

The X-ray crystal structure of **23** contains four tetraphenylphosphonium cations, one iron-sulfur anion, and some solvent. The anion structure was shown in Figure 5-3. The anion possesses two [4Fe-4S] cubane cores, which are directly linked via each Fe-S bond. This

structure is termed "edge-bridged double cubane". Non-bridged iron atoms are coordinated by thiolate from $TefpS_3^{3-}$. The metric parameters of **23** were listed in Table 5-2. The distances of edge-bridged Fe1-Fe1* and Fe1-S3* (2.7346(7) Å and 2.2894(9) Å, respectively) are similar to those of intercubane Fe-Fe and Fe-S (2.6436(8)-2.7694(8) Å and 2.2439(9)-2.4064(9) Å), and therefore the bonding between two [4Fe-4S] cores is as strong as inter-cubane bonding. In cubane core, the Fe-S distances and the Fe-S-Fe angles around S3 and S3* (2.3665(9)-2.4064(9) Å and 66.90(3)-68.44(3)º) are different from the other Fe-S distances and Fe-S-Fe angles (2.2439(9)-2.3059(9) Å and 70.31(3)-74.91(3)º) because of the μ^4-geometry of S3 and S3*. Compared with previous reported $\{[4Fe\text{-}4S]^+\}_2$ clusters $[Fe_8S_8(P^iPr_3)_4(SSiPh_3)_2]$ and $[Fe_8S_8(P^iPr_3)_4(SSi^iPr_3)_2]$,[13de] the geometry of bridged S (S3 and S3*) atoms of cluster **23** are resemble those of previous clusters. However, the Fe-Fe distances of cluster **23** (average: 2.71 Å) are slightly longer than those of previous clusters (average: 2.67-2.68 Å). The longer Fe-Fe bonds would be due to electron-donation from six thiolate ligands.

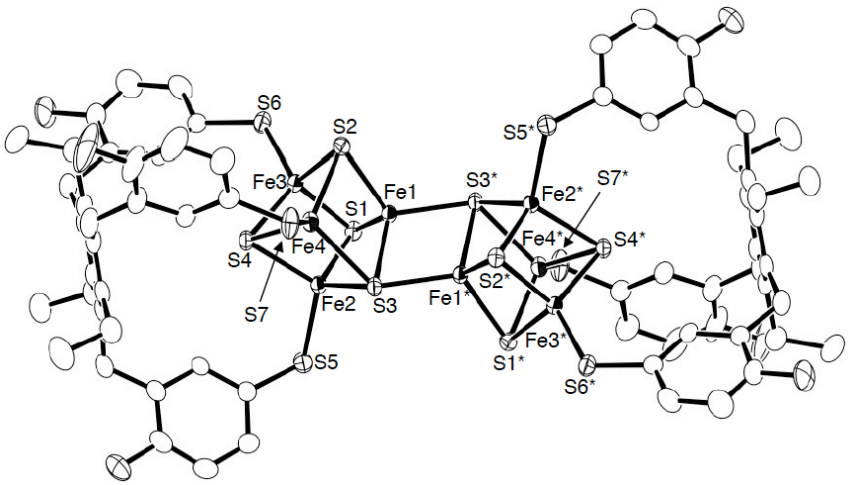

Figure 5-3. Molecular structure of the anion of **23** with 50% thermal ellipsoids. Hydrogen atoms are omitted for clarity.

Table 5-2. Selected bond distances (Å) and angles (deg) for **23**.

Fe1-Fe2	2.6746(7)	Fe1-S1	2.2767(10)
Fe1-Fe3	2.7654(8)	Fe1-S2	2.2981(10)
Fe1-Fe4	2.6436(8)	Fe1-S3	2.3895(10)
Fe2-Fe3	2.7694(8)	Fe2-S1	2.3017(10)
Fe2-Fe4	2.6589(9)	Fe2-S3	2.3665(9)
Fe3-Fe4	2.7456(10)	Fe2-S4	2.3059(9)
Fe1-Fe1*	2.7346(7)	Fe3-S1	2.2703(10)
		Fe3-S2	2.2740(9)
Fe1-S3*	2.2894(9)	Fe3-S4	2.2439(9)
Fe2-S5	2.2969(10)	Fe4-S2	2.2929(9)
Fe3-S6	2.2708(10)	Fe4-S3	2.4064(9)
Fe4-S7	2.3011(13)	Fe4-S4	2.2914(9)

Table 5-2. (cont)

S1-Fe1-S2	102,22(3)	S1-Fe3-S2	103.18(4)	Fe1-S1-Fe2	71.49(3)
S1-Fe1-S3	107.10(4)	S1-Fe3-S4	104.45(3)	Fe1-S1-Fe3	74.91(4)
S1-Fe1-S3*	111.90(4)	S1-Fe3-S6	110.00(4)	Fe2-S1-Fe3	74.56(3)
S2-Fe1-S3	109,08(4)	S2-Fe3-S4	104.18(4)	Fe1-S2-Fe3	74.43(3)
S2-Fe1-S3*	117.48(3)	S2-Fe3-S6	111.22(4)	Fe1-S2-Fe4	70.31(3)
S3-Fe1-S3*	108.51(3)	S4-Fe3-S6	122.03(4)	Fe3-S2-Fe4	73.91(3)
S1-Fe2-S3	107.06(4)	S2-Fe4-S3	108.67(3)	Fe1-S3-Fe1*	71.49(3)
S1-Fe2-S4	101.50(3)	S2-Fe4-S4	102.07(4)	Fe1-S3-Fe2	68.44(3)
S1-Fe2-S5	109.66(4)	S2-Fe4-S7	117.31(4)	Fe1-S3-Fe4	66.90(3)
S3-Fe2-S4	108.64(4)	S3-Fe4-S4	107.76(4)	Fe2-S3-Fe4	67.70(3)
S3-Fe2-S5	114.64(3)	S3-Fe4-S7	103.92(4)	Fe2-S4-Fe3	74.97(3)
S4-Fe2-S5	114.31(4)	S4-Fe4-S7	116.75(4)	Fe2-S4-Fe4	70.67(3)
				Fe3-S4-Fe4	74.51(3)

The redox potentials of **23** were also recorded in acetonitrile (Figure 5-4). The CV shows one oxidation event at $E_{1/2}$ = –1.03 V and two reduction events at $E_{1/2}$ = –1.64, –1.96 V, which are attributable to the $\{[4Fe\text{-}4S]_2\}^{2+}/\{[4Fe\text{-}4S]_2\}^{3+}$, $\{[4Fe\text{-}4S]_2\}^{2+}/\{[4Fe\text{-}4S]_2\}^{+}$, and $\{[4Fe\text{-}4S]_2\}^{+}/\{[4Fe\text{-}4S]_2\}^{0}$ process, respectively. The previous reported edge-bridged double

cubane cluster $[\{Fe_4S_4(P^iPr_3)_2(SSiPh_3)\}_2]$ has $\{[4Fe\text{-}4S]_2\}^{2+}/\{[4Fe\text{-}4S]_2\}^{3+}$ and $\{[4Fe\text{-}4S]_2\}^{2+}/\{[4Fe\text{-}4S]_2\}^{+}$ redox couples at –0.33 and –1.18 V, respectively.[13d] The potentials of cluster **23** are more negative, which is reasonable because of having six anionic thiolate ligands.

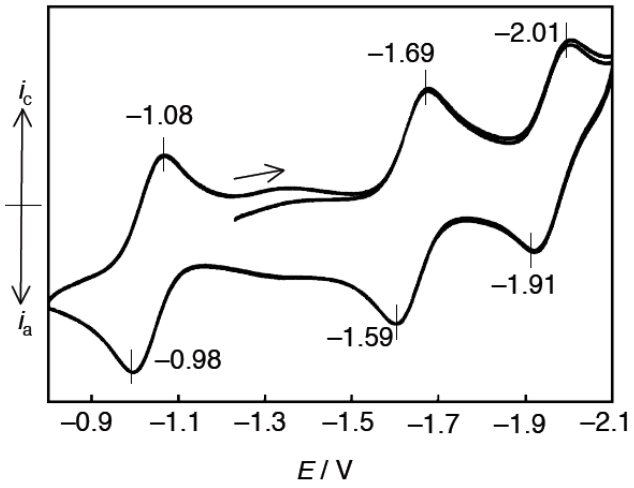

Figure 5-4. CV spectrum of **23**.

5.2.3 Synthesis, Structure, and Magnetic Property of $(PPh_4)_3[Fe_4S_4(SPh)(TefpS_3)]$ (24)

The cluster **23** has two $[4Fe\text{-}4S]^+$ cores, and therefore this cluster is useful for the synthesis of [3:1] site-differentiated $[4Fe\text{-}4S]^+$ cluster. 2 Equiv of tetraphenylphosphonium benzenethiolate in acetonitrile was added to acetonitrile solution of cluster **23**. After stirred overnight, the solvent was removed under vacuum, and then the intended reduced [4Fe-4S] cluster $(PPh_4)_3[Fe_4S_4(SPh)(TefpS_3)]$ (**24**) was produced as black powder. Layering hexane and ether on the acetonitrile solution of **24** gave black crystals in 60% yield, and the molecular structure was elucidated by X-ray analysis (Figure 5-5, Table 5-3). This compound contains three tetraphenylphosphonium as cations and one [4Fe-4S] cluster having a tridentate thiolate $TefpS_3^{3-}$ and a benzenethiolate as anion, which is corresponding to $[4Fe\text{-}4S]^+$ cluster. While

the Fe-Fe distances in cubane core of **24** (average: 2.73 Å) do not change from those of **5b** having a $[4Fe\text{-}4S]^{2+}$ core (average: 2.73 Å), the Fe-S(core), the Fe-S(thiolate) distances of **24** (average: 2.31 Å, 2.31 Å) are longer than those of **5b** (average: 2.29 Å, 2.27 Å). The difference of the metric parameters of **5b** and **24** is consistent with that of previous clusters $[Fe_4S_4(SPh)_4]^{2-}$ [14] and $[Fe_4S_4(SPh)_4]^{3-}$.[3f,15]

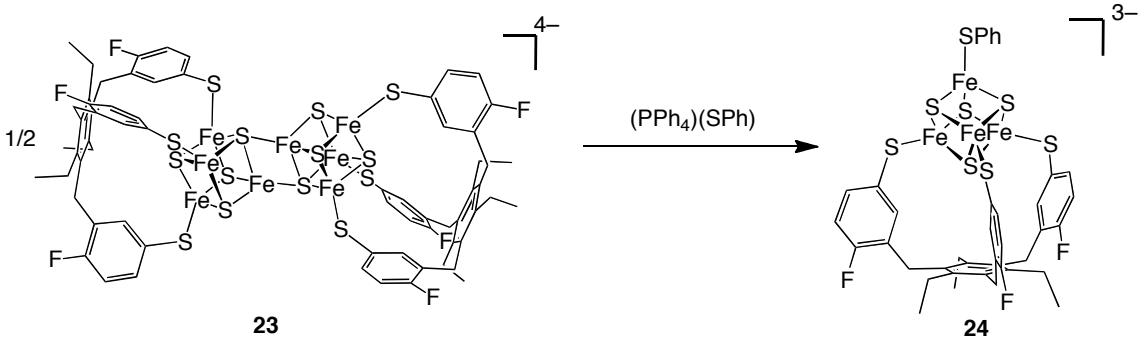

Scheme 5-3. Synthesis of **24**.

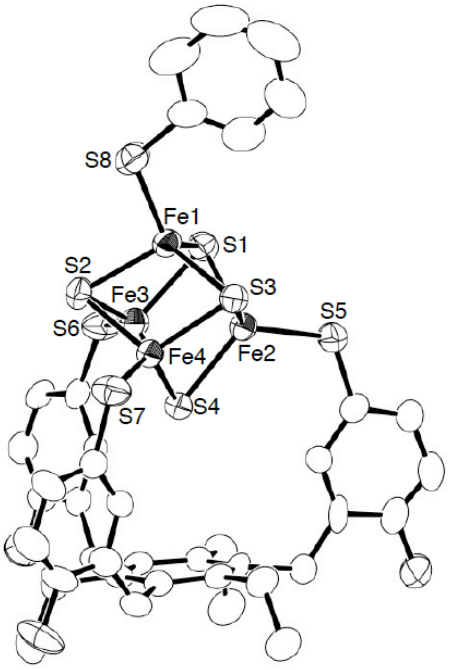

Figure 5-5. Molecular structure of the anion of **24** with 50% thermal ellipsoids. Hydrogen atoms are omitted for clarity.

Table 5-3. Selected bond distances (Å) for **24**.

Fe1-Fe2	2.768(2)	Fe1-S1	2.253(3)
Fe1-Fe3	2.7570(19)	Fe1-S2	2.326(3)
Fe1-Fe4	2.657(3)	Fe1-S3	2.330(3)
Fe2-Fe3	2.661(2)	Fe2-S1	2.335(4)
Fe2-Fe4	2.792(2)	Fe2-S3	2.295(3)
Fe3-Fe4	2.764(2)	Fe2-S4	2.334(3)
		Fe3-S1	2.349(3)
Fe1-S8	2.313(4)	Fe3-S2	2.270(3)
Fe2-S5	2.315(3)	Fe3-S4	2.326(3)
Fe3-S6	2.299(3)	Fe4-S2	2.315(3)
Fe4-S7	2.315(3)	Fe4-S3	2.350(3)
		Fe4-S4	2.259(3)

The electron spin resonance (ESR) spectrum of **24** in acetonitrile is displayed in Figure 5-5. The signal at 4 K shows the rhombic spectrum with g = 2.06, 1.95, and 1.91, which is consistent with paramagnetic compound. The values around 2.00 are similar to previous reported [4Fe-4S]$^{+}$ clusters[15,16] such as $[Fe_4S_4(SPh)_4]^{3-}$ (g = 1.93, 2.06, axial shape in acetonitrile),[14] $[Fe_4S_4(SCys)_4]^{3-}$ in *Bacillus polymyxa* ferredoxin$_{red}$ (g = 1.88, 1.93, 2.06, rhombic shape in aqueous buffer).[16a] The temperature-dependent magnetic susceptibility of **24** was also measured (Figure 5-6). The magnetic momentum at 2K (μ_{eff} = 1.35 μ_B) supports the S =1/2 ground state, which is consistent with [4Fe-4S]$^{+}$ cluster, similar to previous cluster.[15,17]

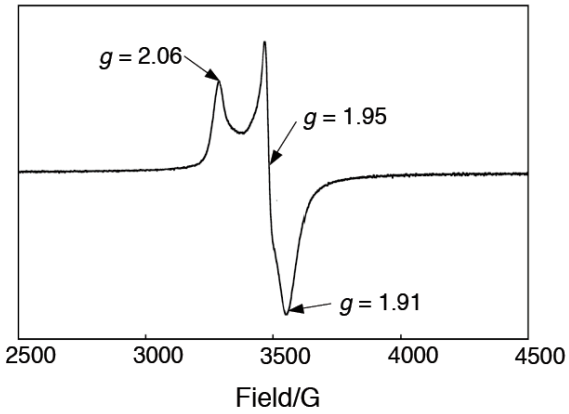

Figure 5-5. ESR spectrum of **24** in acetonitrile at 4 K.

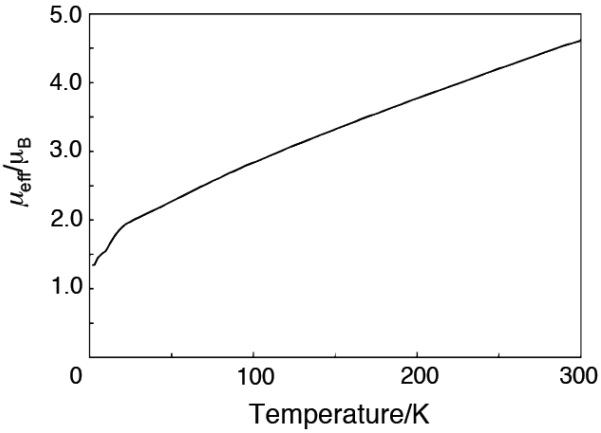

Figure 5-6. The temperature-dependence of magnetic susceptibility of **24**.

5.3 Summary

In this chapter, the synthesis of [4Fe-4S] cluster having a chloride and tridentate thiolate $TefpS_3^{3-}$ was reported. The reaction of chloride-ligation with sodium tetrahydroborate gave the edge-bridged double cubane cluster containing two $[4Fe\text{-}4S]^+$ cores. The addition of 2 equiv of tetraphenylphosphonium benzenthiolate to the edge-bridged double cubane cluster gave $[4Fe\text{-}4S]^+$ cluster having a benzenethiolate and a $TefpS_3^{3-}$, of which magnetic property is reasonable of reduced $[4Fe\text{-}4S]^+$ cluster.

5.4 Experimental Section

General:

All air-sensitive compounds were handled under an atmosphere of pure nitrogen gas using standard Schlenk techniques or glove boxes. Hexane, ether, acetonitrile, and DMF were degassed and purified by the method described by Grubbs, in which the solvents were passed over columns of activated alumina and a copper catalyst supplied by Hansen & Co., Ltd. ^{1}H NMR spectra were acquired by using a JEOL ECA-600. NMR assignments were supported by additional 2D NMR experiments. Cyclic Voltammograms were recorded on a BAS-ALS-660B electron analyzer using a glassy carbon working electrode and 0.1 M nBu$_4$NPF$_6$ as the supporting electrolyte, and the potentials are referenced to the Ag/AgNO$_3$ electrode. Electrospray ionization time-of-flight mass spectrometry (ESI-TOF-MS) spectra were obtained from a Micromass LCT TOF-MS spectrometer or Bruker micrOTOF II-NUT. UV/Vis spectra were recorded in 10-mm quartz glass cells with a JASCO V560 spectrometer. Elemental analyses were performed on Elementar Analysensysteme GmbH varioMICRO where the samples were sealed in tin or silver capsules under nitrogen. The ESR spectrum was recorded on a Bruker EMX-plus spectrometer at X-band frequencies. The magnetic susceptibility was measured using a Quantum Design MPMS-XL SQUID-type magnetometer, and the crystalline samples were sealed in quartz tubes. (PPh$_4$)$_2$[Fe$_4$S$_4$(SEt)(TefpS$_3$)] (**4b**) was synthesized according to chapter 2.

Synthesis:

(PPh$_4$)$_2$[Fe$_4$S$_4$(Cl)(TefpS$_3$)] (22): Benzoylchloride in acetonitrile (0.047 M, 5.8 mL, 0.27 mmol) was added to (PPh$_4$)$_2$[Fe$_4$S$_4$(SEt)(TefpS$_3$)] **(4b)** (455 mg, 0.27 mmol) in acetonitrile (90 mL) at 0 ºC. After stirring for 1 h at r.t., the black solution was evaporated to dryness, and the residue was washed with ether, which gave **22** as a black solid (367 mg, 0.22 mmol, 83%

yield). Single crystals of **22** suited to X-ray analysis was obtained by layering hexane and ether onto the acetonitrile solution. ^{1}H NMR (600 MHz, CD_3CN, δ); 7.90 (s, $P(C_6H_5)_4$), 7.79 (s, arom, 3H), 7.76-7.68 (m, $P(C_6H_5)_4$), 7.68-7.62 (m, $P(C_6H_5)_4$), 6.36 (br, arom, 3H), 5.58 (br, arom, 3H), 3.43 (s, $ArCH_2Ar$), 2.36 (br, CH_2CH_3), 1.13 (s, CH_2CH_3). Anal. Calc. for $ClC_{81}Fe_4S_7H_{70}P_2F_3$: C, 59.12; H, 4.29; S, 13.64. Found: C, 59.09; H, 3.97; S, 13.49. Cyclic voltammetry (acetonitrile, 0.1 Vs^{-1}); $E_{1/2}$= –1.32 V. UV/Vis (CH_3CN): λ_{max} [nm] (ε [$M^{-1}cm^{-1}$]) = 454 (9.9×10^3), 291 (2.2×10^4) sh.

$(PPh_4)_4[Fe_4S_4(TefpS_3)]_2$ (23): Sodium tetrahydroborate in acetonitrile (0.12 M, 2.2 mL, 0.26 mmol) was added to **22** (367 mg, 0.22 mmol) in acetonitrile (60 mL), and the solution was stirred overnight. After removal of all the volatiles in vacuo, the residue was extracted acetonitrile (20 mL). The solution was layered with hexane and ether, which gave **23** as black crystals (203 mg, 0.061 mmol, 55% yield). ^{1}H NMR (600 MHz, CD_3CN, δ); 11.93 (br), 11.11 (br), 10.64 (br), 7.89 (br, $P(C_6H_5)_4$), 7.72 (br, $P(C_6H_5)_4$), 7.68-7.63 (m, $P(C_6H_5)_4$), 5.71 (br), 3.92 (br), 3.45 (br), 2.61 (br), 2.38 (br), 1.28 (br), 1.24 (br). Anal. Calc. for $C_{162}Fe_8S_8H_{140}P_4F_6$: C, 60.42; H, 4.38; S, 13.94. Found: C, 59.95; H, 4.88; S, 14.23. Cyclic Voltammetry (acetonitrile, 0.1 Vs^{-1}); $E_{1/2}$ = –1.03, –1.64, –1.96 V. UV/Vis (CH_3CN): λ_{max} [nm] (ε [$M^{-1}cm^{-1}$]) = 419 (3.3×10^4), 286 (5.0×10^4) sh.

$(PPh_4)_3[Fe_4S_4(SPh)(TefpS_3)]$ (24): Tetraphenylphosphonium benzenethiolate (PPh_4)(SPh) in acetonitrile (0.012 M, 5 mL, 0.058 mmol) was added to **23** (80 mg, 0.024 mmol) in acetonitrile (18 mL), and the solution was stirred overnight. After removal of all the volatiles in vacuo, the residue was extracted acetonitrile (6 mL). The solution was layered with hexane and ether, which gave **24** as black crystals (60 mg, 0.029 mmol, 60% yield). ^{1}H NMR (600 MHz, CD_3CN, δ); 12.13 (br, SC_6H_5), 9.33 (br, arom), 7.89 (s, $P(C_6H_5)_4$), 7.72 (br, $P(C_6H_5)_4$),

7.67-7.64 (m, $P(C_6H_5)_4$, 4.41 (br, arom), 3.74 (br, arom), 2.56 (br, $ArCH_2Ar$), 2.48 (br, CH_2CH_3), 1.19 (br, CH_2CH_3), 0.24 (br, SC_6H_5), –1.03 (br, SC_6H_5). Anal. Calc. for $C_{111}Fe_4S_8H_{95}P_3F_3 \bullet C_2H_3N \bullet C_3H_7ON$: C, 64.12; H, 4.87; N, 1.29; S, 11.81. Found: C, 63.86; H, 5.05; N, 0.83; S, 12.29. UV/Vis (CH_3CN): λ_{max} [nm] (ε [$M^{-1}cm^{-1}$]) = 444 (1.8×10^4), 292 (3.2×10^4) sh. ESR (X-band, microwave 1.0 mW, in frozen acetonitrile, 4K): g = 2.06, 1.95, and 1.91. Magnetic susceptibility (B.M.): μ_{eff} = 1.35 μ_B (2 K), μ_{eff} = 4.63 μ_B (300 K).

Crystal-Structure Determination:

Crystal data and refinement parameters for the clusters reported herein are summarized in Table 5-4. Single crystals were mounted on a loop using oil (Paraton, Hampton Research Corp.). Diffraction data were collected at –100 ºC under a cold nitrogen stream on a Rigaku FR-E with a Saturn 70 CCD detector using graphite-monochromated MoKα radiation (λ = 0.710690 Å). Using an oscillation range of 0.5˚, 1080 data images were collected for **23** and **24** while 720 images were measured for **22**. The data were integrated and corrected for absorption using the Rigaku/MSC CrystalClear program package. The structures were solved by a direct method (SIR97, SHELXS97) and were refined by full-matrix least-squares on F^2 by the Rigaku/MSC CrystalStructure program package. Anisotropic refinement was applied to all non-hydrogen atoms except for some crystal solvents. All the hydrogen atoms were put at the calculated positions.

Table 5-4. Crystal data of **22**, **23**, and **24**.

	22•1.5CH_3CN	**23**•8CH_3CN	**24**•CH_3CN•DMF
fomula	$ClC_{81}Fe_4S_7H_{70}P_2F_3$ •$C_3H_{4.5}N_{1.5}$	$C_{162}Fe_8S_{14}H_{140}P_4F_6$ •$C_{16}H_{24}N_8$	$C_{111}Fe_4S_8H_{95}P_3F_3$ •C_2H_3N•C_3H_7ON
Formula wt	1707,23	3548.81	2172.9
crystal system	triclinic	monoclinic	triclinic
space group	*P*-1 (#2)	$P2_1/n$ (#14)	*P*-1 (#2)
a/Å	12.436(2)	14.183(4)	13.289(4)
b/Å	13.487(2)	43.325(10)	18.808(7)
c/Å	24.805(3)	14.169(4)	23.3856(10)
α/deg	86.329(4)	–	72.20(3)
β/deg	77.150(3)	106.477(3)	74.84(3)
γ/deg	75.022(4)	–	71.23(3)
V/Å^3	3918.4(9)	8349(4)	5182(3)
Z	2	2	2
D_{calc}/g cm^{-1}	1.447	1.412	1.392
μ/cm^{-1}	10.393	9.484	8.126
F(000)	1758,00	3668.00	2254.00
$2\theta_{max}$/deg	55.0	55.0	54.7
no. of rflns. (all)	32335	73807	63687
indep. rflns. (R_{int})	17304	19016	23175
no. of params.	923	989	1213
$R1$[a]	0.0463	0.0463	0.0773
w$R2$[b]	0.1230	0.1128	0.1953
GOF[c]	1.050	1.098	1.027

[a] $R1 = \Sigma ||F_o| - |F_c|| / \Sigma |F_o|$ ($I > 2\sigma(I)$). [b] $wR2 = \{[\Sigma w(|F_o| - |F_c|)^2 / \Sigma wF_o^2]\}^{1/2}$ (all data). [c] GOF = $[\Sigma w(|F_o| - |F_c|)^2/(N_o - N_v)]^{1/2}$ (N_o = number of observations, N_v = number of variables).

References for Chapter 5

[1] a) P. J. Stephens, D. R. Jollie, A. Warshel, *Chem. Rev.* **1996,** *96*, 2491–2513, Ferredoxin; b) I. Bertini, A. Sigel, H. Sigel, *Handbook on Metalloproteins*, Marcel Dekker, New York, **2001**, Chapter 10; c) A. Messerchmidt, R. Huber, T. Poulos, K. Wiehardt, *Handbook of Metalloproteins vol. 1,* John Wiley & Sons, Chichester, UK, **2001**, pp543–552, 560–592.

[2] a) M. Teixeira, I. Moura, A. V. Xavier, D. V. Dervartanian, J. Legall, H. D. Peck, Jr, B. H. Huynh, J. J. G. Moura, *Eur. J. Biochem.* **1983**, *130*. 481–484; b) M. H. Emptage, J.-L. Dreyer, M. C. Kennedy, H. Beinert, *J. Biol. Chem.* **1983**, *258*, 11106–11111; c) R. C. Conover, A. T. Kowal, W. Fu, J.-B. Park, S. Aono, M. W. W. Adams, M. K. Johnson, *J. Biol. Chem.* **1990**, *265*, 8533–8541; d) H. Beinert, M. C. Kennedy, C. D. Stout, *Chem. Rev.* **1996**, *96*, 2335–2373; e) U. Müh, I. Çinkaya, S. P. J. Albracht, W. Buckel, *Biochemistry* **1996**, *35,* 11710–11718; f) A. Magalon, M. Asso, B. Guigliarelli, R. A. Rothery, P. Bertrand, G. Giordano, F. Blasco, *Biochemistry* **1998**, *37,* 7363–7370; g) E. Bol, L. E. Bevers, P.-L. Hagedoorn, W. R. Hagen, *J. Biol. Inorg. Chem.* **2006**, *11*, 999–1006.

[3] a) E. J. Laskowski, R. B. Frankel, W. O. Gillum, G. C. Papaefthymiou, J. Renaud, J. A. Ibers, R. H. Holm, *J. Am. Chem. Soc.* **1978**, *100*, 5322–5337; b) J. M. Berg, K. O. Hodgson R. H. Holm, *J. Am. Chem. Soc.* **1979**, *101*, 4586–4593; c) D. W. Stephan, G. C. Papaefthymiou, R. B. Frankel, R. H. Holm, *Inorg. Chem.* **1983**, *22*, 1550–1557; d) K. S. Hagen. A. D. Watson, R. H. Holm, *Inorg. Chem.* **1984**, *23*, 2984–2990; e) M. J. Carney, G. C. Papafthymiou, K. Spartalian, R. B. Frankel, R. H. Holm, *J. Am. Chem. Soc.* **1988**, *110*, 6084–6095; f) M. J. Carney, G. C. Papaefthymiou, M. A. Whitener, K. Spartalian, R. B. Frankel, R. H. Holm, *Inorg. Chem.* **1988**, *27*, 346–352; g) M. J. Carney, G. C. Papaefthymiou, R. B. Frankel, R. H. Holm, *Inorg. Chem.* **1989**, *28*, 1497–1503; h) B. M. Segal, H. R. Hoveyda, R. H. Holm, *Inorg. Chem.* **1998**, *37*, 3440–3443.

[4] a) M. A. Tyson, K. D. Demadis, D. Coucouvanis, *Inorg. Chem.* **1995**, *34*, 4519–4520; b) C. Goh, B. M. Segal, J. Huang, J. R. Long, R. H. Holm, *J. Am. Chem. Soc.* **1996**, *118*, 11844–11853; c) M. Harmjanz, W. Saak, D. Haase, S. Pohl, *Chem. Commun.* **1997**, 951–952; d) J. Han, D. Coucouvanis, *J. Am. Chem. Soc.* **2001**, *123*, 11304–11305; e) H.-C. Zhou, R. H. Holm, *Inorg. Chem.* **2003**, *42*, 11–21; f) T .A. Scott, H.-C. Zhou, *Angew. Chem., Int. Ed.* **2004**, *43*, 5628–5631; g) K. S. Hagen, M. Uddin, *Inorg. Chem.* **2008**, *47*, 11807–11815; h) L. Deng, A. Majumdar, W. Lo, R. H. Holm, *Inorg. Chem.* **2010**, *49*, 11118–11126.

[5] a) M. A. Tyson, K. D. Demadis, D. Coucouvanis, *Inorg. Chem.* **1995**, *34*, 4519–4520; b) M. Harmjanz W. Saak, D. Haase, S. Pohl, *Chem. Commun.* **1997**, 951–952; c) J. Han, D. Coucouvanis, *J. Am. Chem. Soc.* **2001**, *123*, 11304–11305; d) H.-C. Zhou, R. H. Holm, *Inorg. Chem.* **2003**, *42*, 11–21, e) L. Deng, A. Majumdar, W. Lo, R. H. Holm, *Inorg. Chem.* **2010**, *49*, 11118–11126.

[6] a) T. D. P. Stack, R. H. Holm, *J. Am. Chem. Soc.* **1987**, *109,* 2546–2547; b) T. D. P. Stack, R. H. Holm, *J. Am. Chem. Soc.* **1988**, *110*, 2484–2494.

[7] a) T. D. P. Stack, M. J. Carney, R. H. Holm, *J. Am. Chem. Soc.* **1989**, *111*, 1670–1676; b) J. A. Weigel, R. H. Holm, K. K. Surerus, E. Münck, *J. Am. Chem. Soc.* **1989**, *111,* 9246–9247; c) S.

Ciurli, M. Carrie, J. A. Weigel, M. J. Carney, T. D. P. Stack, G. C. Papaefthymiou, R. H. Holm, *J. Am. Chem. Soc.* **1990**, *112*, 2654–2664; d) J. A. Weigel, K. K. P. Srivastava, E. P. Day, E. Münck, R. H. Holm, *J. Am. Chem. Soc.* **1990**, *112,* 8015–8023; e) J. A. Weigel, R. H. Holm, *J. Am. Chem. Soc.* **1991**, *113*, 4184–4191; f) C. Zhou, R. H. Holm, *Inorg. Chem.* **1997**, *36*, 4066–4077.

[8] C. Baudin, M. Ephritikhine, *J. Organomet. Chem.* **1989**, *364*, Cl–C2.

[9] H. Werner, U. Meyer, *J. Organomet. Chem.* **1989**, *366*, 187–196; b) T. Arliguie, D. Baudry, M. Ephritikhine, M. Nierlich, M. Lance, J. Vigner, *J. Chem. Soc., Dalton Trans.* **1992**, 1019–1024; c) M. Tamm, B. Dreßel, T. Bannenberg, J. Grunenberg, E. Herdtweck, *Z. Naturforsch. B*, **2006**, *61b*, 896–903; d) P. Perrotin, I. El-Zoghbi, P. O. Oguadinma, F. Schaper, *Organometallics* **2009**, *28*, 4912–4922.

[10] M. Koutmos, D. Coucouvanis, *Inorg. Chem.* **2004**, *43*, 6508–6510.

[11] The peak of $[Fe_4S_4(BH_4)(TefpS_3)]^{2-}$ was detected by Micromass LCT TOF-MS spectrometer, while the peak of $[Fe_4S_4(H)(TefpS_3)]^{2-}$ was detected by Bruker micrOTOF II-NUT.

[12] The ^{1}H NMR of the reaction of **22** with $NaBH_4$: (600 MHz, CD_3CN, *d*); 7.90 (s, $P(C_6H_5)_4$), 7.83 (s, arom, 3H), 7.72 (s, $P(C_6H_5)_4$), 7.68-7.63 (m, $P(C_6H_5)_4$), 6.43 (br, arom, 3H), 5.50 (br, arom, 3H), 3.39 (s, $ArCH_2Ar$), 2.32 (br, CH_2CH_3), 1.11 (s, CH_2CH_3).

[13] a)L. Cai, B. M. Segal, J. R. Long, M. J. Scott, R. H. Holm, *J. Am. Chem. Soc.* **1995**, *117*, 8863–8864; b) C. Goh, B. M. Segal, J. Huang, J. R. Long, R. H. Holm, *J. Am. Chem. Soc.* **1996**, *118*, 11844–11853; c) M. Harmjanz, W. Saak, D. Haase, S. Pohl, *Chem. Commun.* **1997**, 951–952; d) H.-C. Zhou, R. H. Holm, *Inorg. Chem.* **2003**, *42*, 11–21; e) L. Deng, R. H. Holm, *J. Am. Chem. Soc.* **2008**, *130*, 9878–9886; e) L. Deng, A. Majumdar, W. Lo, R. H. Holm, *Inorg. Chem.* **2010**, *49*, 11118–11126.

[14] a) L. Que, Jr., M. A. Bobrik, J. A. Ibers, R. H. Holm, *J. Am. Chem. Soc.* **1974**, *96*, 4168–4178; b) L. Guodong, Z. Hongtu, H. Sheng-Zhi, T. C. W. Mak, *Acta Cryst.* **1987**, C*43*, 352–353; c) J. Gloux, P. Gloux, H. Hendriks, G. Rius, *J. Am. Chem. Soc.* **1987**, *109*, 3220–3224; d) P. Excoffon, J. Laugier, B. Lamotte, *Inorg. Chem.* **1991,** *30*, 3075–3081.

[15] E, J. Laskowski, R. B. Frankel, W. O. Gillum, G. C. Papaefthymiou, J. Renaud, J. A. Ibers, R. H. Holm, *J. Am. Chem. Soc.* **1978**, *100*, 5322–5337.

[16] a) N. A. Stombaugh, R. H. Burris, W. H. Orme-Johnson, *J. Biol. Chem.* **1973**, *248*, 7951–7956; b) R. Mathews, S. Charlton, R. H. Sands, G. Palmer, *J. Biol. Chem.* **1974**, *249*, 4326–4328; c) R. Cammack, *Biochem. Soc. Trans.* **1975**, *3*, 482–488

[17] G. C. Papaefthymiou, E. J. Laskowski, S. Frota-Pessôa, R. B. Frankel, R. H. Holm, *Inorg. Chem.* **1982**, *21*, 1723–1728.

Acknowledgement

This thesis summarizes the author's study that has been carried out under the direction of Prof. Dr. *Kazuyuki Tatsumi* at Group of Inorganic Chemistry, Department of Chemistry, Graduate School of Science, Nagoya University, during the period of from April 2007 to December 2013.

The author would like to express her science gratitude to Prof. Dr. *Kazuyuki Tatsumi* for his constant supervision, fruitful discussion, and hearty encouragement throughout all of this work. The author is grateful to Dr. *Yasuhiro Ohki* and Dr. *Tsuyoshi Matsumoto* for their useful advice, suggestions and kind encouragements. The author is grateful to Ms. Sayaka Ohike, Mr. *Takuya Wakimoto*, Mr. *Dong Liu*, Mr. *Kiyohisa Hirabayashi*, Mr. *Tomohiko Nakamura*, Ms. *Kaho Tanaka,* Mr. *Jichun Li* for supporting this work. The author would like to thank Dr. *Jun-ici Nishigaki* and Dr. *Shun Ohta* for their useful advice, and Dr. *Takayoshi Hashimoto* for his friendship for six years. The author also would like to thank all of the members of the Tatsumi's research group for their friendship and assistance. The author thanks to Prof. Dr. *Roger E. Cramer* (University of Hawaii) for kind help in the X-ray crystallographic analysis and careful reading of the manuscripts for publications.

The author would like to acknowledge to Prof. Dr. *Gerhard Erker* for giving the opportunity to work in his laboratory at Organisch-Chemisches Institut der Universität Münser (Germany). The author would also like to acknowledge Dr. *Gerald Kehr* for direction of the studies there. The author would like to thank all of the members of *Erker*'s Group for their friendship and assistance. The author also thanks to Ms. *Yuko Kihara* (Research Center for Materials Science, Nagoya University) for the careful arrangements of the externship.

The author is thankful to Global-COE program, Program for Leading Graduate Schools, and so on, on the Nagoya University for the financial support in the form of teaching and researching assistantship. The author is also thankful to Strategic Young Research Overseas Visits Program for Accelerating Brain Circulation (February 2012 - July 2012) for the financial support in the externship. The author also would like to thank to the scholarship of *The Shoshi-Sha Foundation in Takeda Pharmaceutical Company Limited* (April 2010 - March 2013).

Finally, the author would like to acknowledge the help, encouragement, and support for her family, *Munesato Terada*, *Yumi Terada*, *Tamasa Terada*, *Masaki Terada*, and would like to dedicate this thesis.

Tamaki Terada

December 2013

Publication list

(1) New Tridentate Thiolate Ligands: Application to the Synthesis of the Site-Differentiated [4Fe-4S] Cluster having a Hydrosulfide at the Unique Iron

Tamaki Terada, Takuya Wakimoto, Tomohiko Nakamura, Kiyohisa Hirabayashi, Kaho Tanaka, Jichun Li, Tsuyoshi Matsumoto, and Kazuyuki Tatsumi

Chem. Asian J. **2012**, *7*, 920–929.

(2) [3:1] Site-Differentiated [4Fe-4S] Clusters Having One Carboxylate and Three Thiolates

Tamaki Terada, Kiyohisa Hirabayashi, Dong Liu, Tomohiko Nakamura, Takuya Wakimoto, Tsuyoshi Matsumoto, and Kazuyuki Tatsumi

Inorg. Chem. **2013**, *52*, 11997–12004